POLITECNICO
MILANO 1863

SCUOLA DI INGEGNERIA INDUSTRIALE
E DELL'INFORMAZIONE

Selection strategies of resident space objects for active debris removal missions through the resident space object network

TESI DI LAUREA MAGISTRALE IN
SPACE ENGINEERING
INGEGNERIA SPAZIALE

Author: **Luca Perfetti**

Student ID: 10538068
Advisor: Prof. Camilla Colombo
Co-advisor: Jérôme Daquin, Matteo Romano
Academic Year: 2022-23

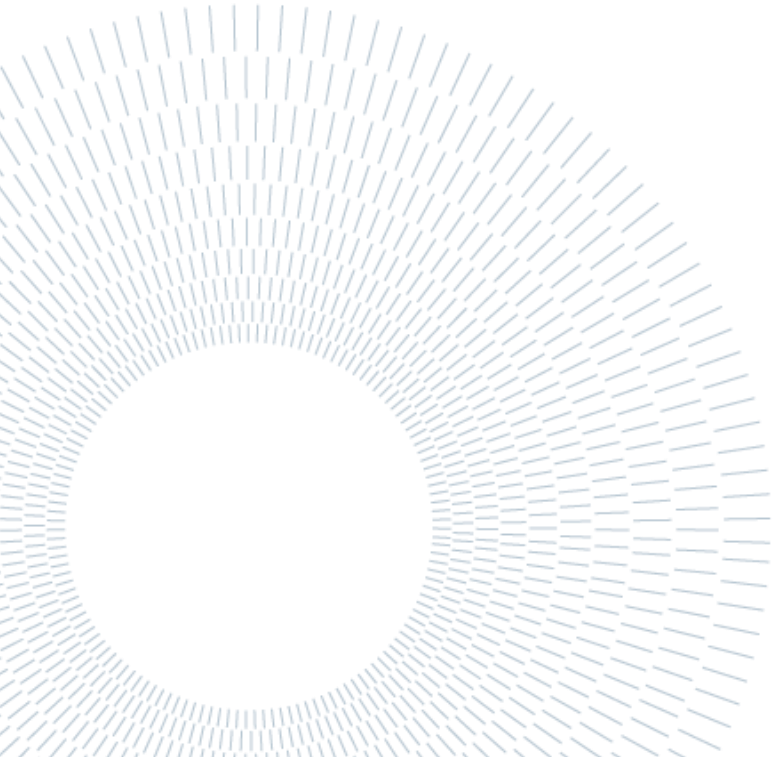

This work is part of the WALSAT (WALlonia Space Awareness Technology) project, which received funding via the BEWARE programme by the government of the Wallonia region of Belgium and by the European Commission (Marie Skłodowska Curie Actions grant agreement 847587) as part of the Horizon 2020 research and innovation programme.

Perfetti Luca, “Selection strategies of resident space objects for active debris removal missions through the resident space object network”. 2024, Politecnico di Milano, Master Thesis in Space Engineering, Supervisors: Camilla Colombo (Politecnico di Milano), Daquin Jérôme (Université de Namur), Romano Matteo (Université de Namur). Printed in Italy.

Abstract

This work focuses on the problem of congestion of Earth orbits by proposing a new method to analyse them and a novel approach to select strategies for debris removal.

The developed tool applies network theory to Resident Space Objects (RSOs), namely orbiting Earth objects, to analyse their positional interactions. Particularly, RSOs represent nodes of a network, while links between nodes are established whenever a conjunction is predicted over a specific period. The obtained network, called Resident Space Object Network (RSONet), is used as a guide to define new metrics called RSONet scores. These scores combine, for each RSO, the likelihood of direct collisions with other RSOs and collisions with debris generated by other objects.

Within this framework, it is analysed the space population through the network connectivity and a novel metric, called "danger score", which merges network-related characteristics and collisional severity factors, such as object mass, probability of collision, etc. More precisely, the main contribution of this work is, by utilising the RSONet, to address the influence of specific RSOs on the rest of population after their removal by quantifying the change of the mentioned metrics. Employing this methodology, two scenarios are analysed to assess the global influence of space debris and mega-constellations on the rest of the RSO population.

Moreover, two complementary approaches are followed to select candidates for debris removal missions. The first one is based on network centrality measures (degree, betweenness, closeness), whilst the second one is based on weighted measures (probability of collision, strength, RSONet scores).

Based on those strategies, a set of nodes to be removed from the RSONet is obtained. Thus, it is analysed the changes in RSONet connectivity and danger score to assess the effectiveness of each strategy.

The findings emphasize that the optimal strategy to weaken the network connectivity involves removal of objects with highest degree. However, the analysis also identifies alternative strategies based on a RSONet score that yield more optimal results in terms of danger score.

Key-words: space debris, space sustainability, ADR target selection, network theory.

Abstract in italiano

Questo lavoro si concentra sul problema della congestione delle orbite terrestri proponendo un nuovo metodo per analizzarle e un nuovo approccio per selezionare strategie di rimozione dei detriti.

Lo strumento sviluppato applica la teoria delle reti agli Oggetti Spaziali Residenti (RSO), cioè gli oggetti orbitanti la Terra, per analizzare le loro interazioni posizionali. In particolare, gli RSO rappresentano i nodi di una rete, mentre i collegamenti tra nodi sono stabiliti ogni volta che una congiunzione è prevista, in un periodo specifico. La rete ottenuta, chiamata RSONet (Resident Space Object Network), viene utilizzata come guida per definire nuove metriche chiamate punteggi RSONet. Questi punteggi combinano, per ogni RSO, la probabilità di collisioni dirette con altri RSO e collisioni con detriti generati da altri oggetti.

In questo quadro di riferimento, la popolazione spaziale è analizzata attraverso la connettività di rete e una nuova metrica, chiamata "punteggio di pericolo", che unisce caratteristiche legate alla rete e fattori di severità collisionale, come la massa dell'oggetto, la probabilità di collisione, ecc. Più precisamente, il principale contributo di questo lavoro è, utilizzando RSONet, affrontare l'influenza di RSO specifici sul resto della popolazione dopo la loro rimozione quantificando il cambiamento delle metriche menzionate. Utilizzando questa metodologia, due scenari sono analizzati per valutare l'influenza globale dei detriti spaziali e delle mega-costellazioni sul resto della popolazione RSO.

Inoltre, vengono seguiti due approcci complementari per selezionare i candidati per le missioni di rimozione dei detriti. Il primo si basa su misure di centralità della rete (grado, betweenness, vicinanza), mentre il secondo si basa su misure ponderate (probabilità di collisione, forza, punteggi RSONet).

Sulla base di queste strategie, un insieme di nodi da rimuovere dal RSONet sono ottenuti. I cambiamenti nella connettività del RSONet e il punteggio di pericolo per valutare l'efficacia di ogni strategia vengono così analizzati.

I risultati sottolineano che la strategia ottimale per indebolire la connettività della rete comporta la rimozione di oggetti con il massimo grado. Tuttavia, l'analisi identifica anche strategie alternative basate su un punteggio RSONet che danno risultati più ottimali in termini di punteggio di pericolo.

Parole chiave: detriti spaziali, sostenibilità spaziale, selezione target per ADR, teoria delle reti

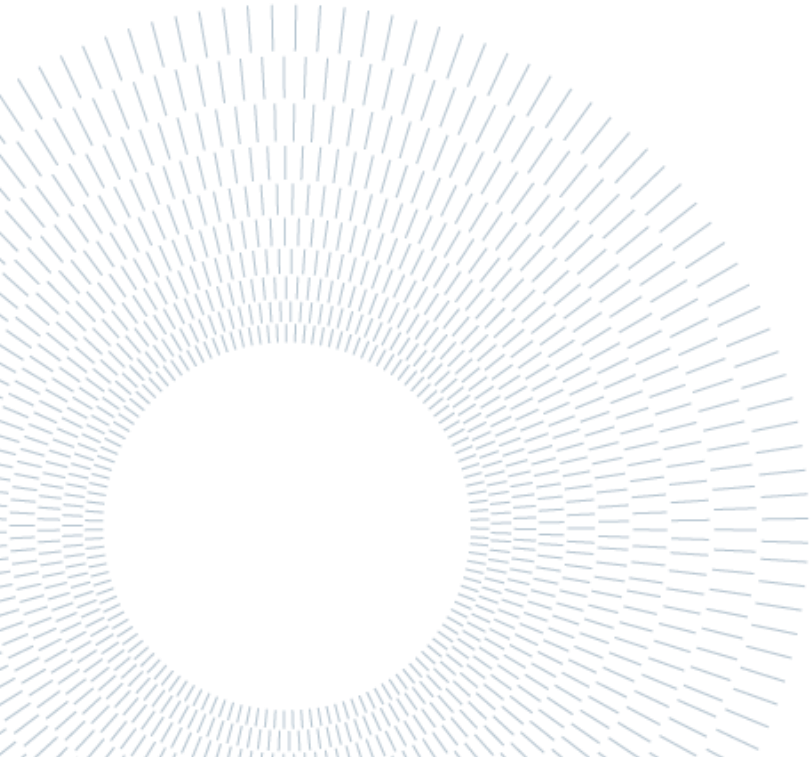

Contents

Introduction

The thesis focuses on the current concern of near-Earth space sustainability, which nowadays is gathering the attention of the worldwide space community. Specifically, in this work, a newly developed method to analyse the near-Earth space object population is described. Moreover, new improvements and extensions in the aforementioned method have been made during the completion of this work. The proposed technique is based on complex systems, aiming to a radical distinct perspective of the problem. While most current prediction methods study the individual break-up events between objects, this framework focuses on an overall look at the whole Earth population of orbiting objects. The latter can be represented through networks, which are defined by vertices (i.e., nodes) and edges (i.e., links). In this context, conjunction events are expressed as links between nodes, while nodes correspond to orbiting space objects. Within this framework, the network can be defined as "Resident Space Objects Network" (RSONet). Furthermore, weighted measures, such as the probability of collisions among linked objects, can be used as weighting factors for the edges, leading to weighted networks. Other measures are introduced to weight object's influence onto other members of the population: these measures are called RSONet scores. In conclusion, the danger score, completely developed for this work, is presented as a measure of evaluation.

The presented approach could prove to be a useful and systematic instrument not only for prediction purposes, but also for mission design. The thesis focuses on assessing the effects of different events, such as removing targeted debris or operative satellites, on the rest of the space population, analysing the variation of network representation, metrics, and danger score. Furthermore, sensitivity analysis addressing the effect of new insertions in orbit onto the rest of orbiting objects, can be a turning point in the design phase of a space mission, in future developments.

Since removal of targeted debris is nowadays gathering the attention of stakeholders involved into clean space activities, the presented methodology represents a straightforward way for selecting target for that kind of activities. Besides the statistics directly connected to the network, the effects of the removals of different objects from the population are investigated in terms of the danger metric. In addition, further removal scenarios are examined: firstly, the influence of space debris is studied within the network framework, by idealistically removing all debris from the current population; similarly, the role of mega constellations, such as SpaceX Starlink and

Eutelsat OneWeb, are evaluated from the complex system's perspective, exploiting this powerful tool.

The rest of the introduction is structured as follows:

1. Brief history of the Earth space population and its main sources are introduced.
2. The space debris problem, together with a summary of possible solutions, are discussed.
3. The Resident Space Object Network (RSONet) methodology, the main concept behind this thesis, is briefly introduced.
4. The precise goals of the thesis, and its structure, are described.

Background of space objects orbiting the Earth

The definition of *space debris* commonly accepted is delineated in the Space Debris Mitigation Guidelines, the backbone paper issued in 2002 by the Inter-Agency Space Debris Coordination Committee (IADC). Accordingly, "Space Debris are all non-functional, artificial objects, including fragments and elements thereof, in Earth orbit or re-entering into Earth's atmosphere" [1]. Hence, space debris include derelict spacecrafts, rocket bodies, payloads and all the fragments related to them. The family of space debris together with operational satellites orbiting the Earth, can be named as Resident Space Objects (RSOs). Since the 4th of October 1957, when the first satellite, Sputnik 1, successfully reached an elliptical low Earth orbit, space debris have grown continuously along with operational satellites, congesting the terrestrial orbit. In this instance, the core stage of the rocket body to launch the Sputnik 1, as a part of the Soviet Space Program, ended its life re-entering the atmosphere after only 2 months. Then, the payload did the same after 1 month, on the 4th of January 1958 [2]. However, this mission was considered a success throughout the Space Race. Meanwhile, the United States of America prepared their response: following the first launch of Explorer 1, a deserved mention of the Vanguard 1 is required. The latter, launched on the 17th of March 1958, is still orbiting the Earth in Medium Earth Orbit (MEO), after more than 65 years. The same goes for Vanguard 2 and 3, and the rocket bodies that have been used to launch them. At the current date, Vanguard 1 is the longest-lasting debris in space history. Since the first successful mission in 1957, US Air Force keeps note of orbiting objects, cataloguing them in the Satellite Catalog (SATCAT). They are identified by two unique distinct codes: the International Designation and the NORAD Catalog Number. The first one is made of 3 parts: the year of launch, the launch of that year (from 000 to 999) and the piece of that launch (from A through ZZZ). The second identifier indicates the sequence in which space objects have been added to the SATCAT. For instance, the Sputnik Launcher (SL-1) is identified as 1957-001A 1 while its payload as 1957-001B 2 [3]. In June 1961, the first critical break-up event occurred: the US Transit-4A was launched on a Thor-Ablestar rocket. 77 minutes after the injection and separation of the payload, the upper stage of the rocket body exploded,

producing more than 298 trackable fragments in orbit [4]. In October 1968, the first known Anti-SATellite (ASAT) test was conducted, using the commanded explosion of the Soviet Cosmos-249 to destroy its predecessor, Cosmos-248. At least 110 trackable objects were generated [5]. Afterwards, many other American and Soviet ASAT tests are considered to be the main cause of space debris from the 70s. Between 1975 and 1981, it is estimated that 9 Delta second stages naturally exploded, increasing by 27% the number of objects in Low Earth Orbit (LEO). The explosions were due to a manufacturing fault. Remedial actions were taken by the stage manufacturer, solving the issue. This can be considered as one of the first space debris mitigation measures adopted in space history. In July 1981, the American Institute of Aeronautics and Astronautics (AIAA) Technical Committee on Space Systems published the first major position paper on the orbital debris issue, in which the probability of collision between space objects would eventually reach unacceptable level in the next decade. The paper expressed the need of urgent actions against the problem. Moreover, it called for national and international space regulations as well as operational and design procedures to mitigate the eventual collision with space debris. Between 1978 and 1990, the astrophysicist Donal J. Kessler had elaborated a theory including a critical scenario, called *Kessler syndrome*. In order to ensure safety and sustainability, space cannot overcome a certain capacity limit, in terms of mass in orbit. Otherwise, if the limit were reached, the instability of space population would lead to an irreversible and exponential increment of space debris. The so-called *domino effect* would bring the number of objects orbiting Earth over the threshold for which space cannot be considered safe and practicable. This would be a rapid process while affecting space activity for several generations. Nowadays, considering a *business-as-usual* scenario, or even with no launches, the space debris population is expected to grow for many decades. This is due to the predicted collisions between space objects. By the 1970s, near-Earth space presented the possibility of accommodating humans for longer periods of time than a simple space travel. Firstly, the Soviet Salyut and American Skylab were launched, then the Mir and ISS. Those missions required designing precautions regarding the presence of debris: passive and active systems were consistently implemented through the years to protect the spaceships and their crews. The first accidental collision recorded between an operational satellite and a debris happened on July 24th 1996, when CERISE satellite collided with a debris of an Ariane V16 upper stage. Both of them were catalogued before the accident. The collision produced one fragment and the CERISE satellite remained operational with degraded performance.

The first significative step towards a sustainable space was made in the mid-October 2002, when the Inter-Agency Space Debris Coordination Committee (IADC) published its space debris mitigation guidelines. The document provides recommendations and best practices for preventing the creation of new space debris and minimizing the growth of existing debris. In 2007, the 63 member nations of the UNCOPUOS Scientific

& Technical Subcommittee (STSC) approved the IADC guidelines as voluntary high-level mitigation measures. As shown in Figure 1, the most critical turning point event, occurred in the early 2007, when China deliberately destroyed the weather satellite FengYun-1C (FY-1C), conducting an anti-satellite missile test. At an altitude of 865 km, a kinetic kill vehicle impacted with a relative velocity of 8 km/s the satellite. More than 3500 debris scattered in LEO. In 2015, NASA predicted that by the end of 2035, still the 25% of fragments larger than 10 cm would be in orbit [6]. Even though the latter percentage depends on solar activity, the number of orbiting debris from FY-1C will be still considerable.

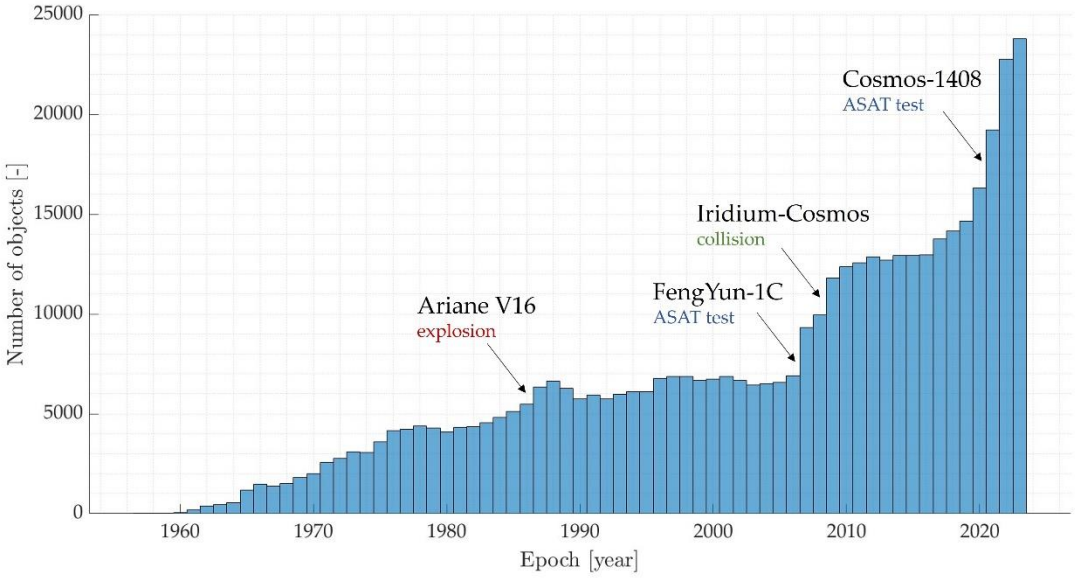

Figure 1: Number of resident space objects in LEO from 1957 to 2023. Most critical debris generator events are highlighted. Initial data from Space-Track.org

The first in-orbit collision between two satellites occurred the 10th of February 2009, between a privately owned American satellite, Iridium-33, and a Russian military satellite, Cosmos 2251. The accidental strike spread up more than 2300 trackable fragments, some of them still in orbit.

The miniaturisation and privatisation of the space industry, on the one hand, has brought huge technology improvements. On the other hand, a concern about space sustainability has arisen on the international level. The number of launched payloads has been increasing yearly, but the crucial break-up point came with the deployment of constellations of satellites. As illustrated in Figure 1, the recent slope increase corresponds to 2019, when Starlink and OneWeb began their operativity. As can be seen from Figure 2, at the current date, more than 5 thousand Starlink satellites and more than 6 hundred OneWeb satellites are spread in several low orbits. Eulsat, SpaceX, Amazon are some of the many private companies which have deployed their mega-constellations or have intent to do so in the near future. Their influence cannot be neglected when analysing conjunction events, since their presence increase

effectively the collision rate in LEO [7]. It is expected, for the next decade, that more than 100 thousand satellites will be launched, counting exclusively constellation satellites [8].

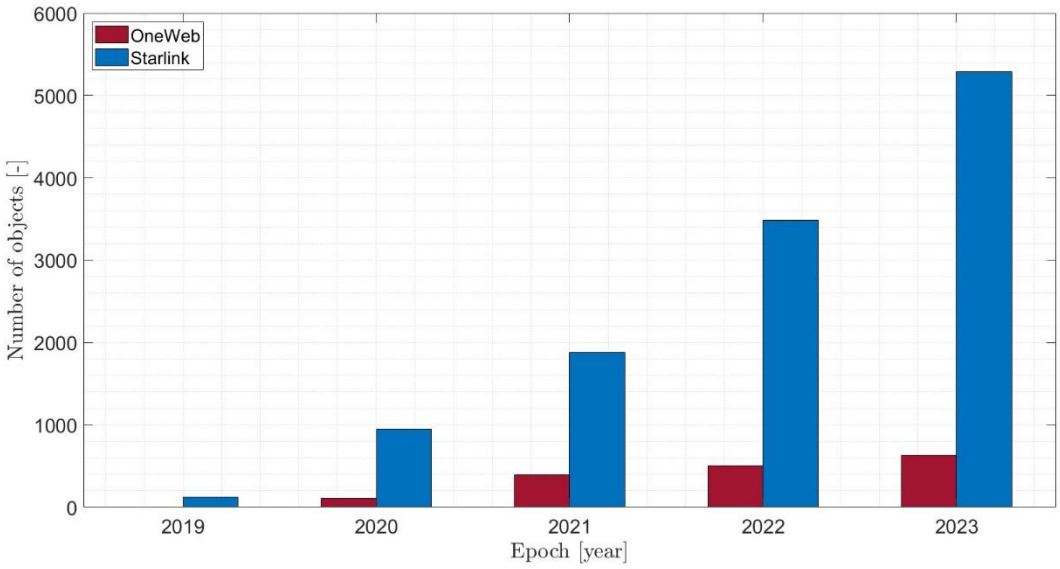

Figure 2: Starlink and OneWeb satellites presence in orbit over time. Initial data from Space-Track.org.

One of the last concerning break-up events happened in November 2021, when the Soviet Cosmos 1408 was destroyed by a ground-based Russian interceptor ASAT system. The mission produced at least 1500 trackable objects [9].

Nowadays, more than a hundred million of RSOs are estimated to orbit the Earth, including also objects smaller than 10 cm. The United States Space Surveillance Network (SSN) constantly tracks and monitors only about 0.03% of the whole estimated population of RSOs, regarding 5-10 cm and larger objects. The tracking data of the latter portion, counting about 35 thousand space debris and active satellites [10], is publicly available online through the Satellite Catalog and updated continuously by the United States Space Command (USSPACECOM).

There are mainly two types of in-orbit fragmentations, either explosions or collisions. The first ones are considered the major cause for break-up events, as, of more than 560 recorded in-orbit fragmentations, only 7 were collisions [11]. Nevertheless, it is predicted that, in few decades, collisions will become the first source of fragmentations [12]. Here, the importance of predict and analyse conjunction events, which may escalate into collisions. Depending on the relative velocity and mass of the objects, the collision between them can be considered catastrophic or not [13]. If the collision includes an operative satellite, a catastrophic collision will lead to the complete loss of it. Therefore, on the one hand, it is fundamental to take care of monitoring the status of the terrestrial orbits. On the other hand, the monitoring is clearly not enough to end

the issue of space debris. A proper and absolute action, including prediction, prevention, mitigation, and elimination approaches, may be the key solution.

The space debris problem and its possible solutions

In recent years, the uncontrolled space objects orbiting Earth have been a concern for the key space stakeholders on international level. The space community is acting against the current negative trend to avoid the total collapse of the usability of space. Nowadays, different debris mitigation standards are adopted and supported by international space agencies. Nevertheless, their worldwide implementation and obligatoriness is still pending, highlighting a still low-level of care. The monitoring and control of the RSOs is crucial for a sustainable space. In the last decades, the principal space companies and institutions have moved steps forward towards a liveable and durable space, elaborating several possible solutions. As reported in the Figure 3, the various approaches can be grouped in three main families:

- Short-term approaches: including prevention, mitigation, and elimination approaches.
- Long-term approaches: including dynamical approaches.
- Prediction using analytical or statistical methods.

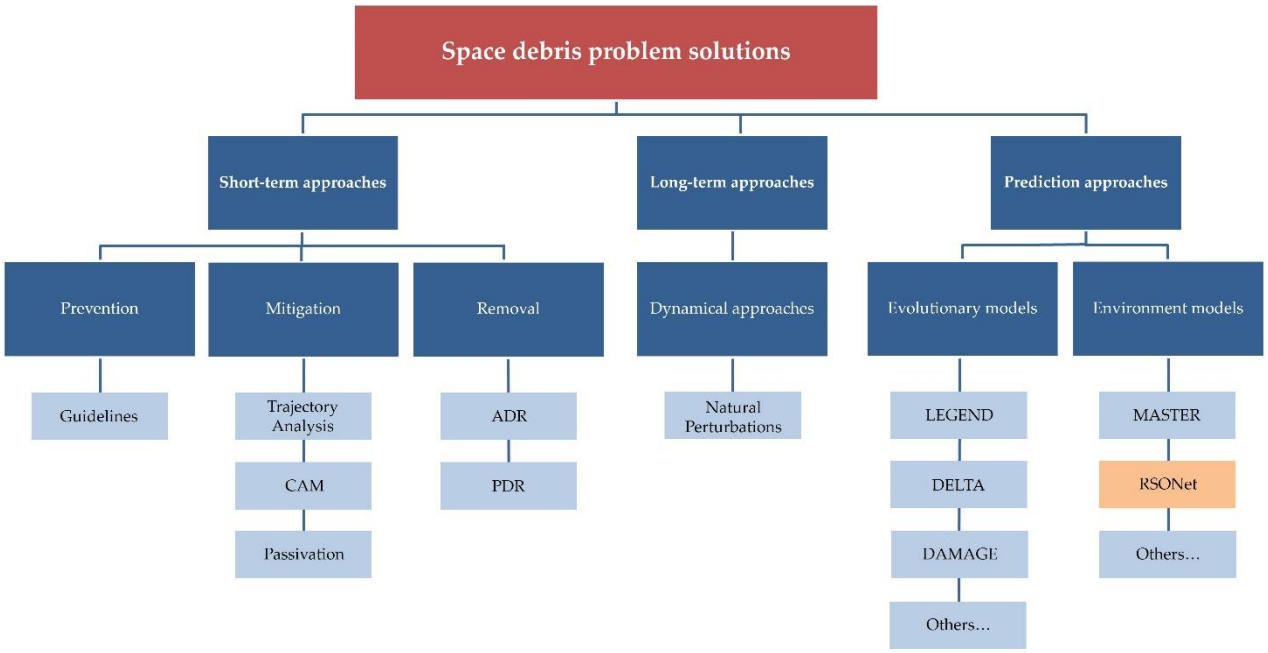

Figure 3: Scheme of possible solutions to debris proliferation.

Prevention strategies are related to the formulation of guidelines and regulations. Many international stakeholders, including global organisations and private companies, are adopting or publishing guidelines for their purposes. Space Debris Mitigation Recommendations by the World Economic Forum [14], Space Debris

Mitigation Requirements by ESA [15], ISO24113:2023 by International Organization for Standardization [16] and the Space Mitigation Guidelines by the Inter-Agency Space Debris Coordination Committee, are only some of principal documents drafted.

Mitigation approaches regard active actions that may be taken during the lifetime of missions, from launch to end-of-life phase. Trajectory analysis, collision avoidance manoeuvres (CAM), and passivation are strategies that, if employed correctly, mitigate the formation of space debris [17].

Removal strategies aim to eliminate targeted debris and group active and passive techniques. Active debris removal (ADR) activities include special satellites capable of interact with targeted debris, to reduce their remaining orbital lifetime [18]. Passive debris removal (PDR) activities have the same scope of ADR, but typically they interact passively with targets, by reducing their kinetic energy [19]. This work highlights a way to narrow down the selection of targets, according to the network embedding and its statistics, and also according to the developed danger metric.

Dynamical approaches regard the exploitation of natural perturbations such as atmospheric drag [20], solar radiation pressure [21], or perturbation resonances [22] to cause an atmospheric re-entry, or insertion into graveyard orbits.

Evolutionary and environment models group sets of different algorithms, techniques and tools to analyse the evolution of the space population in time, in terms of number of objects and break-up events. Particularly, evolutionary models simulate historical and future space object populations, while environment models describe current space populations. LEGEND [23], DELTA [24], DAMAGE [25], SDM [26], GEODEEM and LEODEEM [27], LUCA2 [28], and MEDEE [29] are some examples of evolutionary models, while MASTER [30] and ORDEM 2000 [31] are environment ones. The network application for prediction and conjunction screening can be included in the prevention family. Accordingly, contributions to network exploitation for the analysis of space populations are reported hereafter.

Lewis et al. in 2008 firstly highlighted the possibility of application of the network theory to the space field. Specifically, the authors described two case studies with two types of networks, respectively: unweighted uni-relational networks to represent conjunctions and multi-relational ones to represent the heritage of objects. Here, the DAMAGE tool based on Monte Carlo approach was used to provide a simulation of the historical and future LEO to GEO debris population. The statistic properties of the embedded network highlight the vulnerability to the targeted nodes removal, opening an additional way to the ADR target selection [32].

Newland et al. in 2009 introduced a weighted network based on the object's mass and its probability of collision. Weighting factors (and their combination) can be chosen as driving parameter for assessing targeted ADR. The DAMAGE tool was used to predict the objects' LEO to GEO population for more than 20 years [33].

Newland in 2012 proposed a PhD thesis project in which another tool was used alongside DAMAGE: SOCRATES, for short propagation of conjunction events. It is based on SGP4 propagator and STK/CAT conjunction detector, with short periods of propagation. After the conjunction detection, the robustness of the network was evaluated by removing objects according to centrality measures, namely a certain number of objects with highest degree, highest betweenness, and lowest closeness. Results highlight that the best strategy, in terms of network robustness is highest degree-based removal approach. Moreover, other strategies based on weighted measures including strength, mass, probability of collision, and their combinations, are analysed [34].

Acciarini and Vasile in 2020 applied multi-layers dynamic networks to space population. Specifically, they considered two layers: a physical layer and an information one. The physical layer keeps the link between objects capturing their distance (to model their chance of collision) while the information layer tracks the flow of information among them. In this framework, the authors modelled the propagation of disruptive events using stochastic epidemic model [35].

Acciarini and Vasile in 2021 went a step further focusing on the first layer, the physical one. They proposed a versatile dynamical network able to assess interactions among RSOs: the model includes source and sink patterns to evolve the given population of objects for extended periods [36].

Stevenson et al. in 2022 presented a novel method to detect conjunctions. It is based on the graph neural network theory, applied to RSOs. After the detection of possible close encounters (through a simple apogee-perigee filter), the previous graph becomes an input for a pruning process, in order to have an output graph with predicted conjunction events. The method's power consists of training and overfitting the graph neural network for study and control the space traffic, through machine learning [37].

Stevenson et al. in 2023 evaluated different input data representations and model architectures in the deep learning framework. The work proposes a benchmark of several deep learning techniques in aiding RSOs conjunction screening [38].

Wang et al. in 2023 proposed a multi-layer temporal network applied to space objects. Relationships regard physical collisions or cyberattacks. The dynamics of nodes is depicted by source and sink phenomena, described by mathematical equations [39].

In the next section, the focus is on the central object of this thesis, i.e., the Resident Space Object Network.

RSONet robustness and danger assessment

This work is based on the extension and improvement of the work from Romano et al., who proposed in 2022 a novel method to analyse the past, the current and short-term future population of RSOs [40]. The latter can be mapped as a network, whose nodes represent the space objects while links represent the conjunction events. If two objects are likely to collide, the link is established, and it can be weighted with the probability of such event. Moreover, other metrics besides the probability of collision are used to obtain weighted networks. One example is the *conservative* probability of collision, namely one of the RSONet scores in this work, expressed for each object, defined through the combination of 3 different contributions: the first one estimates the direct probability of collision with neighbours of the object, that are set of nodes connected to one; the second contribution addresses the probability of collisions between the neighbours of that object; the third contribution introduces the probability of collision between the object and debris created by a cascade starting outside the neighbourhood of the object. The conservativeness lies in the assumption, that the conjunctions are considered to happen with no dependence on time. The conservative probability is computed for every node in the network embedding and it can be used as parameter to select objects to be removed from the network, assessing the network robustness. Specifically, removing a certain number of objects from the network, with the highest previous score, is one removal strategy analysed of the several adopted in the thesis. Other removal strategies rely on focusing on other metrics, such as the network centrality measures, the strength, the probability of collision, etc. Moreover, also the danger score, which depends on the conservative probability of collision and the mass of each object, is evaluated after the application of removal strategies.

In summary, the evaluation of the different scenarios and strategies have been made through the analysis of the variation of network representations, measures, and danger metric, which represents the novelty compared to the works by Romano et al.

As explained in the Appendix A, the robustness of RSO networks is related to their vulnerability to the removals of nodes. In this work, space network vulnerability to strategical targeted objects removal compared to random one is investigated. The stability of RSO population is clearly affected by the generation of conjunctions, which may cause cascade of events. Mega-constellations are also main actors for the population's instability, due to their high contribution in terms of objects. In the next chapters, the processes to construct the network, RSONet and danger scores, together with strategies and scenarios selected, are explained, in detail.

Goals of the thesis

The aim of the thesis is the proposal of an extension and improvement of a method based on complex systems, in order to analyse the effects of specific events such as the

removal of crucial satellites in specific orbits, and the influence of debris and mega constellations on the rest of the population of RSOs. In particular, many removal strategies based on different measures are proposed, to assess the influence on network statistics and on the danger metric. Here, the goal is to find the best strategy that may represents a straightforward way to select target for ADR or PDR activities. Moreover, the impact of mega-constellations and debris on the rest of population, is assessed by removing their presences and by evaluating the network measures, to quantify their influences. Lastly, by using the developed danger metric, the aim is to give an effective score of collisional danger, and to have a diverse yardstick for strategy evaluations.

Thesis structure

In Chapter 1, the construction of RSONet is reviewed in depth. In Chapter 2, the RSONet scores and the danger score are presented. In Chapter 3, the previously introduced process is applied to a recent population environment, namely the one of May 2023. In Chapter 4, both the aforementioned scenarios are reported: firstly, the influence of debris is assessed by their removal and by the consequences onto the network embedding; secondly, the role of mega-constellations, such as Starlink and OneWeb, is highlighted with the same previous approach. Afterwards, all the removal strategies, based on different approaches, are presented, focusing on their implications and their quantitative influence on the population's vulnerability, in terms of robustness and danger score. Finally, the conclusion summarises results and discusses potential future improvements and research directions.

1 RSONet building process

The subsequent chapter comprehensively outlines the procedural scheme governing the construction process of the RSONet. The Figure 1.1a elucidates the methodology to generate the network embedding, including representations, related measures, and the scores. Representations consist of network visualisations, highlighting:

- Object type: various types of nodes are distinguished by shapes and colours, assigned to different categories of space objects: debris, operational payload, non-functional payload, rocket body, unknown [41]. The classification adheres to the categorization outlined in the SANA Registry of Object Types [42], accepted by the 18th Space Defense Squadron (18 SDS), the responsible for tracking Earth orbiting objects. Particularly, the differentiation between operative and non-operative satellites is established based on data published on Celestrack.org, one of the web-based services publishing space situational awareness data. The detailed classification extends beyond the scope of this thesis; thus, a simplified version is employed herein. CelesTrack defines various status: operational, partially operational, in backup or standby, spare (waiting for activation), extended mission, decayed, non-operational, and unknown. Non-operational satellites can group the previous three categories, while any satellite not falling within these types, is considered operational [43].
- Orbit type: including LEO, MEO, Geostationary Orbit (GEO), Highly Elliptical Orbit (HEO). The definitions of the types of orbits are presented in Table 1.1, wherein the classification adhere to the official one provided by Space-Track, another frequently utilised website that grants access to US space tracking data [44].
- Network centrality measures (degree, betweenness, clustering, closeness): each node in the network can be weighted for each centrality measures. Consequently, these representations illustrate nodes with varying colours and sizes based on their respective numerical values for each measure. The detailed interpretations of these measures are elucidated in the Appendix A.
- Weighted measures: similarly to the previous category, weighted measures can weight each node. Within this group, these measures pertain to characteristics directly related to the individual node, such as its mass, probability of collision, object type classification, and other parameters outside the network environment. On the contrary, degree, betweenness, clustering, and closeness

do not take into account any specific information related to individual nodes, while they depend only on the network structure and topology. Weighted measures include the network strength, the RSONet scores, and the probability of collision. Specifically, the latter is employed to assign weights to links, leading to the so-called *weighted networks*, a topic widely discussed in network literature.

Table 1.1: Types of orbits: Space-Track definitions.

	Eccentricity e [-]	**Orbital Period T_O [min]**	**Mean Motion u [rev/day]**
LEO	< 0.25	T_O> 128	u > 11.25
MEO	< 0.25	$600 \leq T_O \leq 800$	$1.8 \leq u \leq 2.4$
GEO	< 0.01	$1425.75 \leq T_O \leq 1454.54$	$0.99 \leq u \leq 1.01$
HEO	> 0.25	-	-

The measures (i.e., metrics or statistics) and the scores include:

- Network general measures: order, size, and connectivity.
- Network centrality measures: degree, betweenness, clustering and closeness, defined for each node and on average over the whole network. Detailed formulas are reported later in this chapter.
- Weighted measures: probability of collision (PoC) defined for each link and on average and strength, RSONet scores, danger score reported per each node and on average. Detailed formulas are reported hereafter in this chapter and in the next one.

Furthermore, ranking lists for each measure are provided, which are utilised in the subsequent developments of this project.

The building process for the RSONet is divided in two sections: processing and post-processing part. As depicted in Figure 1.1b, the first section has been developed using *Fortran* and *Python*, whereas the post-processing has been realized within *MATLAB* environment (see Appendix B for the detailed scheme of the post-processing section). *Fortran* is a compiled programming language with built-in functions for numerical calculations. Specifically, for the thesis purposes, *Fortran* has been utilised for the orbital determination of each RSO and the conjunction detection process. *Python* is a common programming language, in this work employed for data extraction from online databases and for selecting code settings. The starting point of the RSONet building process coincides with the selection of initial population, namely the chosen RSOs which will be elaborated through the developed tool. The end goal of the processing section is the creation of a list of conjunction events, which clearly depends on the initial selected RSOs. Lastly, *MATLAB* is a software with built-in functions and tools, useful for numerical and technical computing. The post-processing part entails

generating the network embedding (i.e., network visualizations, measures, scores) of the selected population. For the elaboration of this thesis, mainly the post-processing part has been improved and extended. Indeed, the processing part (on *Fortran, Python*) has been considered as a black box: only initial data and input parameters have been set to have desirable outputs. The logic behind both code parts is thoroughly explained in the following sections.

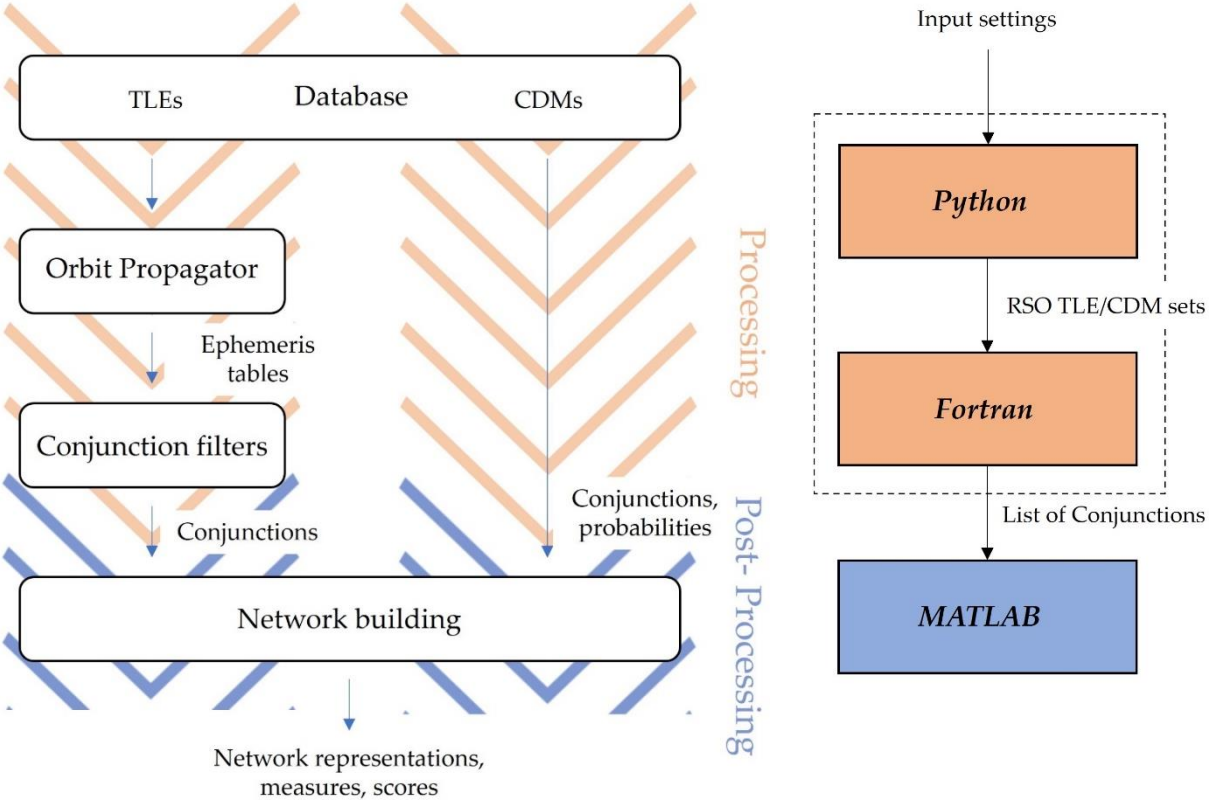

(a) Procedural scheme (b) Environments

Figure 1.1: Scheme of the process to build RSONet.

At the current date, the initial data utilised for this project are publicly accessible online. The processing code is able to extract and elaborate two different formats of data: Two Line Elements (TLE) and Conjunction Data Messages (CDM). On the one side, TLE format provides standardized data on a space object in the form of averaged orbital parameters and additional information, all at a specific time instant. Downloading the most recent TLE available, the aforementioned time instant aligns with the latest tracking of the related object, if available. On the other side, CDM format already contains information regarding predicted conjunction events which can be directly processed in *MATLAB* for the completion of the RSONet. In the next section, TLE and CDM formats are further described.

Since TLE sets have to be propagated over time, to be compared for conjunction detection, CDM and TLE format follow two different paths in the scheme for constructing the RSONet: selecting initial data in terms of TLE sets, a brief description of the adopted orbital propagation method is given. Afterwards, a list of position and

velocity vectors over time is created (called *ephemeris tables*), for each RSO in the population. Subsequently, conjunction events are detected by comparing each computed ephemeris table. The computational effort needed for the previous calculation is quite huge, therefore, filters to cut down the numbers of operations have been implemented, further explained in the following section. The processing phase ends with a list of conjunction events, accompanied by their main information. On the contrary, CDM sets directly feed the post-processing section.

Finally, the list of conjunctions permits the computation of the whole network embedding, including graphical representations, network centrality measures, and weighted measures.

In the following sections, the workflow from data selection up to computation of weighted measures is thoroughly described.

1.1. Initial data

As previously explained, the method englobes two distinct types of initial data: TLEs and CDMs. Both TLE sets and CDMs are publicly available online. For this work, *Space-Track*, *CelesTrak* [45], and *DISCOSweb* [46] have been selected to retrieve initial data. Space-Track is utilised to obtain sets of TLE and CDM. CelesTrack publishes the current status of tracked payloads, categorizing them in different levels of operational status. For the thesis purposes, the subdivision has been simplified to obtain just operational and non-operational satellites classification, following CelesTrack's guidelines. Lastly, DISCOSweb also provides information on masses of certain objects currently orbiting the Earth. Mass data are useful to compute the danger score. The three databases have been merged, in the post-processing part and, typically, they are updated three times per day, approximately every 8 hours [47]. Table 1.2 summarises the data extracted from selected online databases.

Table 1.2: Database and retrieved information.

	Retrieved data
Space-Track	Complete TLE, CDM sets
Celestrack	Status (operational, non-operational)
DISCOSweb	Mass

For this work, initial data coincide with the RSO population of the 1st of May 2023 (8:00 AM).

A TLE is a series of characters (numbers and letters) associated to each tracked RSO, individually indicating the object concerned. It is a list of orbital parameters averaged according the SGP4 theory and other data at a specific time instant. For that reason, TLE are then propagated to compute the states (i.e., position and velocity vectors) for

the period of interest (e.g., 30 days), through a pre-built orbital propagator. An example of one TLE is in Figure 1.2:

```
1 42000U 17008BE  24044.92386936  .00089662  00000-0  12183-2 0  9990
2 42000  97.1625 104.0960 0003639 222.8407 137.2565 15.57298373389306
```

Figure 1.2: TLE of the nano-satellite DIDO 2 (downloaded the 14th, February 2024, 3:00 PM).

For the way they are built, TLEs need to be propagated with a dedicated orbital propagator, such as SGP4.

A Conjunction Data Message is a file of data regarding a single conjunction between two objects. It contains the IDs of the objects, the Time of Close Approach (TCA), the minimum distance between the objects at TCA, the probability of collision, and other information. At the current date, Space-Track publicly makes available CDM sets for a restricted timeframe: it provides CDMs over the 3 days following the date of creation, which remain available for 30 days. It does not permit to select parameter such as the threshold for distance detection of conjunctions, fixed at 1 km. This means that distances of conjunction events predicted to be greater than 1 km are not reported. An example of CDM for one conjunction is in Figure 1.3:


```
{"CDM_ID":"629291692",  "CREATED":"2023-12-22  10:21:41.000000",
"EMERGENCY_REPORTABLE":"Y",  "TCA":"2023-12-22T19:59:33.045000",
"MIN_RNG":"237",     "PC":"0.0001329665",     "SAT_1_ID":"7274",
"SAT_1_NAME":"METEOR     1-17",     "SAT1_OBJECT_TYPE":"PAYLOAD",
"SAT1_RCS":"LARGE", "SAT_1_EXCL_VOL":"5.00", "SAT_2_ID":"37048",
"SAT_2_NAME":"FENGYUN   1C   DEB",   "SAT2_OBJECT_TYPE":"DEBRIS",
"SAT2_RCS":"SMALL", "SAT_2_EXCL_VOL":"1.00"}
```


Figure 1.3: CDM of conjunction between the payload METEOR 1-17 and a debris of the FengYun-1C satellite.

Since TLEs do not contain any information on conjunction events, after the orbital propagation, they need to be compared one with each other to obtain the list of conjunction events. Afterwards, the latter must be supplied with the probability of collision for each item in the list, to have all the complete inputs to build the RSONet embedding.

1.2. TLE sets Propagation

The final goal of the orbital propagation phase is to obtain position and velocity states of each object in the selected population over time, provided by each TLE set. Since TLE data are defined as mean values obtained by the removal of periodic variations associated to space perturbations, they must be re-elaborated to add again those periodic perturbations, in order to have accurate orbital states prediction. The propagation method utilised in the current work is the one employed in SGP4 tool, compatible with TLE format. SGP4 is an orbital propagator, developed by Ken

Cranford in 1970 and suitable for near-Earth orbital objects (period less than 225 minutes) [48].

The mentioned tool is implemented in *Fortran*, enabling to compute a table of position and velocity vectors over time (ephemeris table) for each object. Ephemeris tables are defined in the True Equator Mean Equinox (TEME) coordinate system [49]. The time of propagation (i.e., the time in which the conjunction detection is performed) is settable by the user, together with the time step. The computational effort depends on both parameters, increasing for longer periods of propagation and smaller time steps. For this work, 30 days of propagation and 1 minute of time step have been set.

SGP4, and especially the TLE format, can be considered accurate for only few days of propagation time: unaccounted perturbations and un-modelled forces result into limited precision [50]. However, the conclusion of the work applies despite the precision of the orbital propagator.

1.3. Conjunctions detection process and filtering

The detection of conjunction events starts right after the computation of every ephemeris tables. Each ephemeris table must be compared with others, to find close position state vectors in similar time instants. The number of computations to perform this detection is:

$$n \times (n-1) \times t \tag{1.1}$$

where n is the number of objects while $t = T/t_s$ is the number of time instants, given by the propagation time T [s] and the time step t_s [s]. Since typically the number of objects n is relatively high (at current date, tracked and published RSOs are more than 35 thousand) and accuracy is preferred (small time step), a method to decrease the number of comparisons is needed. With a time step of 60 s (1 minute) and a propagation time of 2592000 s (30 days), considering 35000 objects, the number of computations is more than 50 thousand of billions. The method to reduce the number of computations exploits geometrical criteria to filter out pairs of objects that cannot perform conjunctions. Essentially, before comparing ephemeris tables of two objects, filters allow us to exclude objects that cannot interact, either because their orbits do not intersect or because the minimum distance between their orbits exceeds the selected distance threshold. In this work, a three-filters approach, and a threshold of minimum distance of 3 km are used.

Filters are consecutive, therefore only pairs of objects which go through all of them are not discarded.

1.3.1. Literature Review of Conjunctions Filters

Hereafter, a brief review of the main papers to elaborate the adopted filter method is presented.

Hoots et al. in 1984 proposed a filter sequence to calculate the times of future close approaches between two objects. The first described filter is a simple perigee-apogee test: if the difference between the larger of the two perigees and the smaller of the two apogees is above a given threshold, the pair can be discarded. Otherwise, the second filter activates. It is considering the relative geometry of the two ellipses. Specifically, it is computing the minimum distance in space between the two paths: if it is below a certain amount, the pair can continue the filtering process. Lastly, the final filter includes the time constraint, for which two satellites must also simultaneously pass through regions of closeness, in order to have a close approach [51].

Casanova et al. in 2014 proposed some improvements: using similar algorithms, they have changed the first and second filters proposed by Hoots, speeding up the process [52].

1.3.2. Adopted method

The adopted strategy is based on the three-filter sequence proposed by Casanova. The same method is implemented in PUZZLE software [53].

As it is showed in Figure 1.4, it consists of three steps:

1. Computing whether the orbits can cross via the apogee-perigee distance.
2. Computing the Minimum Orbital Intersection Distance (MOID) between the closest points of the two orbits.
3. Comparing cartesian coordinates of the objects.

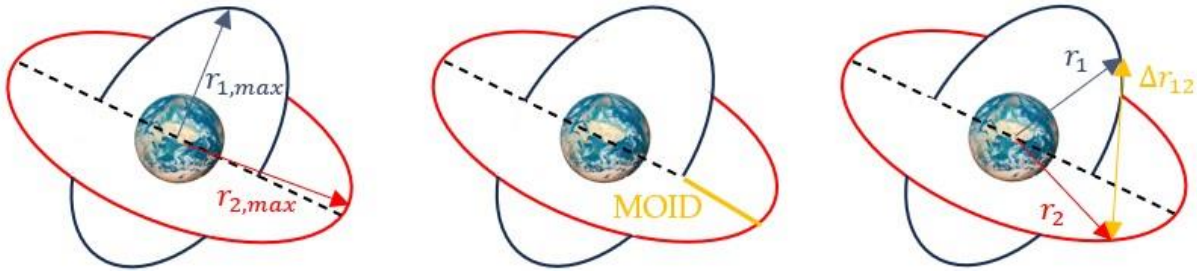

Figure 1.4: Three-filters approach.

Specifically, the first filter is comparing the minimum and maximum geocentric distances of the two orbits in order to define the possibility of orbital crossing. Given the two orbits of two objects 1 and 2, it can be defined:

$$a = max(r_{1,min}, r_{2,min}) \tag{1.2}$$

$$b = min(r_{1,max}, r_{2,max}) \tag{1.3}$$

Where $r_{1,min}$ and $r_{2,min}$ are the minimum geocentric distances reached by the two orbits, while $r_{1,max}$ and $r_{2,max}$ are the maximum ones.

If $|a - b| < d$ is satisfied, the two orbits can cross, therefore the pair passes to the second filter. Note that d is the distance threshold to cut out orbits, in this case fixed to 3 km.

The second filter is based on the computation of the Minimum Orbital Intersection Distance (MOID), namely the minimum value of the function representing the distance between each pair of points in two orbits:

$$MOID = min(d_k) \tag{1.4}$$

$$d_k = \left|\overline{X}_1 - \overline{X}_2\right| \tag{1.5}$$

where $\overline{X}_1$ and $\overline{X}_2$ are the Cartesian position vectors of the two objects, while d_k is known as Keplerian distance function. The local minimal points of the Keplerian distance function coincides with possible conjunctions between the two objects. Introducing a scheme proposed by Gronchi et Tommei [54], is possible to compute whenever an orbit crossing actually occurs. If it happens, it means that a conjunction can occur, thus the pair of objects pass the second filter and lead to the last one.

The pairs of objects which pass through filter I and II, are now compared instant by instant. Here, the number of pairs is significantly reduced compared to the complete comparison with no filters. If the condition $\left|\overline{X}_1(t) - \overline{X}_2(t)\right| > d$ is satisfied for every time instant t, the pairs do not perform a conjunction and they are discarded. The Figure 1.5 represents the logical scheme of the three-filters approach.

The output is a list of conjunction events expressed with the SATCAT IDs of the two objects performing the conjunction, the epoch of TCA, the minimum distance at TCA, and the state vectors (position and velocity) at TCA. Afterwards, the list is ready to be processed in the second part of the code, to build network embedding. This is the last step regarding the processing part of the code.

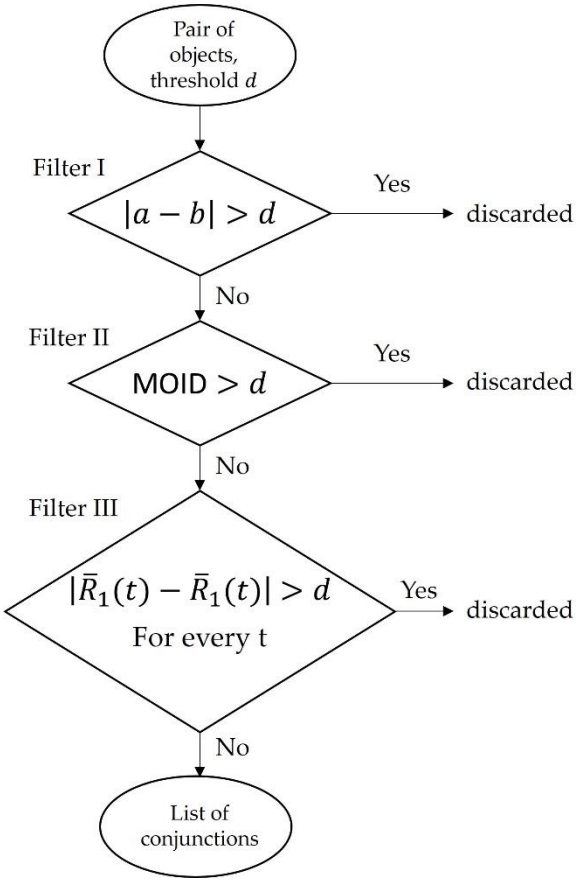

Figure 1.5: Logical scheme of the three-filters approach.

1.4. Probability of Collision

Following the compilation of the list of conjunction events performed by the selected population in the propagation period, the post-processing section begins. The last step preceding the computation of the RSONet embedding involves the association of a probability to each conjunction event occurring. The probability of collision is computed through an algorithm, elaborated in *MATLAB*. It is based on the method developed by the Space Force's 19th Space Defense Squadron (19 SDS), the same utilised to compute the probability of collision already included in CDMs [55]. It propagates in time the uncertainties associated to state position vector. The latter, in this work, is fixed for each object. This assumption is made since TLE format does not contain any information on the uncertainties associated to the state vectors.

After the computation of all the probabilities of collision, for each conjunction event, the RSONet is built. Objects performing at least one conjunction become nodes of the network, while links are determined by conjunctions. In the next chapter, the RSONet and the danger scores are presented, while in Ch. 3 the application of the construction process to the RSO population of the 1st of May 2023 is showed.

1.5. Network Metrics

Hereafter, the methodology for calculations of the network related measures is presented. Considering a network with n nodes connected by m links, defined by the adjacency matrix A, the network metrics include:

- Order (i.e., number of nodes in the network):

$$n \rightarrow A: (n \times n) \tag{1.6}$$

- Size: m (i.e., number of links in the network)

$$m = \frac{1}{2}\sum_{i}^{n}\sum_{j}^{n} A(i,j) \tag{1.7}$$

- Connectivity:

$$\beta = \frac{m}{n} \tag{1.8}$$

- Degree:

$$d_i = \sum_j^n A(i,j) \text{ for each node } i \tag{1.9}$$

$$\hat{d} = \frac{1}{n}\sum_i^n d_i \text{ average} \tag{1.10}$$

- Betweenness:

$$B_i = \sum_{s,t\neq i}^{n} \frac{n_{st}(i)}{2N_{st}} \text{ for each node } i \tag{1.11}$$

$$\hat{B} = \frac{1}{n}\sum_{i=1}^{n} B_i \text{ average} \tag{1.12}$$

where n_{st} is the number of shortest paths between two nodes s and t that pass through node i and N_{st} is the total number of shortest path from s to t

- Clustering:

$$C_i = 2\frac{T_i}{d_i(d_i-1)} \text{ for each node } i \tag{1.13}$$

$$\hat{C} = \frac{1}{n}\sum_{i=1}^{n} C_i \text{ average} \tag{1.14}$$

$$\text{where } T_i = [\text{diag}(\text{A U A})]_i \quad \text{and U is the upper triangular matrix extracted from A} \tag{1.15}$$

- Closeness:

$$clos_i = (\frac{n-1}{L_i})^2 Q_i \text{ for each node } i \tag{1.16}$$

$$\widehat{clos} = \frac{1}{n}\sum_{i=1}^{n} clos_i \text{ average} \tag{1.17}$$

where L_i is the number of reachable nodes from i (i excluded)

Q_i is the sum of distances from node i to all reachable nodes

The comprehensive meaning of the centrality measures previously listed is in the Appendix A.

1.6. Weighted Metrics

Weighted metrics are not strictly related to the network structure and topology, but they depend also on individual node data. Considering that the weighted adjacency matrix is defined as $\check{A}$, the weighted measures are:

- Probability of collision: depending on the initial dataset, it is included in the CDM, or it is computed for each object as explained in Sect. 1.4. It weights each link, it generates the weighted adjacency matrix $\check{A}$ and can be averaged on the size.
- Strength: it englobes network related characteristics, namely the degree, and the probability of collision.

$$s_i = \sum_j^n \check{A}(i,j) \text{ for each node } i \tag{1.18}$$

- RSONet Refined score.
- RSONet Simplified score.
- Danger score.

In the subsequent chapter, the RSONet and danger scores are explained upon in detail.

2 RSONet Scores and Danger Score

In this chapter, newly developed metrics, are proposed and further extended. They include two scores, defined as RSONet "Refined Score" and RSONet "Simplified Score". Moreover, the danger score is directly associated with the RSONet refined score and the mass of each object. RSONet scores are defined for each RSO in the population and can be used to weight nodes in the network. They are used to produce representations and average measures, which are useful to evaluate the removal strategies presented in the next chapter.

The danger score is also an instrument to assess the network response to removal approaches, and it is used as a judging parameter to select the best one. Therefore, the danger score is a complete tool to rank removal strategies: besides its connection with network theory, it also introduces information on mass, probability of collision, object type, number of fragments of possible encounters, etc. Therefore, the choice of targets for ADR/PDR can be based on more reliable factors with respect to standard approaches. Nowadays, the selection process is based only on probability of collision, mass, altitude, or a combination of those, while the novel danger score takes into account a wider set of important parameters.

The three scores rank all the objects in the population. In the next chapter, partial tables with highest scores are reported.

2.1. RSONet Scores

Hereafter, a brief explanation of the two RSONet Scores and their relationships with network theory are reported. The complete meaning and explanation of both scores are presented in the works by Romano et al. [56] and [40].

2.1.1. Refined Score

The refined score is a general tool utilised to compute a conservative probability of different types of collisions in the network. The basic idea is that a collision of one object in the population can happen in three different ways: by directly colliding with another neighbouring object; by colliding with a fragment in a debris cloud generated by the collision of two objects in its neighbourhood; by colliding with a debris cloud generated by a chain reaction of other objects. Here, the primary assumption made for current RSONets is that conjunctions are presumed to occur without dependence on

time. Consequently, this score represents a conservative probability, indicating the likelihood under the worst case scenario.

The refined score depends on:

- Probability of collision.
- Network topology and structure.
- Object type.
- Number of fragments and characteristic length of debris cloud generated by RSOs in the network (estimated via the application of the NASA break-up model [57]).

The collision probabilities of each object are the ones computed in the case of TLE sets, or already available in case of CDM sets.

The network topology and structure are typically defined by the network centrality measures (degree, betweenness, clustering, and closeness).

The object type information is introduced by the mean of a coefficient ψ, defined for each node: if the object is a debris, $\psi = 0$, otherwise $\psi = 1$. This coefficient has been implemented to weight different collisions and to penalize collisions between debris, while to emphasized collision between payloads or rocket bodies.

The NASA break-up model has been implemented to characterise the debris cloud that an object can produce. At this stage, due to partially available data on masses, the latter were estimated based on historical data. Only catastrophic collisions are considered at this level, since the coefficient ψ already addresses the severity of the collision.

As previously explained, the refined score consists of three contributions, and it is defined for each node *i* as:

$$R_i = R_{i,1} + R_{i,2} + R_{i,3} \tag{2.1}$$

As shown in Figure 2.1, the first contribution addresses the total probability of a direct collision of the node a with its neighbours (in this example, a_1, a_2, a_3, a_4). It is defined as:

$$R_{i,1} = \sum_{j}^{d_i} (\psi_i + \psi_j) \cdot p_{ij} \tag{2.2}$$

where ψ is accounting for the type of object, d_i is the degree of node i, which expresses its number of neighbours and p_{ij} is the probability of collision between the node i and its neighbours. If the collision involves two debris, this contribution is null due to ψ. Instead, if it involves at least one other type of objects, the contribution is grater than zero. It is evident that through ψ, it is addressed more severity to collisions involving

rocket bodies and/or satellites, since usually they are larger in size and mass with respect debris, and usually they can produce more severe breakup events.

The second contribution quantifies the total probability of the node a to encounter a debris cloud produced by its neighbours. It is defined as:

$$R_{i,2} = \psi_i \sum_{j}^{d_i} \psi_j \cdot p_{ij} \cdot (1 - (1 - \psi_j \cdot p_{ij}))^{N_f} \tag{2.3}$$

with

$$N_f = 0.1 \cdot L_c^{-1.71} \cdot (m_i + m_j)^{0.75} \tag{2.4}$$

where the coefficients ψ consider the type of objects, d_i is the degree of node i, which expresses its number of neighbours, p_{ij} is the probability of collision between the node i and its neighbours. The catastrophic collision is expressed by the Eq. 2.4, which generates a certain number of fragments N_f, depending on characteristic length of the fragments of the L_c (fixed at 0.1 m) and on the two object's masses involved, m_i and m_j.

The third contribution considers the interaction between node i and debris cloud generated from all chains outside its close proximity. It is defined as:

$$R_{i,3} = \psi_i \cdot B_i \sum_{j}^{d_i} R_{2,j} \cdot p_{ij} \tag{2.5}$$

where the coefficients ψ take into account the type of objects, d_i is the degree of node i, which expresses its number of neighbours, p_{ij} is the probability of collision between the node i and its neighbours, B_i is the betweenness of node i and $R_{2,j}$ is the second contribution of each neighbour of node i.

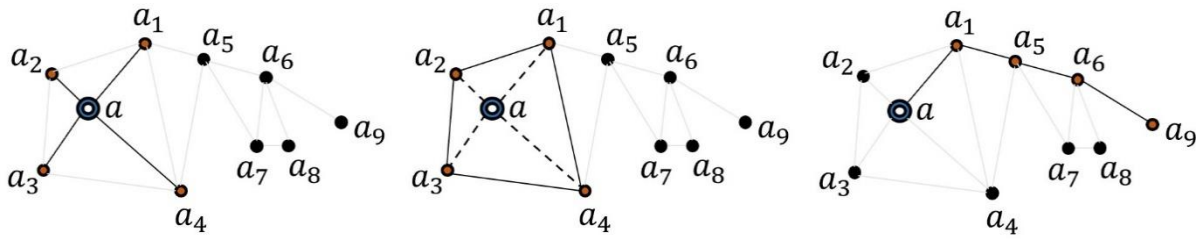

(a) Direct collisions of a (b) Indirect collision of a (c) Chain collision of a

Figure 2.1: The three contributions of the RSONet refined score.

2.1.2. Simplified Score

The simplified score can be seen as a special case of the more general refined score. The assumption for defining this score is as follows: considering fixed probabilities of

collision, equal for all conjunctions, the refined score simplifies a lot. Moreover, the NASA break-up model and the influence of object type have been removed. The score is defined as:

$$S_i = p \cdot d_i + \frac{1}{2} p^2 \cdot C_i \cdot d_i \cdot (d_i - 1) + B_i \cdot p^{(1/clos_i)} \tag{2.6}$$

where d_i is the degree of the node i, C_i is the clustering coefficient of the node i, B_i is the betweenness of the node i and $clos_i$ is the closeness coefficient of the node i. The probability of collision p has been set to 10^{-4}. It is clear that the simplified score is directly related to the network topology and structure, since it depends only on the centrality measures. In this work, it has been considered as a weighted measure, due to its derivation from the refined score. Nevertheless, it bears a closer resemblance to a network measure.

By re-introducing the initial assumptions, the score loses the direct visualization of the centrality measures in the formula, even if it still depends on network topology and structure. It is expected, using simplified and refined score, different conclusions when assessing the robustness of the network (which relies solely on network properties) compared to the danger score (which also incorporates non-network-related characteristics).

2.2. Danger Score

The danger score is the most complete metric utilised in this work: it takes into account every dependence of the refined score, plus the mass. Accordingly, it is used as a judging parameter for the ADR/PDR strategy selection for target choice.

It is dimensionless and defined for each node and computed as:

$$D_i = R_i \cdot \frac{m_i\,[kg]}{1\,[kg]} \tag{2.7}$$

For this purpose, masses are taken directly from DISCOSweb database. Since not all the data are available, the following danger rank lists are partial. However, full data of masses could change the ranking, but not the related conclusions.

3 Recent RSO Population

In this chapter, the application of the procedure to construct the RSONet is showed. In this work, the initial data are the following:

- For the TLE format, TLEs of 1st of May 2023 from Space-track.org.
- For the CDM format, daily CDMs of 1st of May 2023 to 1st of June, 2023 from Space-track.org.

For the TLE set, 30 days of orbital propagation, time step of 1 minute and 3 km of threshold distance for conjunction detection have been chosen.

Even if the two datasets refer to the same period of time (from 1st to 31st May 2023), the generated network embeddings are different. This relies on many causes:

- CDMs report only conjunction below 1 km of distance.
- CDMs do not include Starlink and OneWeb satellites.
- CDMs report conjunctions with probability of collision equal or higher than 10^{-4}.
- TLE sets have been propagated for 30 days with basic SGP4 propagator, whereas CDM sets originate from more sophisticated tools.

3.1. May 2023 Population

After the computation of the list of conjunctions in the case of TLE sets, the network embeddings (for both the initial datasets) are built. The Figure 3.1 is the network representation of the RSOs performing conjunctions in May 2023, highlighting the type of object. This figure describes the population that emerges from the TLE utilisation. The different shapes and colours of each node, indicate different types of objects, as highlighted in the legend. Instead, the Figure 3.2 represents what arises from the CDM exploitation.

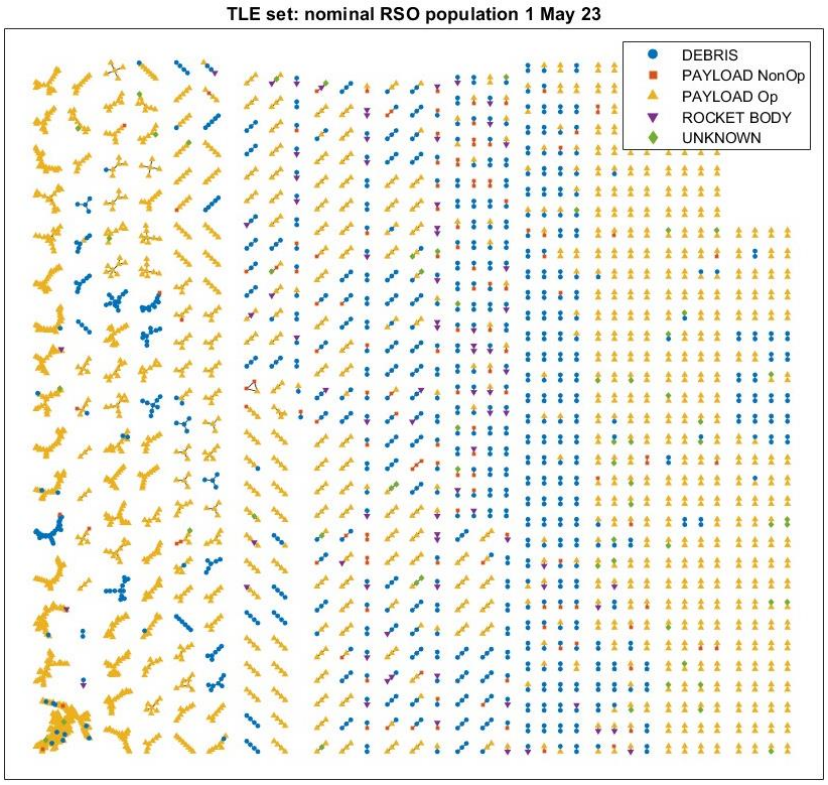

Figure 3.1: TLE dataset, network representation for object type.

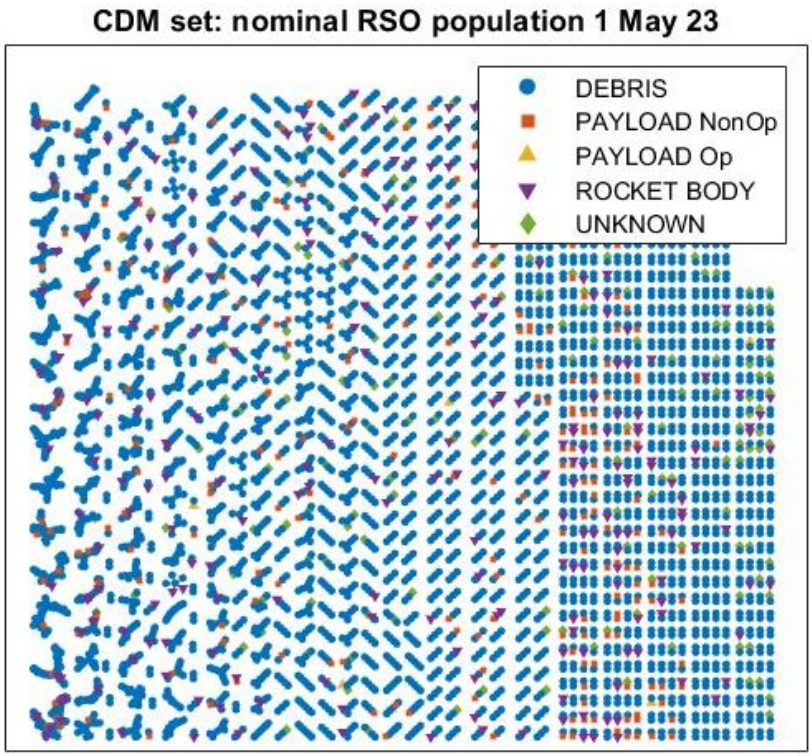

Figure 3.2: CDM dataset, network representation for object type.

The difference between TLE and CDM sets is clearly visible in the previous figures: CDMs include more presence of debris with respect to TLE, which instead have mostly

operational satellites. This is highlighted in Figure 3.3, where numbers of objects per type are reported.

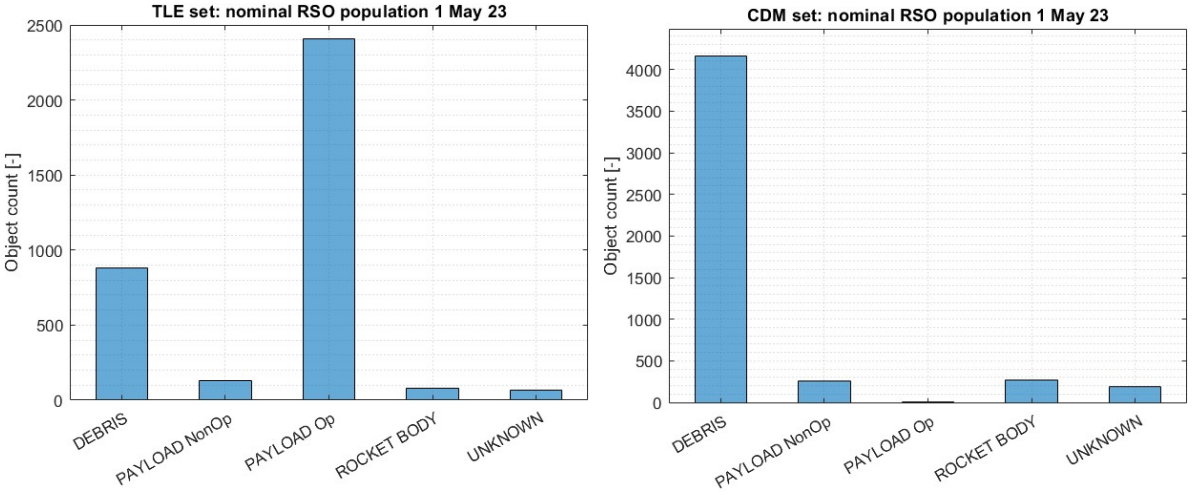

(a) Components of TLE-RSONet (b) Components of CDM-RSONet

Figure 3.3: Number of objects per type.

Out of 3562 objects in the TLE case, 2405 (about 67%) are operative satellites, of which 2080 (about 86%) are Starlink satellites. Other statistics are reported in Table 3.1.

Table 3.1: Statistics of the two RSONets.

	TLE set	CDM set
Order	3562	4694
Size	2590	3406
Connectivity	0.7271	0.7256
# Debris*	1012 (~28.4%)	4248 (~90.5%)
# Operative satellites	2405 (~67.5%)	8 (~0.2%)
# R/B	77 (~2.2%)	270 (~5.7%)
# Unknown	68 (~1.9%)	168 (~3.6%)

* Here, debris include also non-operative satellites.

Hereafter, the largest connected components of both datasets are represented, highlighting the type of object, in Figure 3.4.

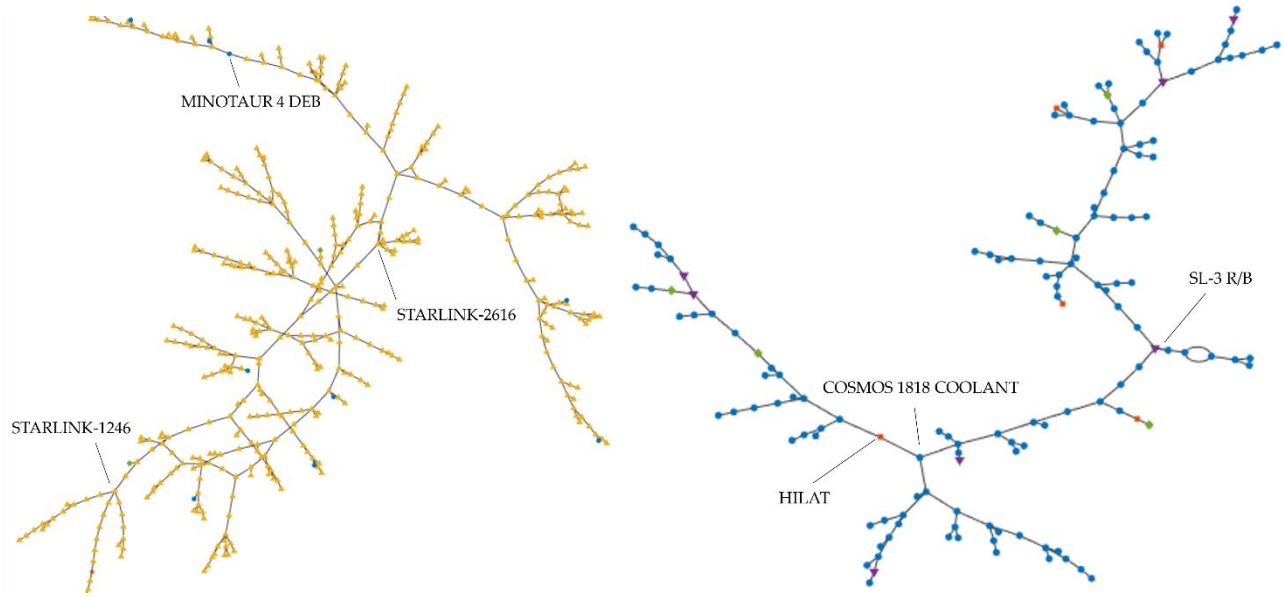

(a) Biggest component using TLE sets (b) Biggest component using CDM sets

Figure 3.4: Largest connected components representations.

LEO is the most crowded orbital region: this is reflected also in the RSONet, as it is shown in Figure 3.5 and in Figure 3.6.

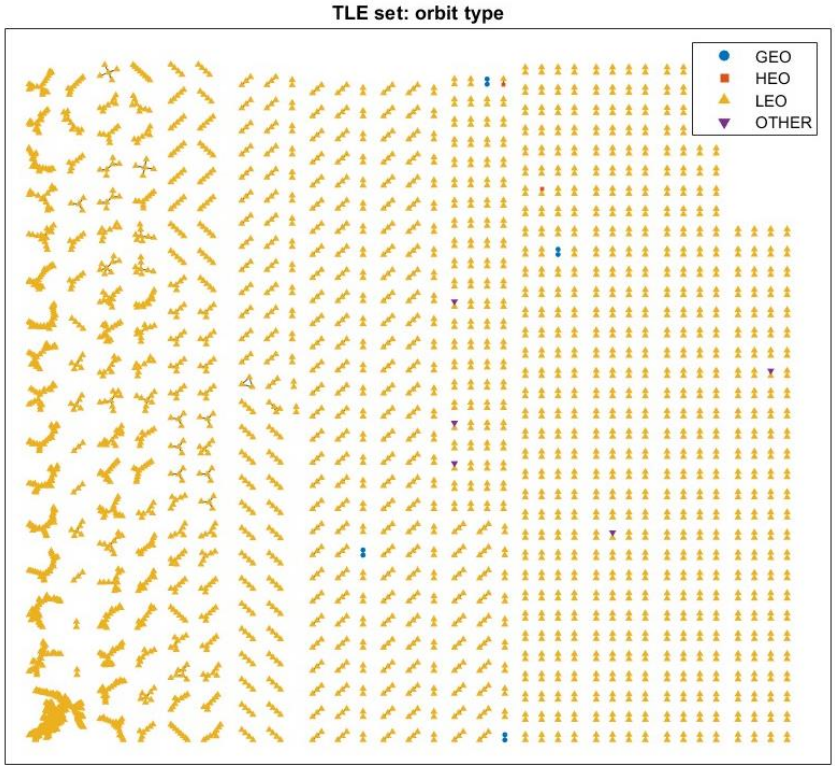

Figure 3.5: TLE dataset, network representation for orbit type.

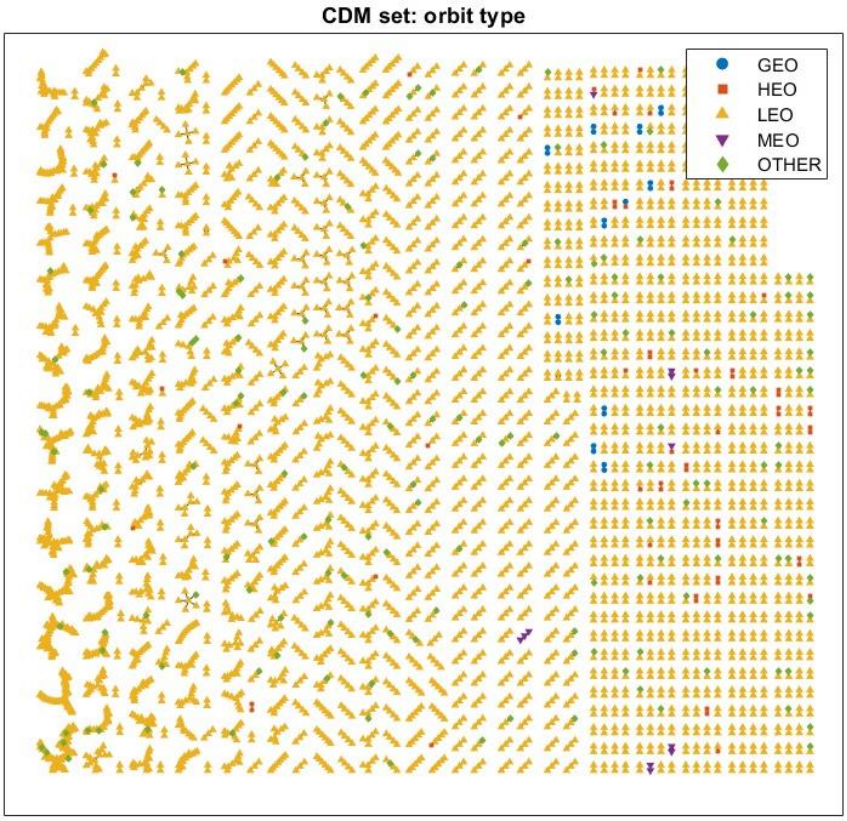

Figure 3.6: CDM dataset, network representation for orbit type.

Hereafter, the largest connected components of both the cases are represented, highlighting the orbit type, in Figure 3.7.

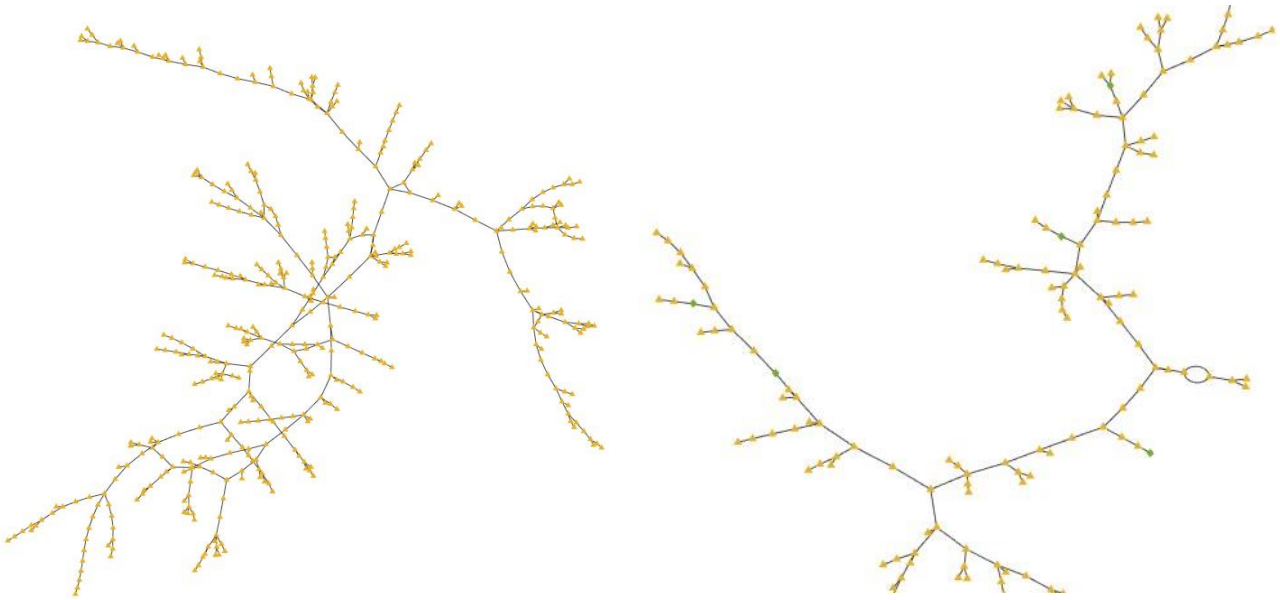

(a) Biggest component using TLE sets (b) Biggest component using CDM sets

Figure 3.7: Biggest components representations.

Nodes and links of the RSONet can be weighted. It is reported, in Figure 3.8, the largest connected component of the TLE RSONet, with weighted nodes for network degree. Similar representations for all the other centrality measures (i.e., betweenness, closeness, clustering) can be reproduced by the developed tool, also in the case of CDM dataset.

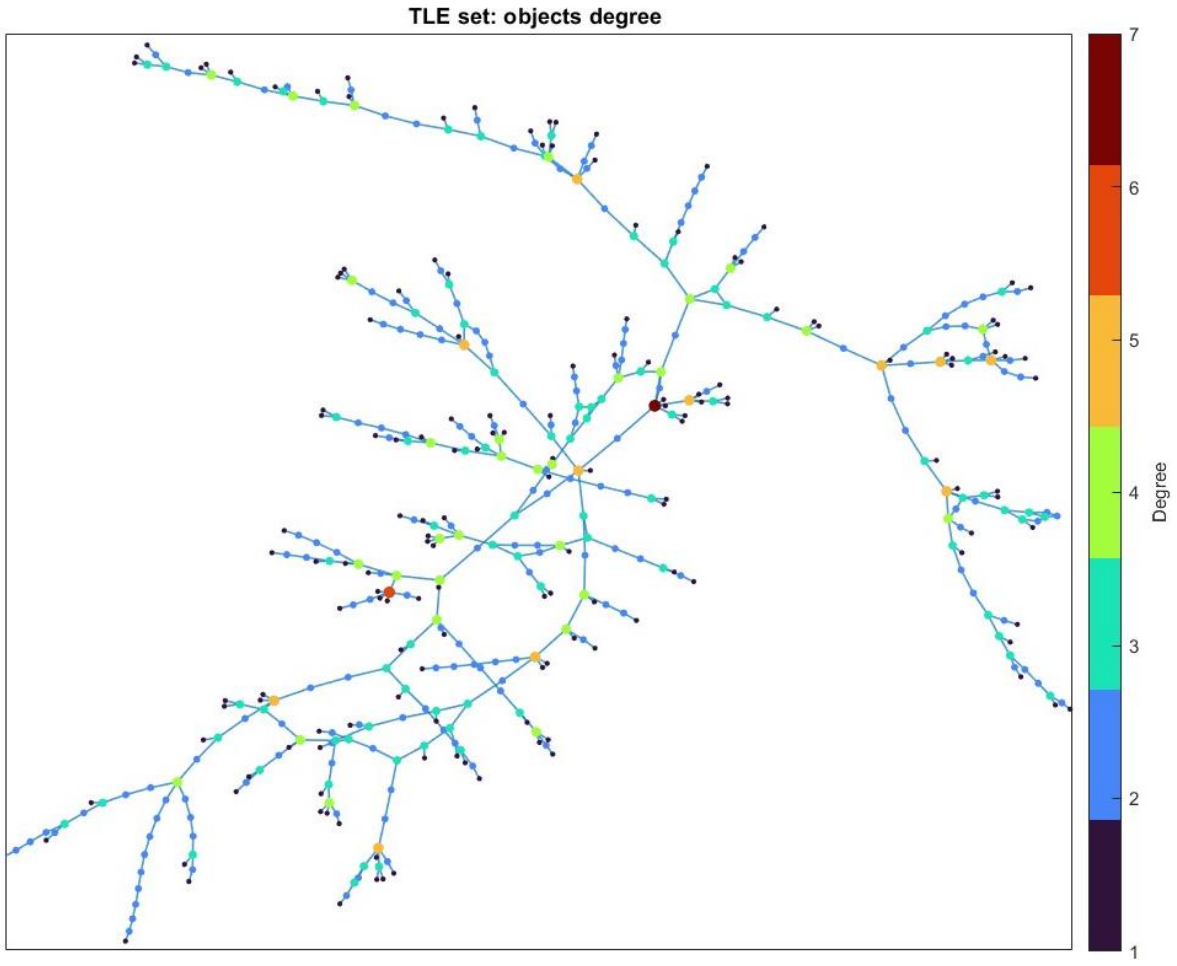

Figure 3.8: TLE dataset, representation of biggest component of the network for degree.

Moreover, the code prints the more connected nodes, i.e., objects with highest degree, as shown in Table 3.2 (only the top 5 are reported).

Table 3.2: The 5 objects with highest degree for both the datasets.

	degree	NORAD ID	Object Name
TLE	7	48695	STARLINK-2616
	6	46382	STARLINK-1769
	6	48689	STARLINK-2617
	6	52370	STARLINK-3827
	6	55544	CZ-6A DEB
CDM	9	16963	COSMOS 1780 (GLONASS)
	9	26565	COSMOS 2376 (GLONASS)
	7	35221	FENGYUN 1C DEB
	6	30121	FENGYUN 1C DEB
	6	31097	FENGYUN 1C DEB

Regarding the TLE-based case, the objects with highest degree are almost all Starlink satellites, this is due to their high presence in the built RSONet. The CZ-6A is one of the more than 780 fragments generated by the explosion of the upper stage of the Chinese rocket body Long March (Cheng Zheng) 6A, occurred the 12th November 2022 [58]. For what concern the CDM-based case, the two objects with highest degree are two Soviet satellites, part of the GLONASS constellation, the Russian Global Positioning System (GPS). These two satellites were launched, respectively, in 1986 and 2000 and they are still in orbit, performing several conjunctions per year. The rest of the table is filled by FengYun-1C debris, related to the worst historical breakup events for number of created fragments.

Similarly, tables for betweenness, closeness and clustering are produced and utilised in the next chapter, to select targets to be removed from the network.

Probability of collision of each conjunction can be used to produce weighted networks. In Figure 3.9 the largest connected component of the CDM RSONet is presented, with the size of the links weighted for each probability of collision. However, the pair of objects with the highest likelihood to collide are not in the biggest component, but in one of the smallest, as seen in Figure 3.10.

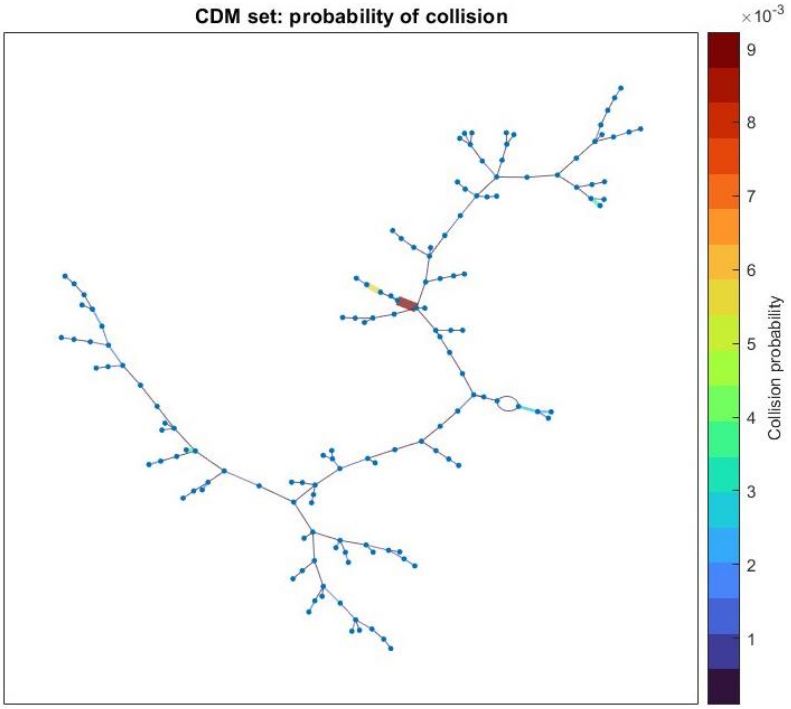

Figure 3.9: CDM dataset, representation of biggest component of the network for probability of collision.

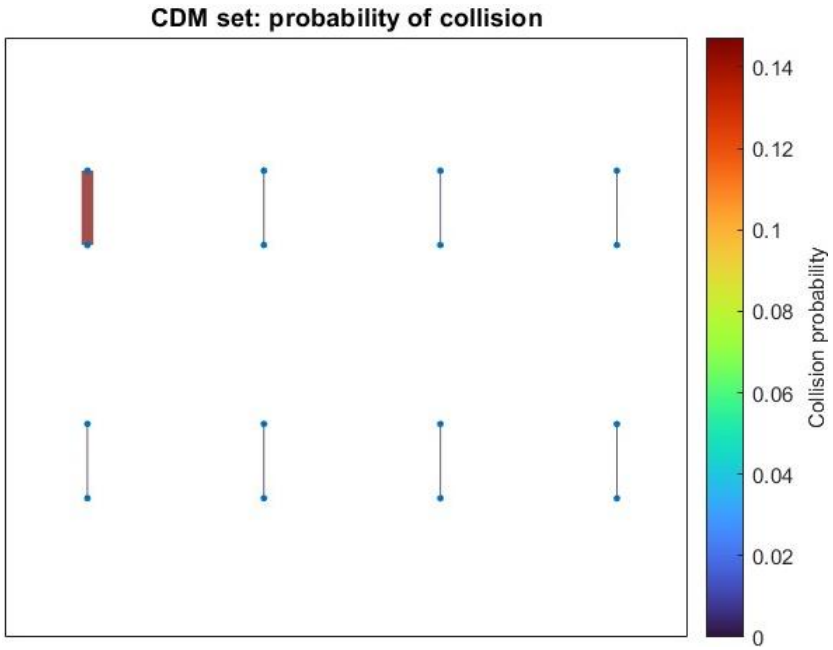

Figure 3.10: CDM dataset, representation of smallest components of the network for probability of collision. The upper-left one is the one with highest PoC.

The maximum probability of collision regards the objects FENGYUN 1C DEB and COSMOS 2251 DEB, two space debris. Their probability to collide was 1 over 7, but this event did not occur.

Lastly, it is reported in Figure 3.11 the representation for one component of the RSONet refined score, using CDM set.

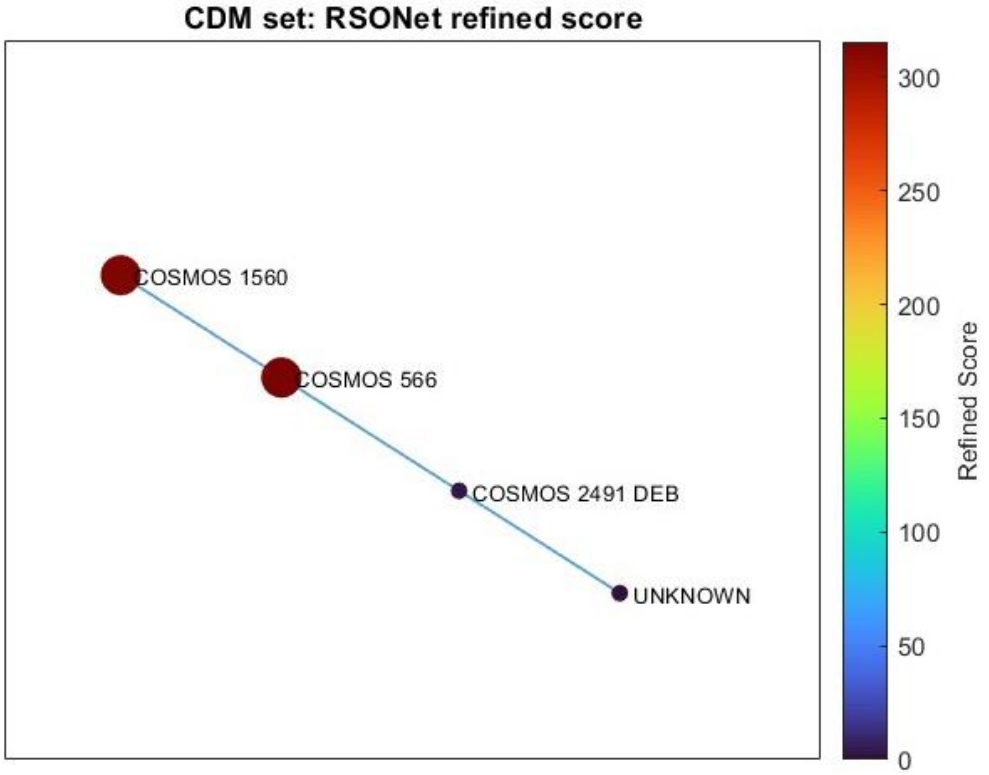

Figure 3.11: CDM dataset, representation of component of the network with the two objects with highest refined score.

Even if they do not have many connections in the network (i.e., low degree, betweenness), they have remarkably high refined score. This is due to the introduction of the dependencies of this score: it does not depend exclusively on network structure but also on the object type, the probability of collision, the number of fragments generated. In this case, COSMOS 1560 and COSMOS 566 are two satellites, with a relatively high probability of collision ($PoC = 0.01565$). Therefore, a relatively high first contribution R_1 for both is expected, as illustrated in Table 3.3.

Table 3.3: Individual contributions of the refined score.

	COSMOS 1560	**COSMOS 566**
Refined score*	313.1983	315.3744
$\boldsymbol{R_1}$	0.0313	0.0315
$\boldsymbol{R_2}$	1.2947e-05	0
$\boldsymbol{R_3}$	0	4.0533e-07

* The refined score has been normalized to 10^{-4}

Since the simplified score, instead, depends strictly on network characteristics, it is expected to have objects with highest simplified score in the largest connected components.

The Figure 3.12 reports the biggest component of the CDM RSONet, valuating the simplified score.

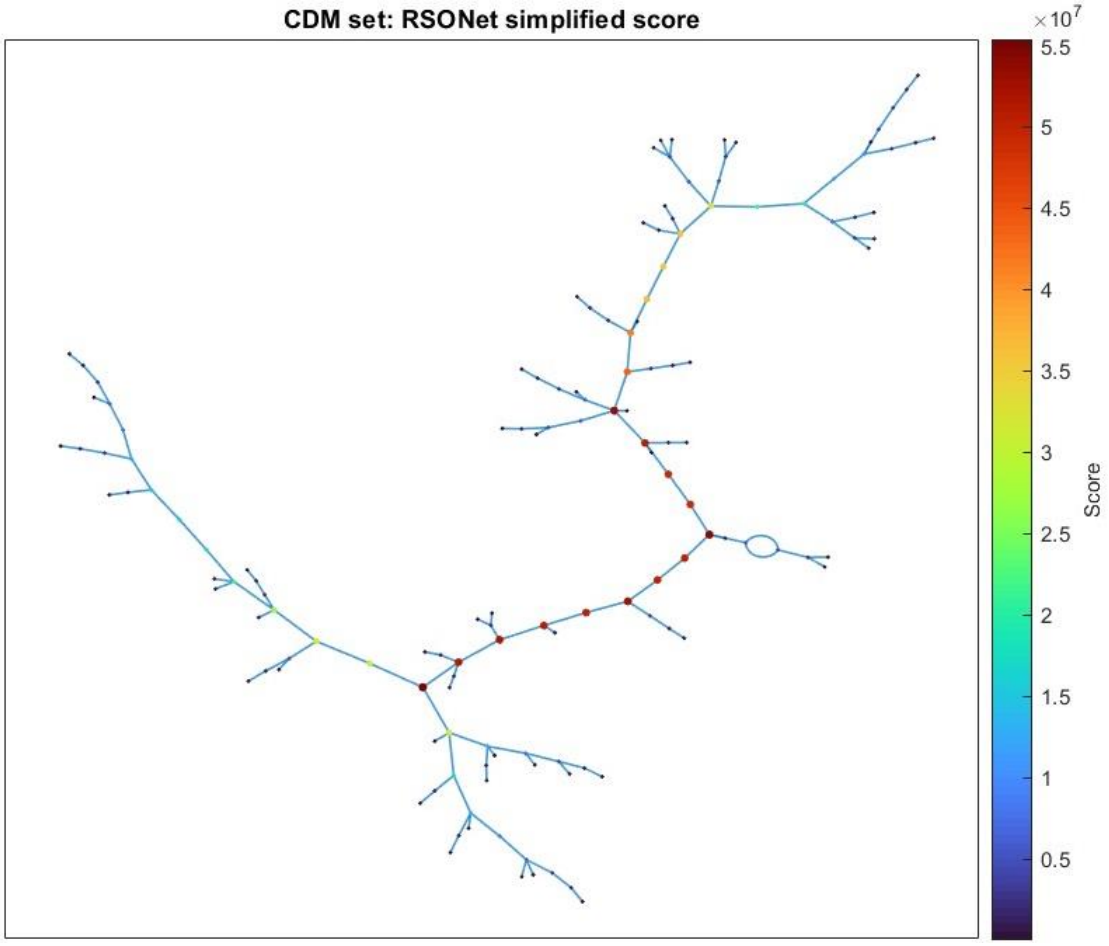

Figure 3.12: CDM dataset, representation of the biggest component of the network for simplified score.

Finally, by introducing also the mass information from the DISCOSweb database, it is possible to compute the ranking for the danger score.

The objects with highest danger score, in both TLE and CDM-based cases, are not the ones with the highest masses or refined score, but with the highest combination of those, as it is illustrated in Table 3.4. In this way a new metric that takes into account other useful parameters, besides the mass and the probability of collision, is introduced.

Table 3.4: Top 5 objects with highest danger score

	Satellite Name	Danger score	Refined score	Mass [kg]
CDM	SL-16 R/B	3.747336e+05	4.555495e+01	8225
	COSMOS 2219	1.619594e+05	5.028219e+01	3220
	SL-16 R/B	1.575417e+05	1.915175e+01	8225
	SL-8 R/B	1.023590e+05	7.202242e+01	1420
	SL-14 R/B	7.278113e+04	5.245449e+01	1390
TLE	CSS (TIANHE-1)	1.044945e+04	1.088485e-01	96000
	TIANZHOU 5	1.854118e+03	1.404635e-01	13200
	OBJECT H	9.604652e+02	2.401163e-01	4000
	SZ-15	8.361079e+02	1.034531e-01	8082
	SL-8 R/B	5.505626e+02	3.873901e-01	1420

4 Removal Scenarios and Strategies

In this chapter, two distinct scenarios and two complementary strategies serve as the case studies. The analysis is developed through the investigation on the connectivity and the network measures.

The two scenarios were built to provide new perspectives on space debris issue and the newly expansion of space utilisation. In the first scenario, space debris are completely removed from RSONet to assess their influence onto the rest of the population. The second scenario, instead, is devoid of any presence of the mega-constellation satellites to analyse their impact on the RSO population. The evaluation of both has been performed through the study of the network embedding before and after the removals. Namely, network representations, measures and weighted scores have been compared, and therefore robustness of the network and danger score are assessed.

The characterisation of TLE and CDM significantly influences the outcomes of the analysis: the RSONet built from TLE sets shows a high presence of mega-constellation satellites, as explained in Ch. 3, and less presence of debris. Nevertheless, in this instance, debris still accounts for 30.6% of appearance (including rocket bodies and non-operative satellites), but they are mostly concentred within the smallest connected components.

Dealing with CDM-built RSONet, it presents the opposite characteristics, with a high presence of debris, also including the largest components.

Assessing the robustness means evaluating the change in the connectivity and in the centrality measures (average degree and betweenness) [59], while analysing the change in the danger score entails comprehending whether the removal is effective not only in terms of parameters within the network domain but also in crucial factors for the space sustainability issue (mass, PoC, operability, etc.).

4.1. Space Debris influence

In this section, the distinction between TLE and CDM datasets, elucidated in the preceding chapter, is substantiated through the analysis of this scenario. Hereafter, all the debris (including object tagged as debris, non-operative satellites, and rocket

bodies) are removed from the RSONet related to the population of the 1st of May 2023. Unknown objects are unidentified types; they could be new fragments resulting from break-up events or recently launched satellites yet to be recognized. Hence, they are not considered in the removal activities.

As shown in Figure 4.1, selecting TLE dataset, most of the debris are located in the smallest components, while the biggest components are mostly made by operative satellites. Even the debris belonging to the largest component exhibit low degree and betweenness. On the contrary, CDM sets produced a radically different situation: debris, rocket bodies, and non-operative satellites are the 96.2% of the total population. By removing them, the network is completely disrupted: the remaining 3.8% includes operative satellites or unknown objects that, after the removal, are left with no conjunctions, thus they are also eliminated from the RSONet. Consequently, before removal, there was not any predicted conjunction between two operative satellites or two unknown objects, or one operative satellite and one unknown object.

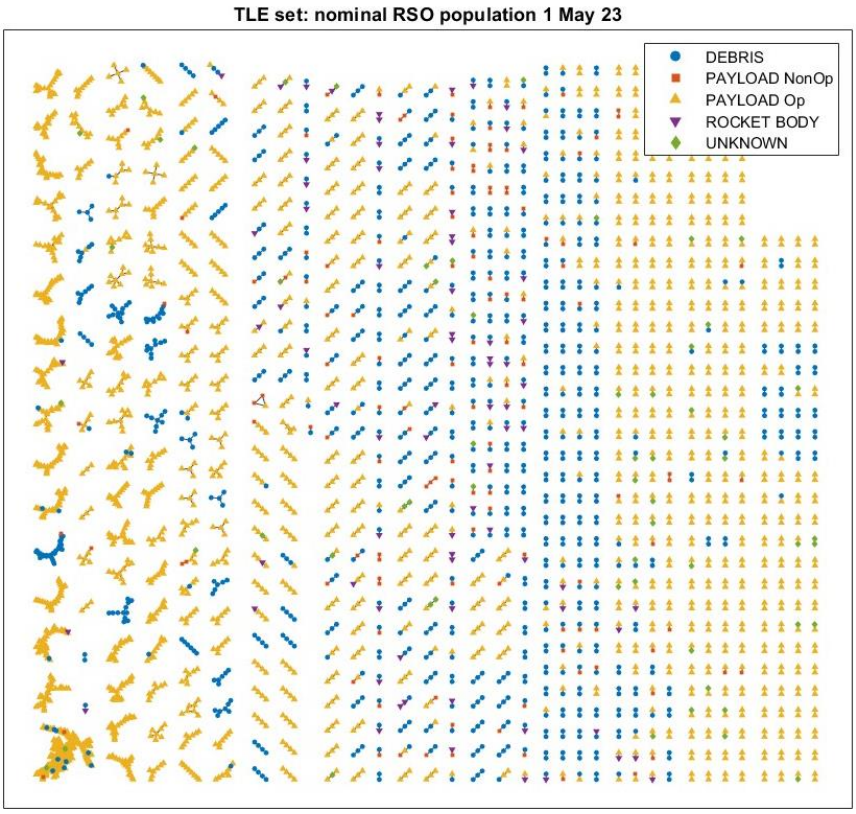

Figure 4.1: TLE dataset, network representation per object type.

The Figure 4.2 and Figure 4.3 display the network representations per object type following the debris removal, in the TLE case. It is notable that the largest component has been split in 3 components, but the division has not significantly disrupted its overall structure.

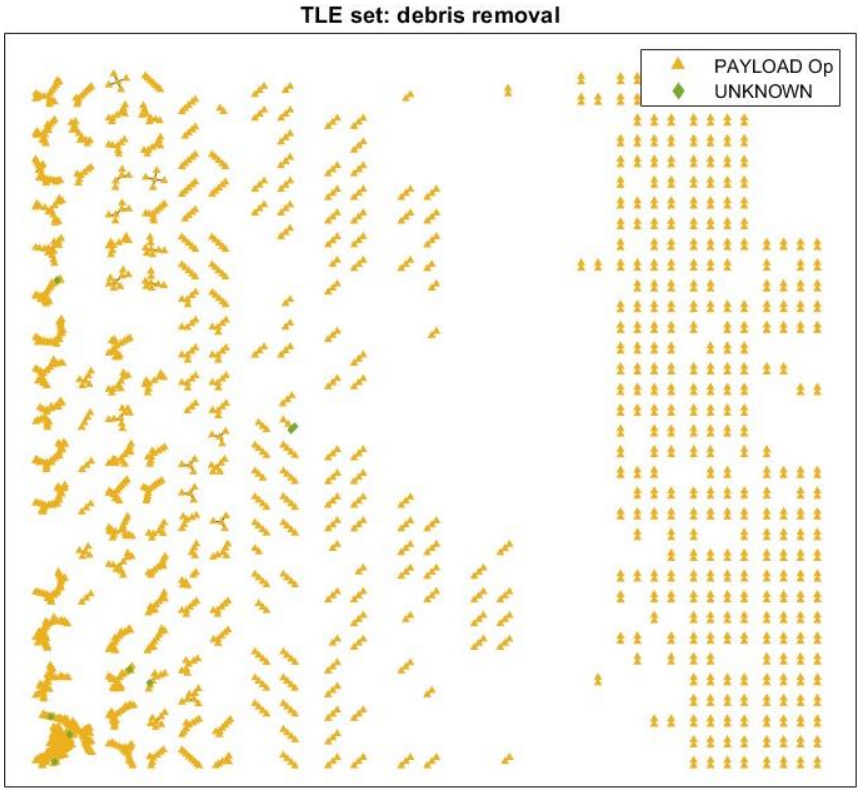

Figure 4.2: TLE dataset, network representation after debris removal.

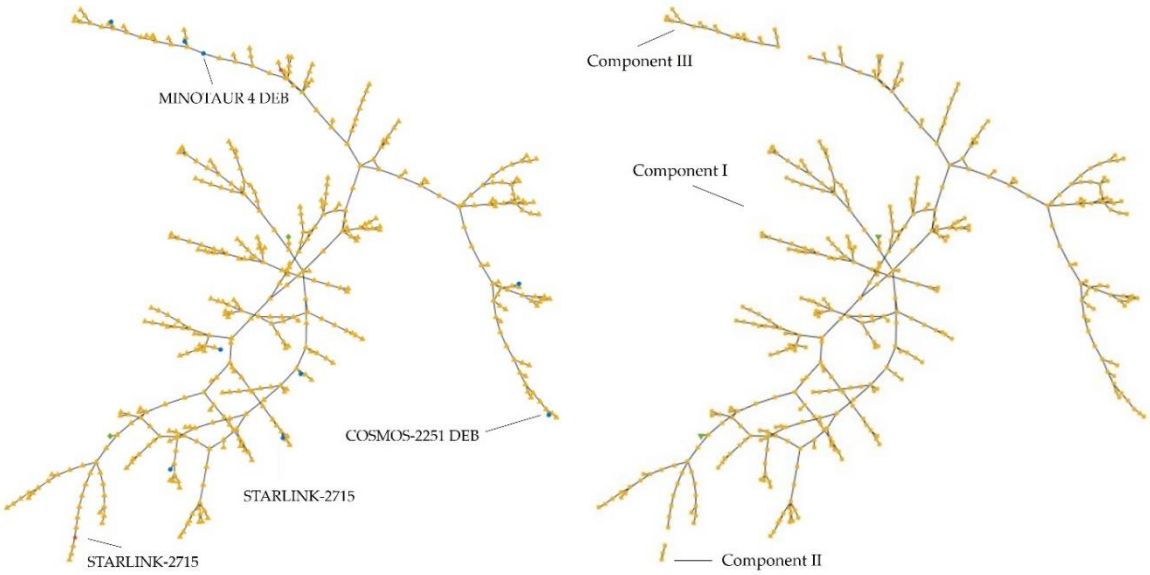

(a) Biggest component (TLE) (b) Biggest component (TLE) after debris removal

Figure 4.3: Biggest components before and after debris removal for TLE dataset.

In Table 4.1 the network measures are reported. Probability of collision, RSONet simplified, refined and danger scores are averaged over the network order. In the case of CDMs, the scenario in which rocket bodies are retained in the network is reported, aiming to elucidate the impact of non-operative satellites and debris fragments.

Table 4.1: Metrics before and after the removal, for both datasets.

	n	m	β	$\hat{d}$	$\hat{B}$	PoC	S	R	D
Nominal TLE	3562	2590	0.73	1.45	4.97e2	2.35e-5	4.97e6	5.81e-2	26.58
Debris Removed	2344	1843	0.79	1.57	5.96e2	2.46e-6	5.96e6	7.72e-2	19.27
Nominal CDM	4694	3406	0.73	1.45	4.41e1	6.25e-4	4.41e5	2.36	9019
Debris Removed*	45	23	0.51	1.02	0.02	5.40e-4	2.21e2	11.31	1201

* Rocket bodies are not removed in this case

In case of TLEs, the total number of debris removed is 1089. Moreover, 129 objects remain disconnected (null degree), therefore they do not perform conjunctions anymore: they are also removed from the network. By focusing on the preceding table, it is evident that the RSONet exhibits robustness to the proposed removal in this scenario: removed objects have not significantly affected the largest components and, consequently, the overall network. Accordingly, the connectivity is increased, together with the average degree and betweenness. The weighted measures (RSONet scores) are increased as well, meaning that the removed objects had relatively low centrality measures and low probability of collision. Moreover, since they are mostly in the smallest components, they present poor network complexity structure, thus low refined score. Nevertheless, the danger score is slightly decreased: this phenomenon arises from the fact that all the rocket bodies which constitute the majority of objects with the highest mass, have been removed.

In case of CDMs, the total number of objects removed is 4264, while 385 objects remain with null degree. As depicted in the Figure 4.4, the network has been nearly completely disrupted, aligning with expectations. This is reflected in the measures in Table 4.1. The connectivity, the average degree, the average betweenness, and the simplified score are significantly decreased. The RSONet is not robust to this removal approach, which could greatly benefit the space environment.

In both cases, order and size are clearly decreased. In a scenario where tracking systems managing predicted conjunctions within a threshold of 1 km (CDM), the hypothetical absence of space debris would markedly reduce the workload, almost to zero. When considering a threshold of 3 km (TLE), the presence of mega-constellation satellites becomes a factor, consequently increasing the effort required for conjunction assessment. Indeed, by changing the distance threshold for conjunction detection in the TLE case to 1 km, yields identical results to those of the CDM scenario.

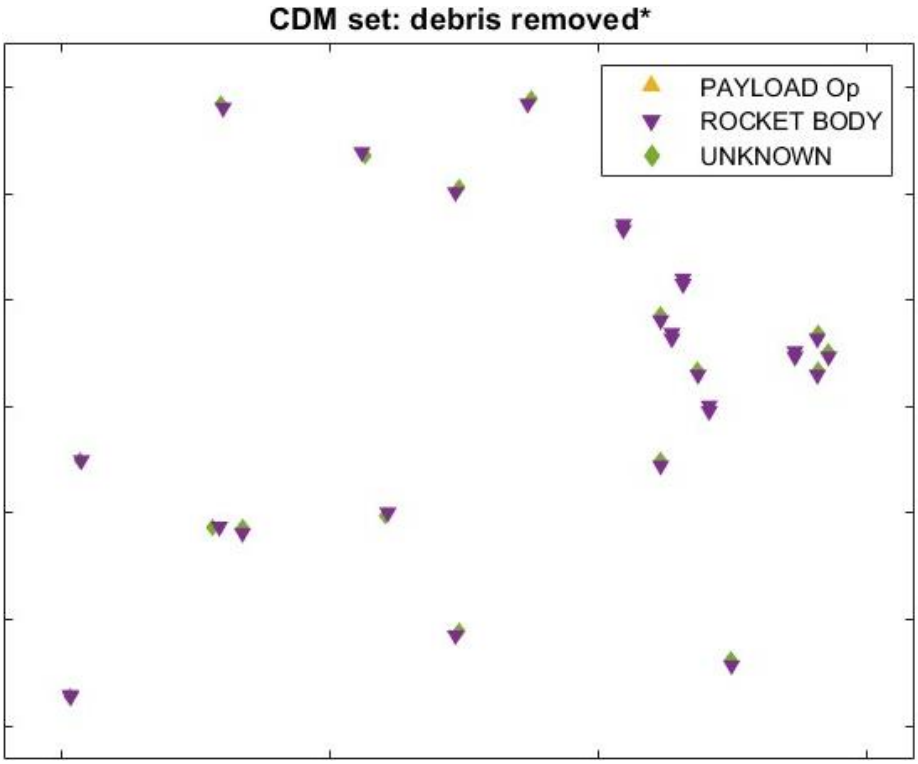

Figure 4.4: CDM dataset, network representation after debris removal (rocket bodies not removed).

4.2. Mega-Constellation Satellites influence

Since TLE sets include the presence of mega-constellation satellites, while CDMs do not, the impact of mega-constellation satellites can be analysed with TLE dataset only.

In the following sections, the current case study is divided in 3 complementary analysis: firstly, the focus is on Starlink satellites by SpaceX, which represent the most numerous fleet among all mega-constellations at the current date; secondly, the following most numerous constellation by Eutelsat, OneWeb, is studied; lastly, to obtain a comprehensive understanding of their influence on the rest of the RSO population, both Starlink and OneWeb are removed from the RSONet at the same time.

4.2.1. Starlink SpaceX

Figure 4.5 illustrates the RSONet following the removal of all the Starlink satellites. As expected from the previous statements, in this instance, the largest components are completely disrupted, except for the ones showed in Figure 4.6. The first one (Fig.4.6a) consists predominantly of debris (from CZ-6A break-up event), with one payload (COSMOS 1934) involved in a conjunction with one of them. In Fig.4.6b instead, all active satellites are depicted, with the majority being constellation satellites.

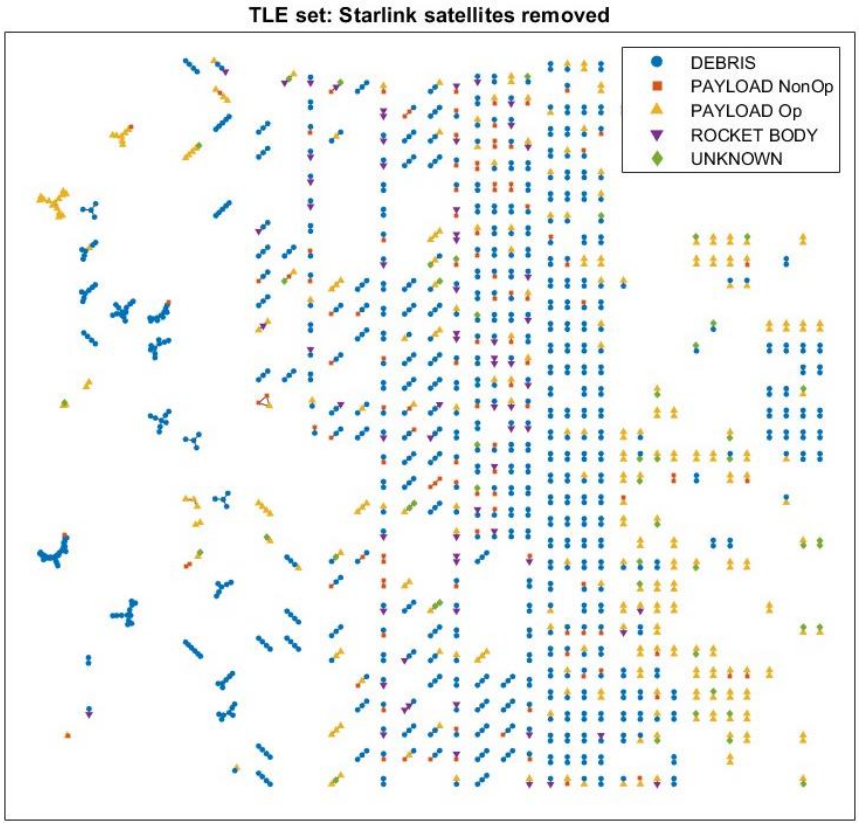

Figure 4.5: TLE dataset, network representation after Starlink satellites removal.

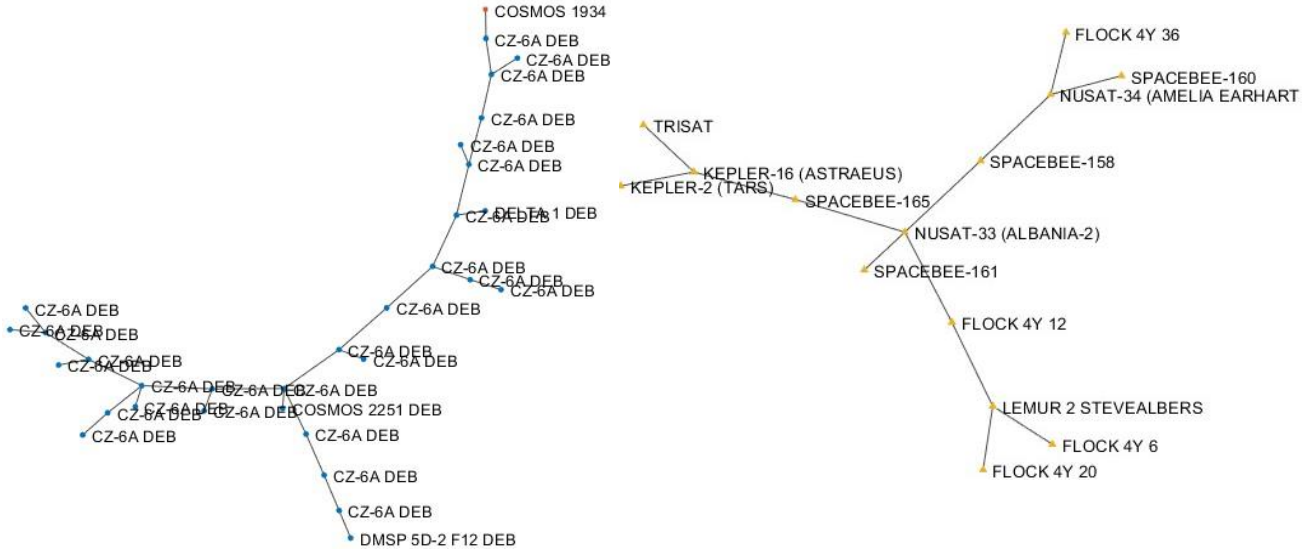

(a) Biggest component (TLE) (b) Second biggest component (TLE)

Figure 4.6: TLE dataset, biggest components after Starlink satellites removal.

In Table 4.2, the comparison between the nominal population of the RSONet and the network after the removal is expressed through the network measures. As expected, due to the high presence of Starlink satellites especially in the biggest components, the network results to be not robust, thus vulnerable to this kind of removal. The order,

size, connectivity, and average degree and betweenness, are significantly decreased. Accordingly, also the simplified and refined score are reduced. On the contrary, the danger score has almost doubled due to the fact that the removals focus on objects with relatively low mass. Even if the refined score is decreases, the danger score still is influenced by the mass of the objects concerned.

Table 4.2: Metrics before and after the Starlink satellites removal, for TLE dataset.

	n	m	β	$\hat{d}$	$\hat{B}$	PoC	S	R	D
Nominal TLE	3562	2590	0.73	1.45	4.97e2	2.35e-5	4.97e6	5.81e-2	26.58
Starlink Removed	1382	815	0.59	1.18	2.49	2.67e-6	2.50e4	2.49e-2	48.29

4.2.2. OneWeb Eutelsat

In Figure 4.7, RSONet after the elimination of OneWeb constellation is depicted.

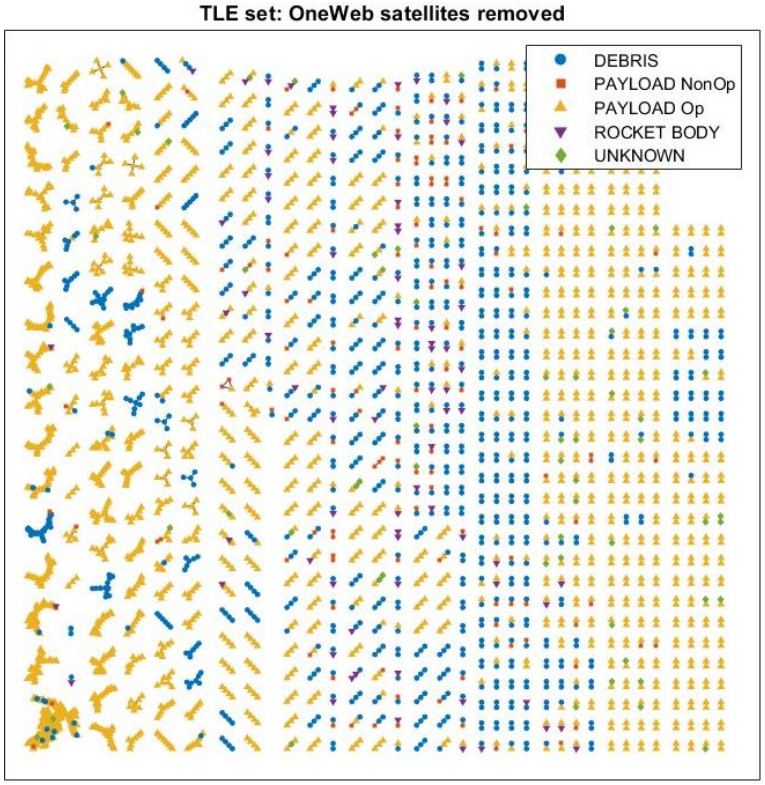

Figure 4.7: TLE dataset, network representation after OneWeb satellites removal.

Only 10 OneWeb satellites were present in the network and, as showed in Figure 4.8, they are located in the smallest components. Order and size almost remain unchanged, 8 other objects are left with no conjunctions and consequently removed. Therefore, as highlighted in Table 4.3, network measures reflect the ineffective removal approach.

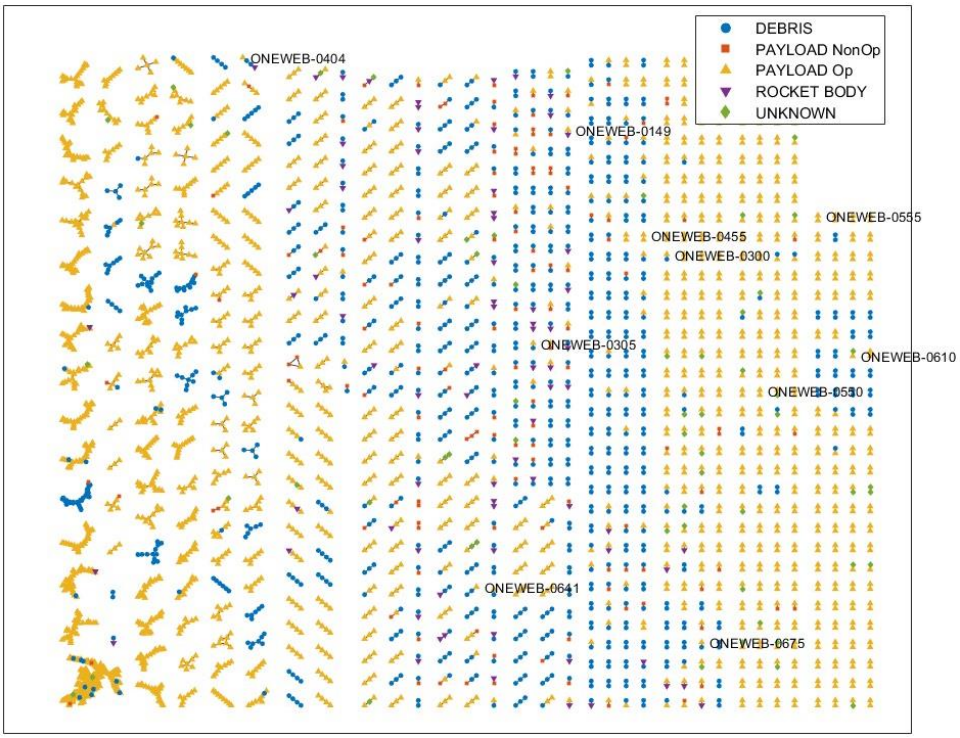

Figure 4.8: TLE dataset, nominal RSONet highlighting OneWeb satellites.

Connectivity, average degree and betweenness, simplified and refined scores slightly increase: the minimal observed variations are attributed to the small number of objects removed, compared to the previous case. However, results remain meaningful: this concept has been proved in Sect. 4.3.4. The danger score is increased due to the removal's emphasis on relatively small-mass objects, as observed previously.

Table 4.3: Metrics before and after the OneWeb satellites removal, for TLE dataset.

	n	m	β	$\hat{d}$	$\hat{B}$	PoC	S	R	D
Nominal TLE	3562	2590	0.73	1.45	4.97e2	2.35e-5	4.97e6	5.81e-2	26.58
OneWeb Removed	3544	2580	0.73	1.45	4.99e2	2.52e-6	4.99e6	5.82e-2	26.66

4.2.3. Both Starlink and OneWeb

The removal of both the selected mega-constellations provides a clear understanding of the effort required for monitoring conjunctions within the specified distance threshold of 3 km. Removing Starlink and OneWeb satellites decreases the number of conjunctions performed from the 1st to the 31st of May 2023 of 1783, approximately 60 less conjunctions per day. It is worth noting that, as indicated in Table 4.4, the danger score exhibits an increase, for same reason observed in the individual cases described previously.

Table 4.4: Metrics before and after the removal of both the mega-constellations.

	n	m	β	$\hat{\mathrm{d}}$	$\hat{\mathrm{B}}$	PoC	S	R	D
Nominal TLE	3562	2590	0.73	1.45	4.97e2	2.35e-5	4.97e6	5.81e-2	26.58
Both MC Removed	1368	807	0.59	1.18	2.52	2.66e-6	2.52e4	2.48e-2	48.97

4.3. Network centrality measures approaches

Hereafter, removal strategies based on network centrality measures are analysed. Specifically, a certain number of objects with highest degree, highest betweenness, and lowest closeness are removed from the network and the changes in the network embedding and danger score are assessed.

The number of objects to be removed is set to $N = 100$, to achieve a clear and visible understanding of the results. However, a sensitivity analysis has been performed to evaluate the sensitivity of the network robustness to the number of objects removed. Thus, the goal was to understand if the conclusions of the work are applicable despite the choice of N.

The motivations behind the choice of removing objects with highest degree and betweenness is readily understandable through their definitions: high degree nodes represent objects with extensive connectivity, contributing to larger network components and higher overall collision probability. It is evident that networks characterised by low connectivity, minimal components sizes, and low-degree nodes are desirable. This concept is directly connected to the real world, where tracking and particularly predicting conjunction events demand significant human and technological resources. Similarly, nodes with high betweenness identify components with large number of members, thus, the same rationale applies.

The reason behind the selection of removing objects with lowest closeness is more general: low values of closeness indicate a highly interactive environment. High interactive network implies an unstable environment, wherein, in the context of space network, the domino effect of collisions could occur more readily.

In the following approaches, the selected dataset exploits CDM sets, because of their higher reliability with respect to TLEs.

4.3.1. Degree

In Figure 4.9, the nominal RSO population performing conjunctions from the 1st to the 31st of May 2023 is depicted, highlighting the types of objects involved.

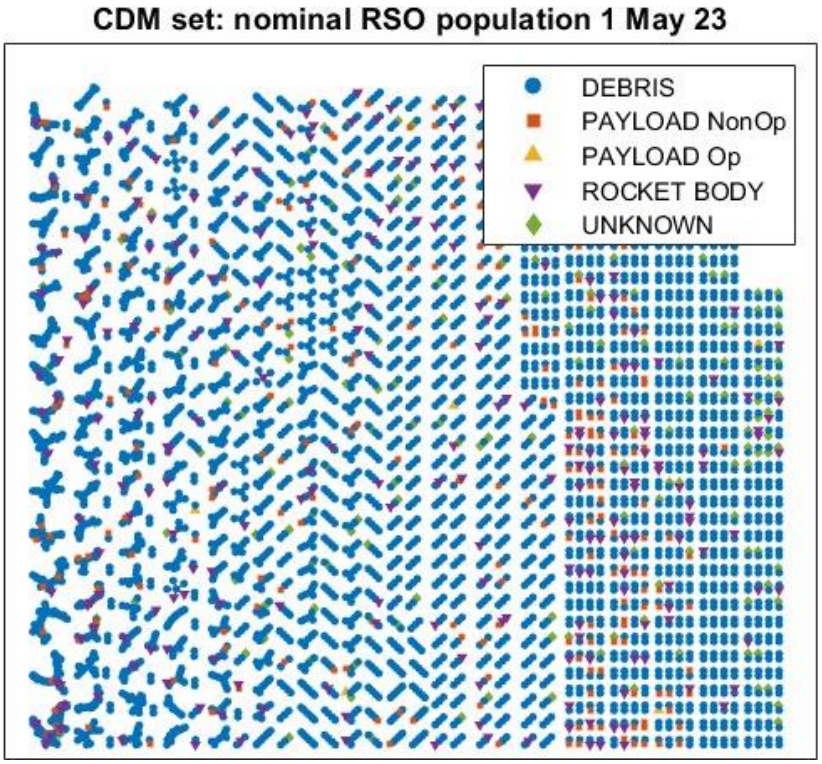

Figure 4.9: CDM dataset, RSONet representation before any removal.

Afterwards, the removal from the RSONet of 100 objects with highest degree is performed, obtaining the mitigated network in Figure 4.10. For visual clarity, the Figure 4.11 depicts the biggest components of the RSONet before and after the strategical removal, respectively, highlighting the degree of each node.

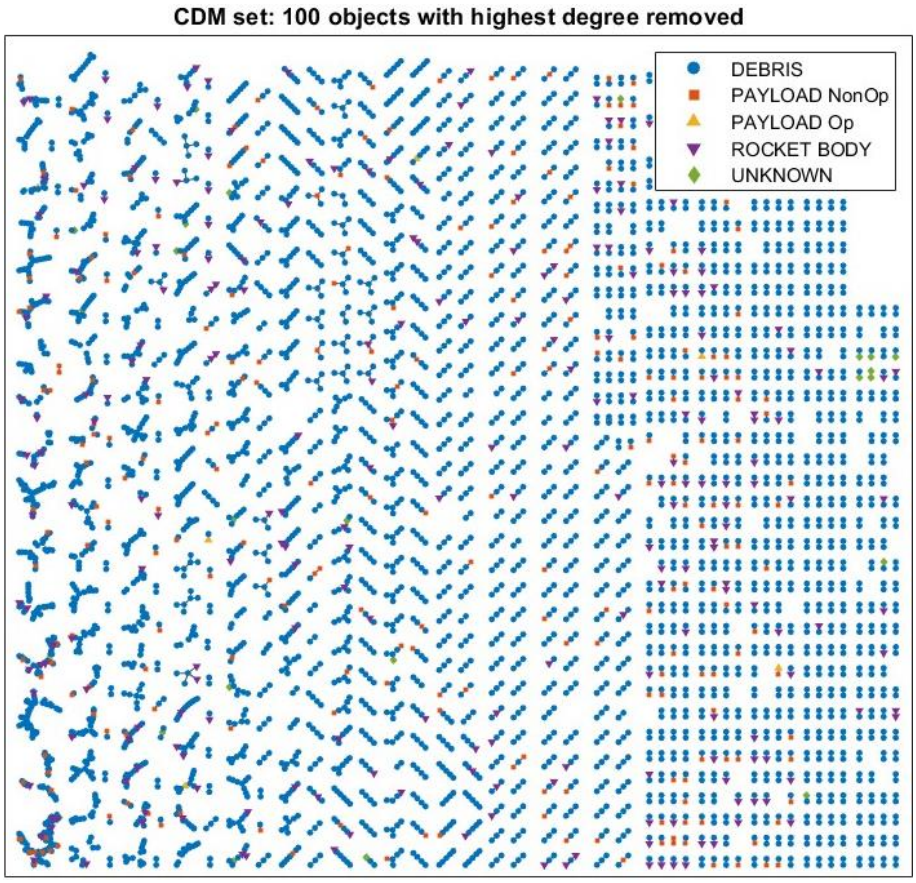

Figure 4.10: CDM dataset, RSONet representation after removal.

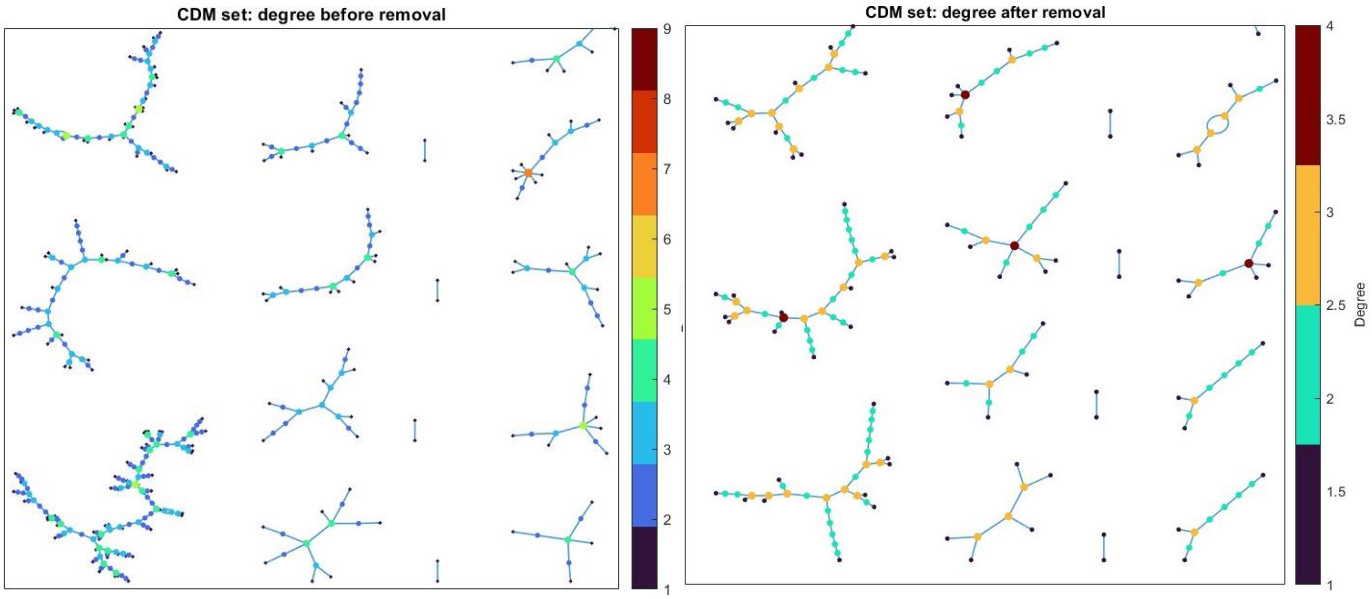

a) Biggest components nominal RSONet. (b) Biggest components mitigated RSONet.

Figure 4.11: CDM dataset, degree representation before and after the removal.

Furthermore, a list of the 5 objects with the highest degrees is reported in Table 4.5.

Table 4.5: Top 5 objects per degree.

	Degree	NORAD ID	Object Name
CDM	9	16963	COSMOS 1780 (GLONASS)
	9	26565	COSMOS 2376 (GLONASS)
	7	35221	FENGYUN 1C DEB
	6	30121	FENGYUN 1C DEB
	6	31097	FENGYUN 1C DEB

The two objects with highest degree, are not in the largest connected components. As shown in the Figure 4.12 they represent one of the smallest components instead. When processing CDMs, multiple conjunction events between the same two objects are filtered out if they are separated one from each other by less than 15 minutes. This is done to avoid counting more than once the same conjunction, which may be predicted multiple times due to corrections in the initial orbit determination of the two RSOs. Consequently, if multiple links appear between the same two nodes in the RSONet, they represent different conjunction events.

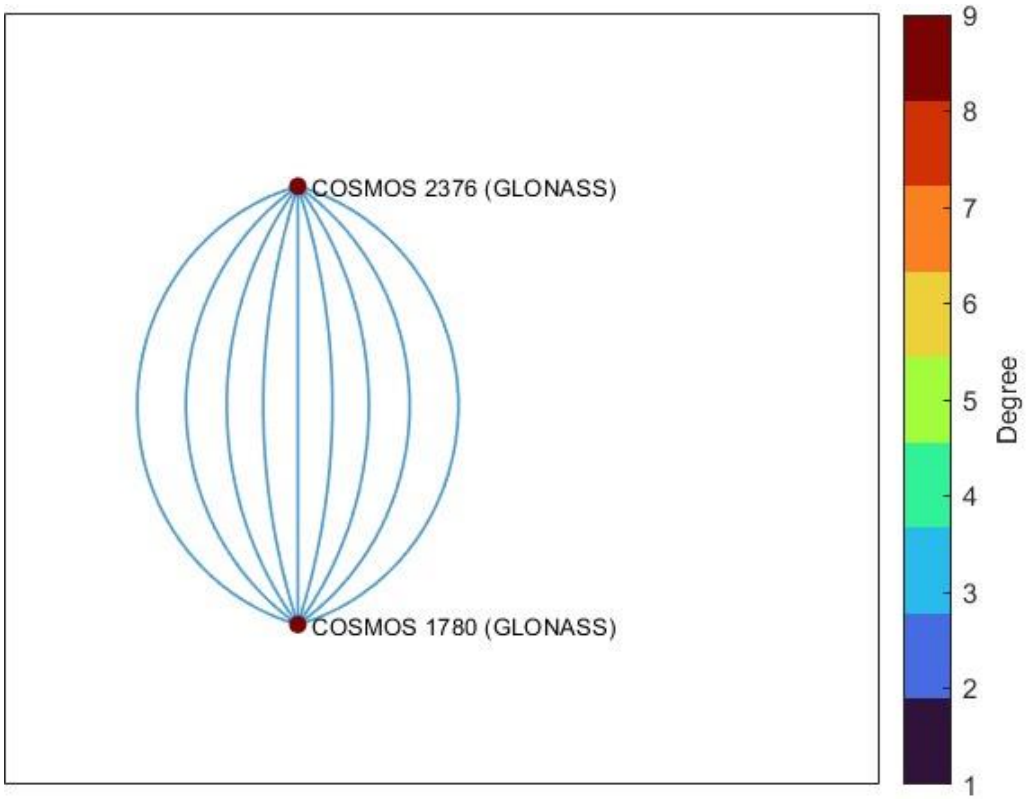

Figure 4.12: Objects with highest degrees.

The maximum value of degree is decreased following the strategy execution, from 9 to 4, as illustrated in Figure 4.13 and Figure 4.14, as indicated by the colorbar.

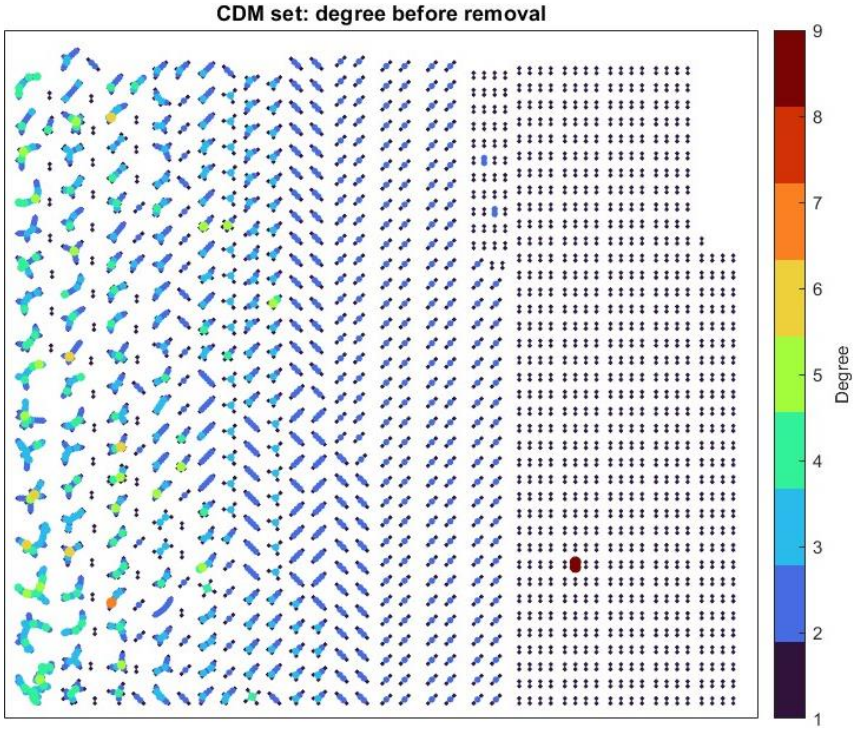

Figure 4.13: CDM set, degree representation before removal.

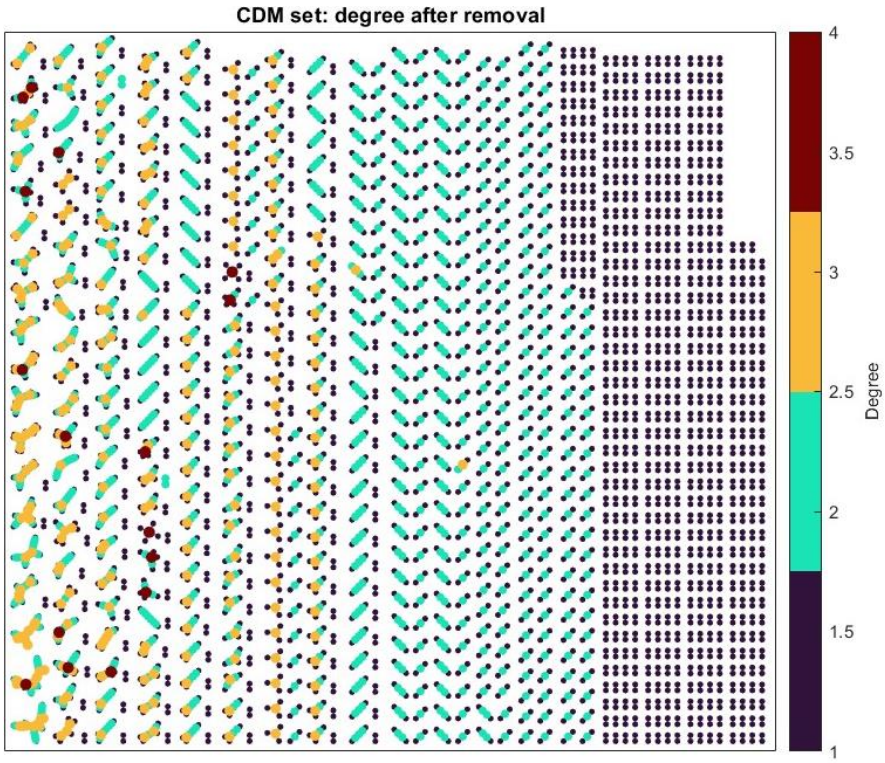

Figure 4.14: CDM set, degree representation after removal.

Besides the network visualizations, the evaluation of the adopted removal strategy based on the network centrality degree is focused on the analysis of the measures, reported in Table 4.6.

Table 4.6: network measures for nominal and mitigated populations.

	n	m	β	$\hat{d}$	$\hat{B}$	PoC	S	R	D
Nominal CDM	4694	3406	0.73	1.45	4.41e1	6.25e-4	4.41e5	2.36	9019
Degree Approach	4406	2989	0.68	1.36	4.20	6.48e-4	4.20e4	2.26	1.3e4

In total, 288 objects are vanished from the network, of which 100 were removed and 188 were left with no conjunctions, thus also eliminated. The connectivity decreased of approximately 7%, together with the average degree and betweenness, meaning that the removal strategy is effective: the network is not robust to this elimination approach. On the contrary, the average danger score is increased, thus, removed objects had lower danger score with respect the average one. The reason is simple: concentrating the removal strategy on the degree, which is a property only related to the network, cannot bring benefits to a less danger environment. Even if the danger score depends on the refined score, which in turn depends on the centrality measures, it also depends on other danger-related properties, such as the object mass, type, probability of collision, etc. For this reason, the appropriate selection of targets to be removed from space should not be based only on this strategy. The same conclusion applies for the following strategies based only on centrality measures.

The Figure 4.15 shows how the RSONet simplified score, clear indicator of the connectivity, is changed after the removal.

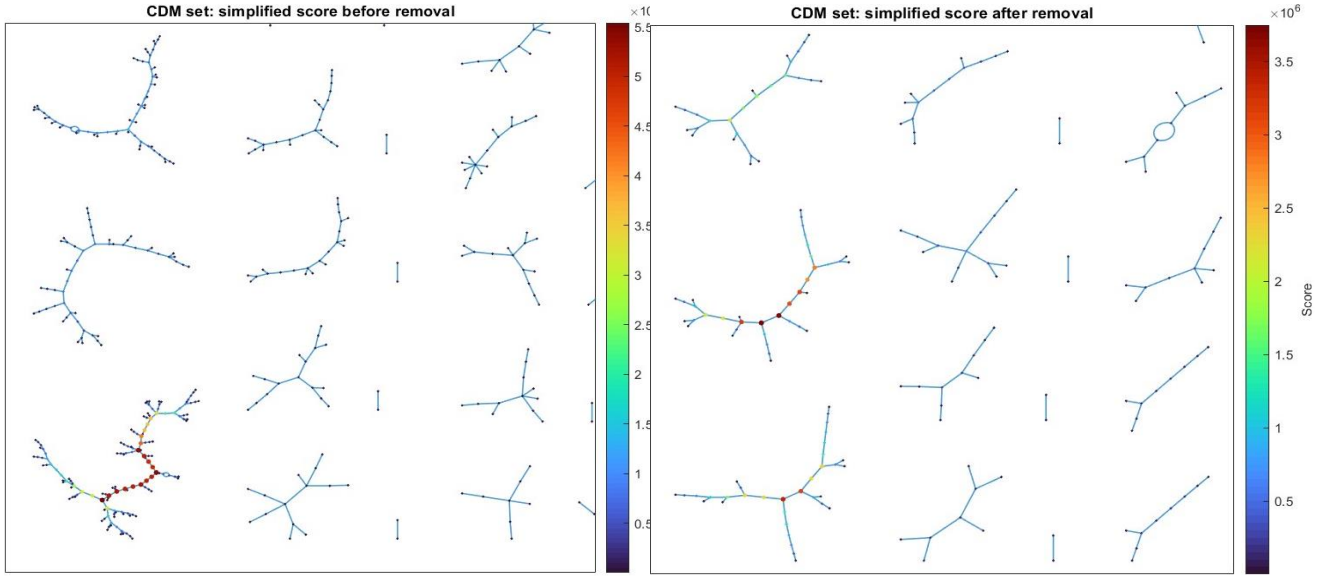

a) Biggest components nominal RSONet (b) Biggest components mitigated RSONet

Figure 4.15: RSONet simplified score for the biggest components, before and after removals.

4.3.2. Betweenness

Hereafter, the same approach as the previous case is applied to the RSONet, removing 100 objects with the highest betweenness values. The Figure 4.16 depicts the mitigated network representation.

A close-up view of the biggest components is in Figure 4.17 and in Figure 4.18, where only the biggest component is represented, completely split in many components.

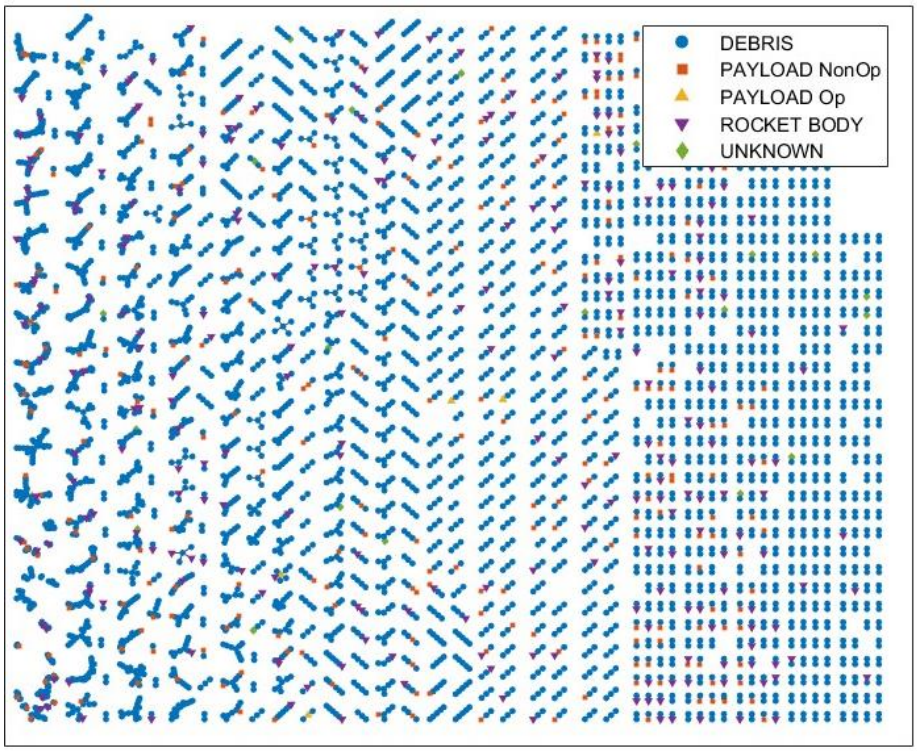

Figure 4.16: CDM dataset, 100 objects with highest betweenness removed.

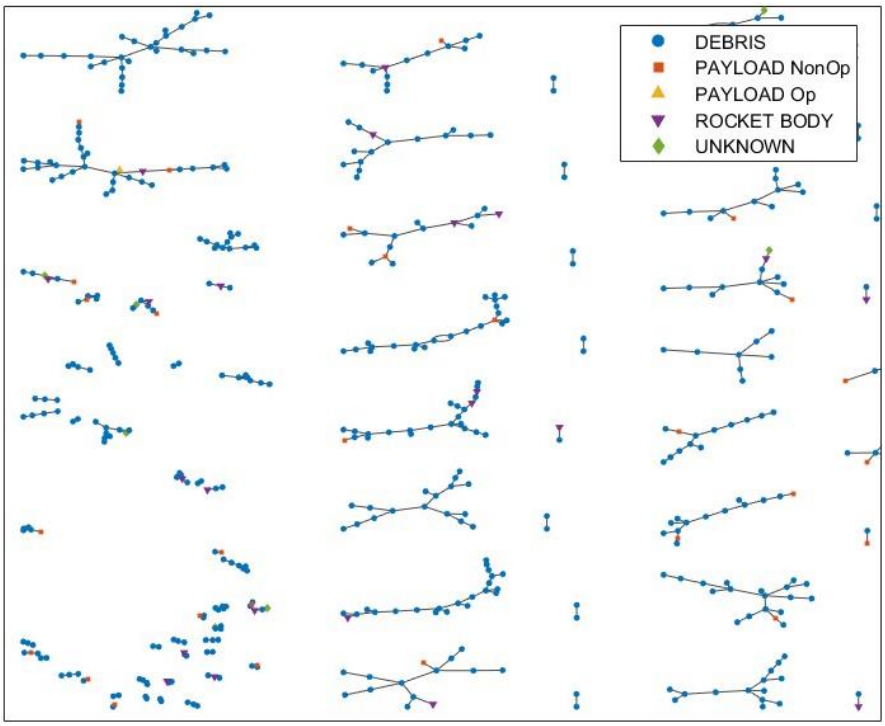

Figure 4.17: CDM dataset, biggest components after removals.

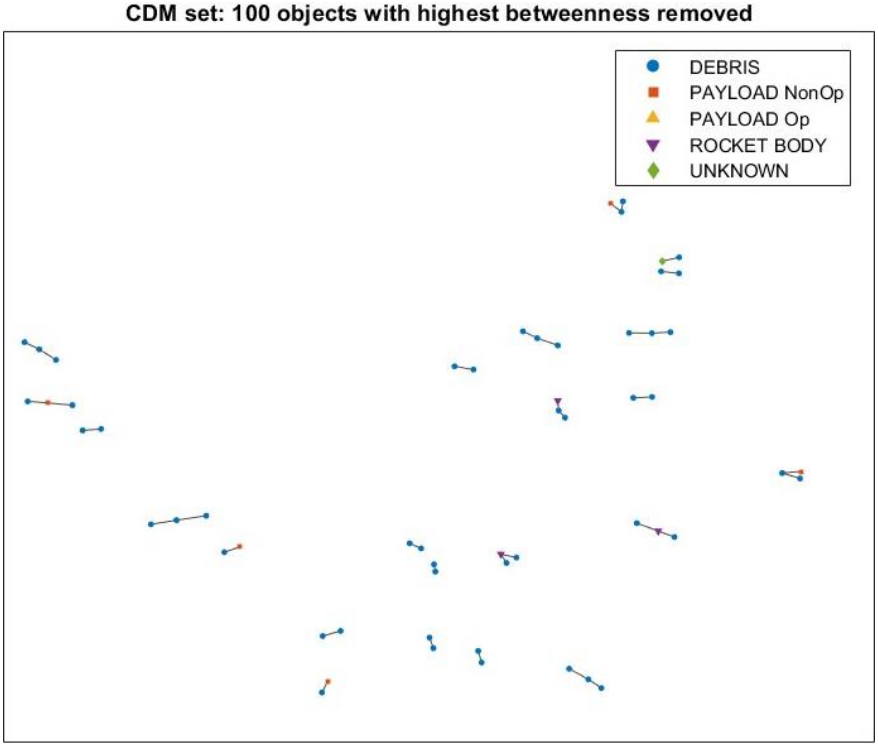

Figure 4.18: Biggest component, representation after removals.

The list of the 5 objects of the RSONet with the highest betweenness is reported in Table 4.7.

Table 4.7: Top 5 objects per betweenness.

	betweenness	NORAD ID	Object Name
CDM	5539	50793	COSMOS 1818 COOLANT
	5409	13719	SL-3 R/B
	5304	38532	METEOR 2-1 DEB
	5245	30092	FENGYUN 1C DEB
	5175	36699	FENGYUN 1C DEB

Figure 4.19, Figure 4.20 and Figure 4.21 show the visual differences in the betweenness, before and after the selected removal strategy. In a different way from the network centrality degree, objects with highest betweenness are all found in the biggest components, since betweenness is directly connected to the number of members in components. If this may seem like a positive aspect at first glance, the contemporaneous removal of the objects with highest betweenness will destroy almost completely the first largest connected components, but it will leave other large components unaltered. This approach can be seen as an overly concentrated and disproportionated removal, because it concentrates mostly on the biggest components.

This is reflected also in the network measures, which indicate a worse strategy with respect to the previous one based on degree.

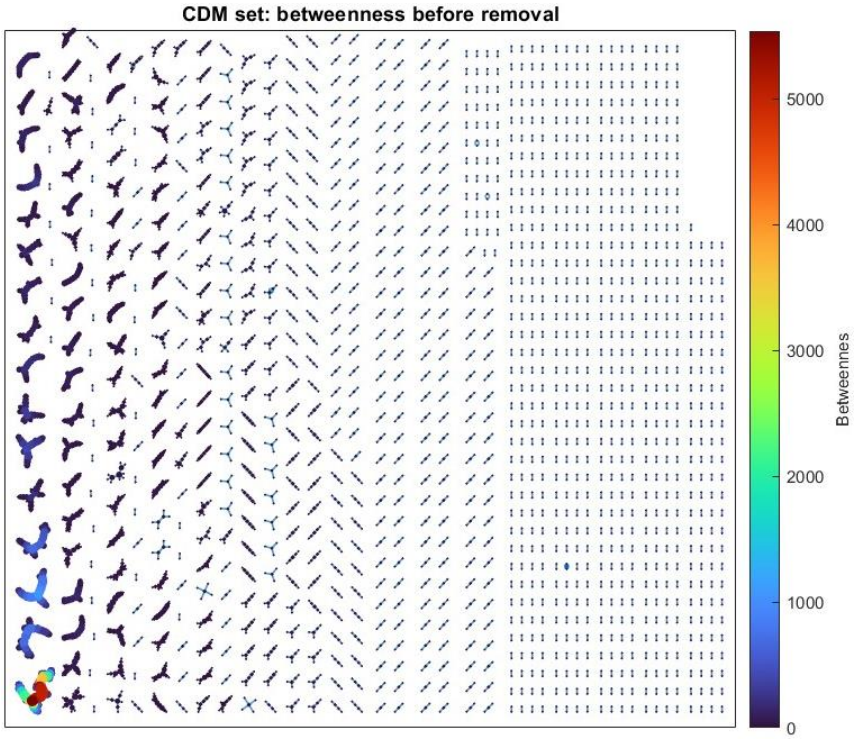

Figure 4.19: CDM dataset, RSONet highlighting the betweenness for each node.

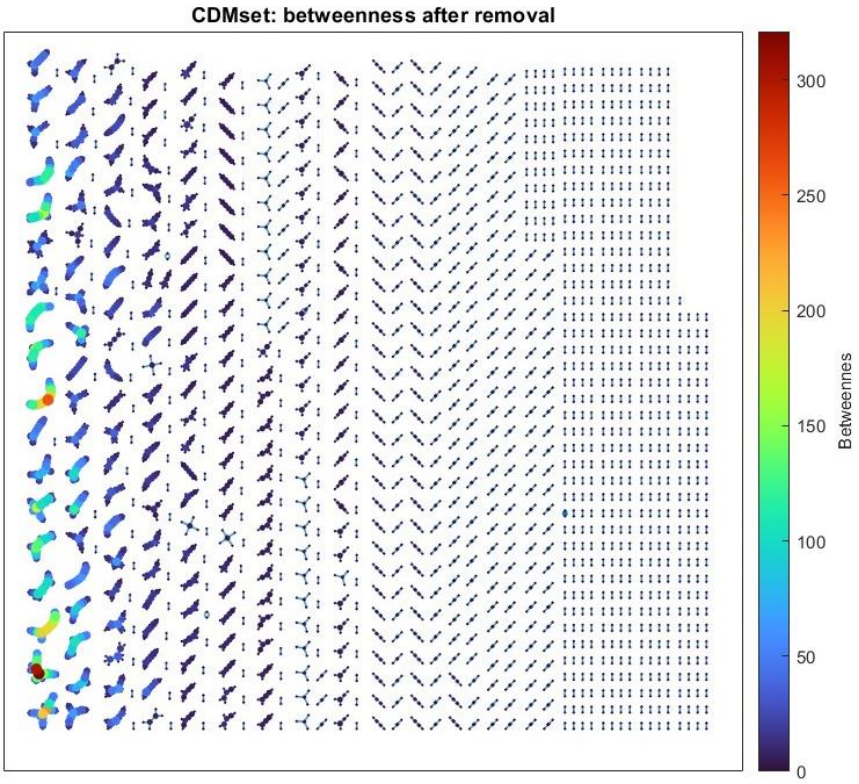

Figure 4.20: CDM dataset, betweenness representation after removal.

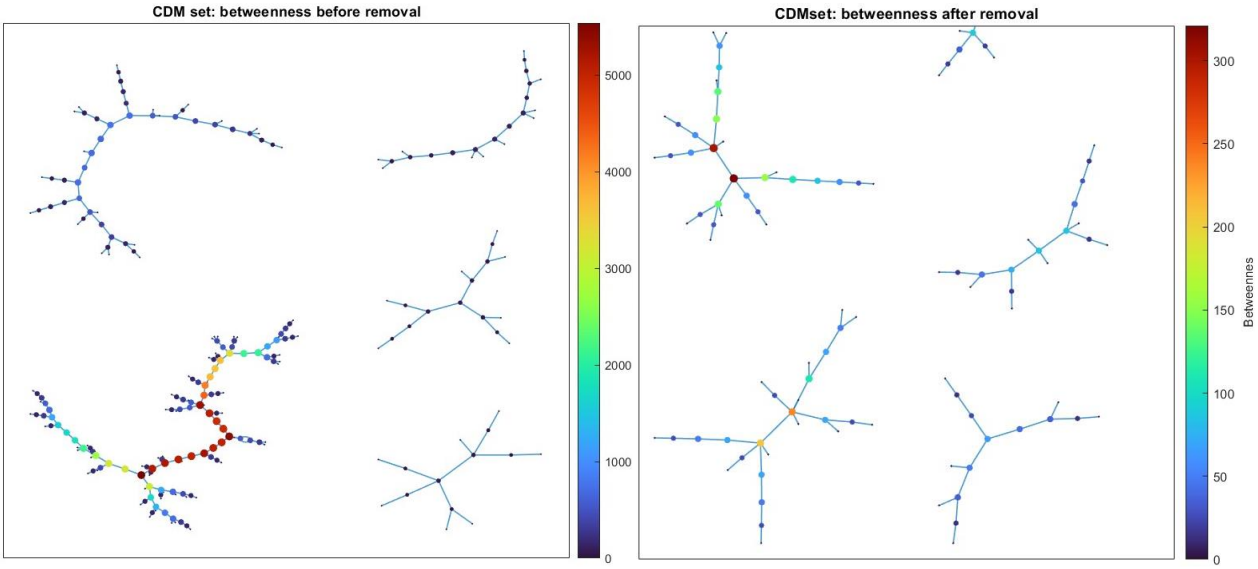

Figure 4.21: Biggest components, betweenness representation before and after removal.

By analysing Table 4.8, it is possible to evaluate the adopted strategy through the robustness of the network and the danger score.

Table 4.8: network measures for nominal and mitigated populations.

	n	m	β	$\hat{d}$	$\hat{B}$	PoC	S	R	D
Nominal CDM	4694	3406	0.73	1.45	4.41e1	6.25e-4	4.41e5	2.36	9019
Betweenness Approach	4542	3204	0.71	1.41	6.11	6.35e-4	6.11e4	2.19	1.2e4

In total, 152 objects are removed, of which 52 were removed because left with no conjunctions. The connectivity, the average degree and the average betweenness are decreased, but less than the previous strategy, indicating the current approach is less optimal in terms of connectivity. The danger score is increased, for the same reason as with the degree-based approach.

4.3.3. Closeness

The final strategy based on network centrality measures involves targeting the closeness. Specifically, 100 objects with lowest closeness are removed by the RSONet, and related measures are evaluated. In the Figure 4.22, the network representation, depicting the RSONet after the removal, highlights the object type of each node.

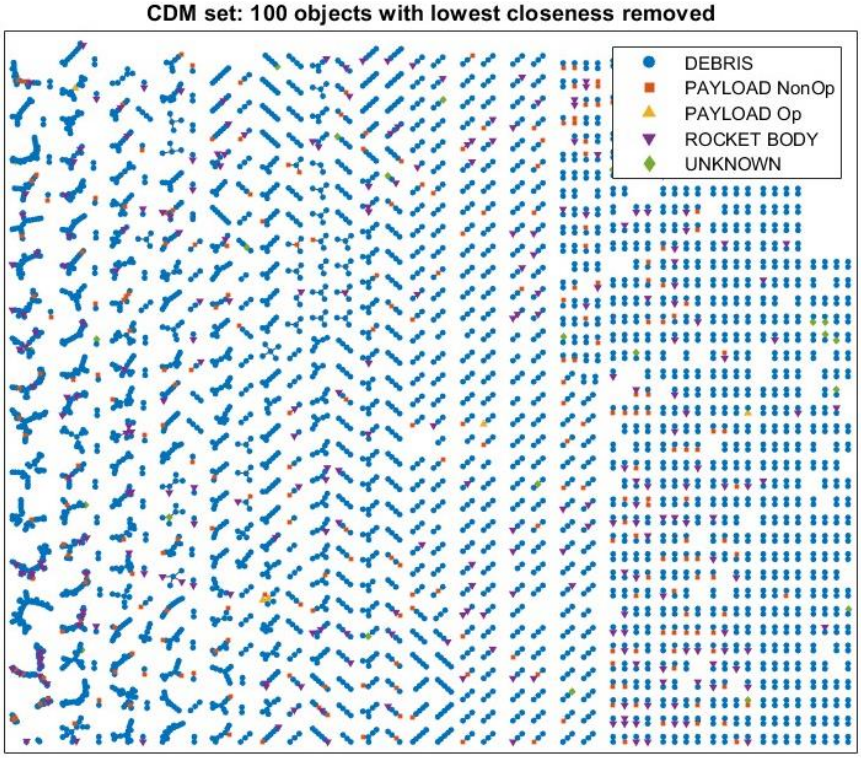

Figure 4.22: CDM dataset, RSONet representation after removal.

The Figure 4.23 is a close-up view of the biggest components, after the removal.

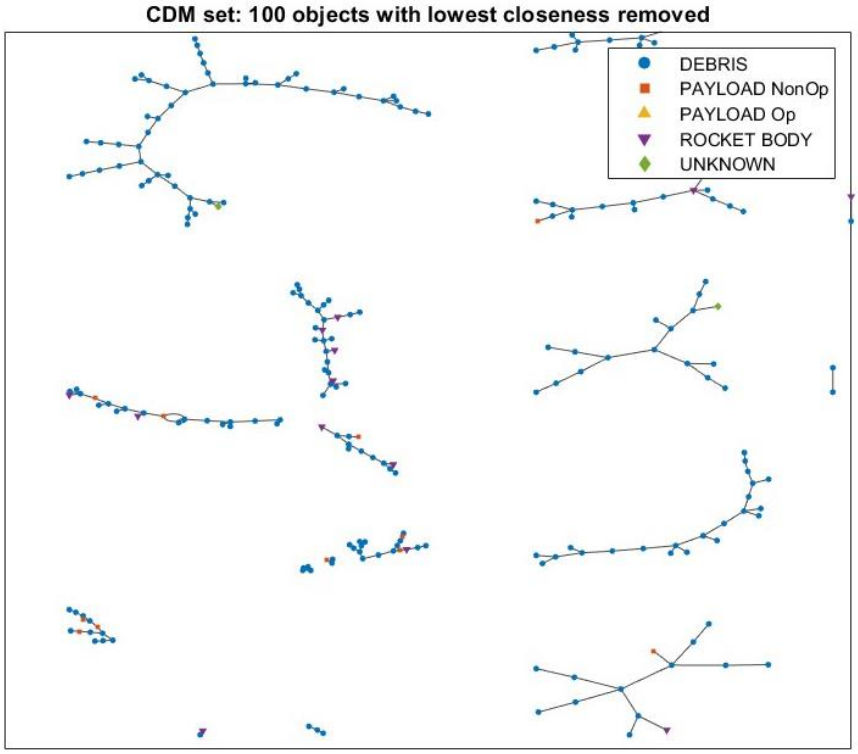

Figure 4.23: Biggest components after removal strategy.

The list of the 5 objects of the RSONet with the lowest closeness values is reported in Table 4.9.

Table 4.9: Top 5 objects per lowest closeness.

	closeness	NORAD ID	Object Name
CDM	2.275091e6	22480	SL-16 DEB
	2.284192e6	39302	SL-16 DEB
	2.284192e6	54553	CZ-6A DEB
	2.318493e6	38022	IRIDIUM 33 DEB
	2.326247e6	31419	FENGYUN 1C DEB

The Figure 4.24, Figure 4.25 and Figure 4.26 show the visual differences in the closeness, before and after the selected removal strategy.

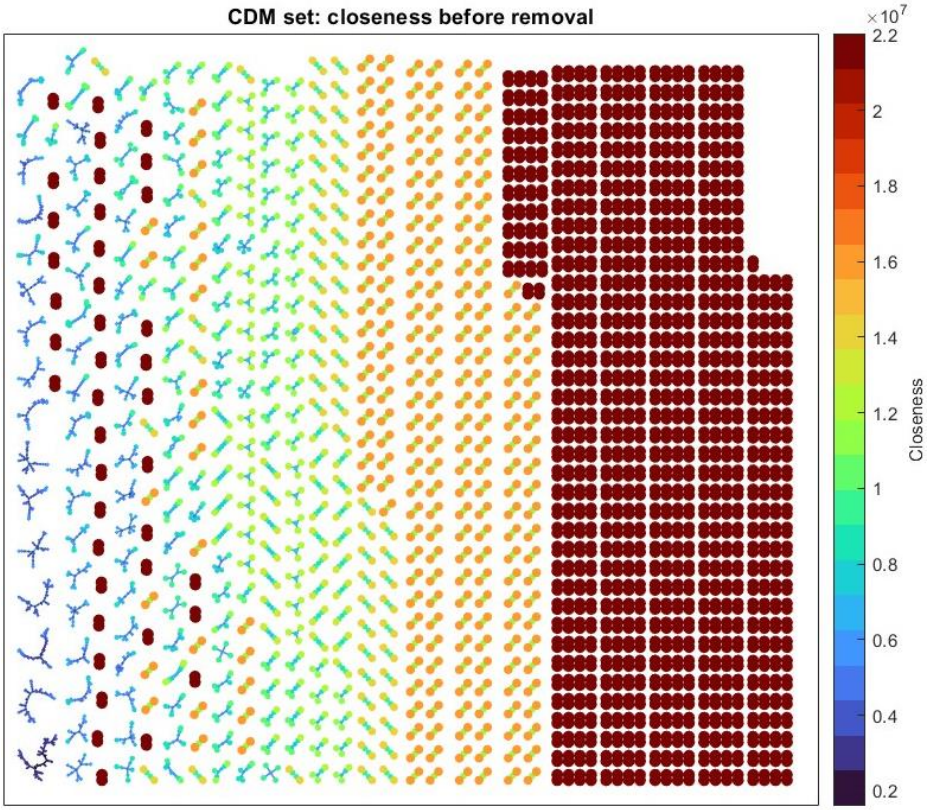

Figure 4.24: CDM dataset, closeness representation before removal.

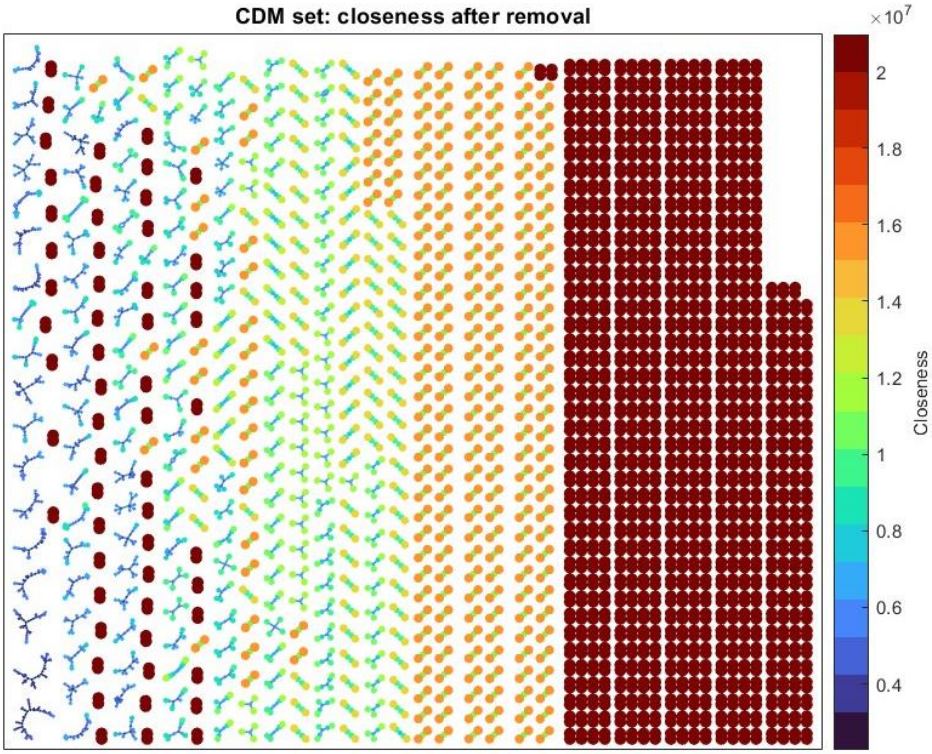

Figure 4.25: CDM dataset, closeness representation after removal.

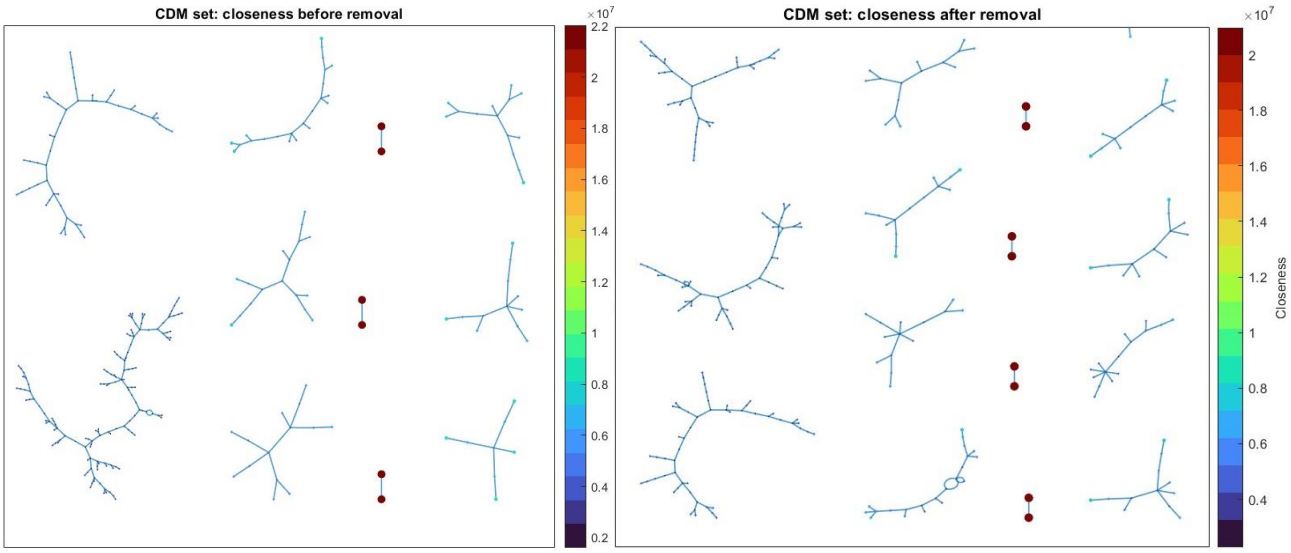

Figure 4.26: Biggest components, closeness representation before and after removal.

Similarly to the previous cases, Table 4.10 reports network measures, thus, conclusions on the robustness of the network and on the danger score to this kind of strategy can be established.

Table 4.10: network measures for nominal and mitigated populations.

	n	m	β	$\hat{d}$	$\hat{B}$	PoC	S	R	D
Nominal CDM	4694	3406	0.73	1.45	4.41e1	6.25e-4	4.41e5	2.36	9019
Closeness Approach	4580	3274	0.72	1.42	1.11e1	6.28e-4	1.11e5	2.29	1.2e4

Thus, 114 objects are removed from the RSONet, of which 14 left with no links after the removal, leading to 132 less conjunction events in the selected period. The connectivity, average degree and betweenness are slightly decreased, implying this strategy is the less effective in terms of network robustness, with respect the previous ones.

The average danger score, as in the preceding strategies, is increased for the same reason explained in Sect. 4.3.1.

4.3.4. Sensitivity Analysis to N

Hereafter, the focus is on the selection of the number of objects to be removed, namely N. The aim is to determine whether there is any connection between the results of the work and the number of nodes to be eliminated. Essentially, the aim is to ascertain whether even removing just one object from the network yields the same conclusions as before. This sensitivity study is crucial because it allows the work to be genuinely

compared to other methods for selecting targets for debris removal activities, especially considering that removing many objects almost simultaneously is currently an impossible challenge.

In Figure 4.27, a three-dimensional histogram reports $\Delta\beta$, for the 3 previous strategies, removing 100 and 200 objects from CDM RSONet. Note that $\Delta\beta$ is the difference between the connectivity of the nominal RSONet and the one after the removals:

$$\Delta\beta = \beta_{nom} - \beta_{case} \tag{4.1}$$

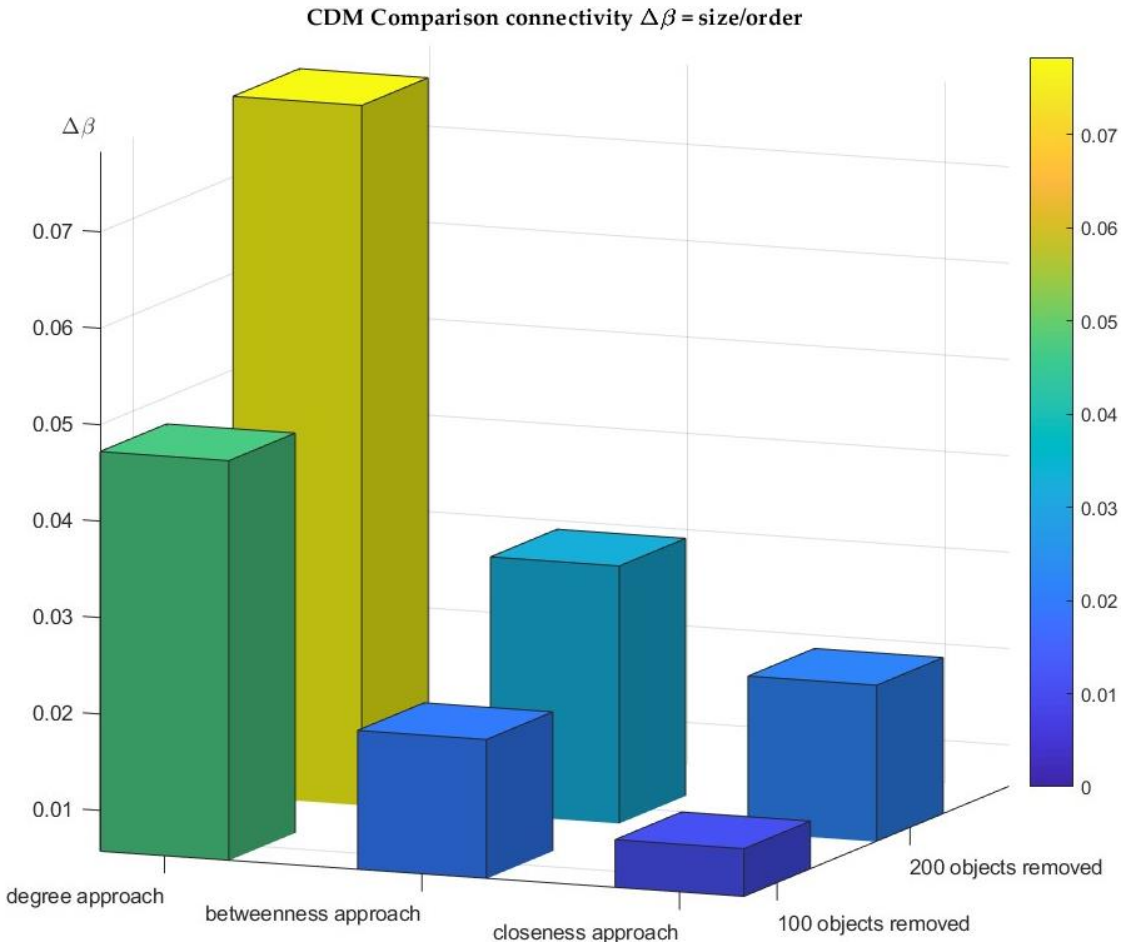

Figure 4.27: Change in connectivity after different strategies of removal (CDM).

It is evident that, by increasing N, the influence on the network robustness increases. In essence, removing more objects results in greater effects on the connectivity and robustness.

For completeness, also the case of TLE RSONet is documented, in Figure 4.28.

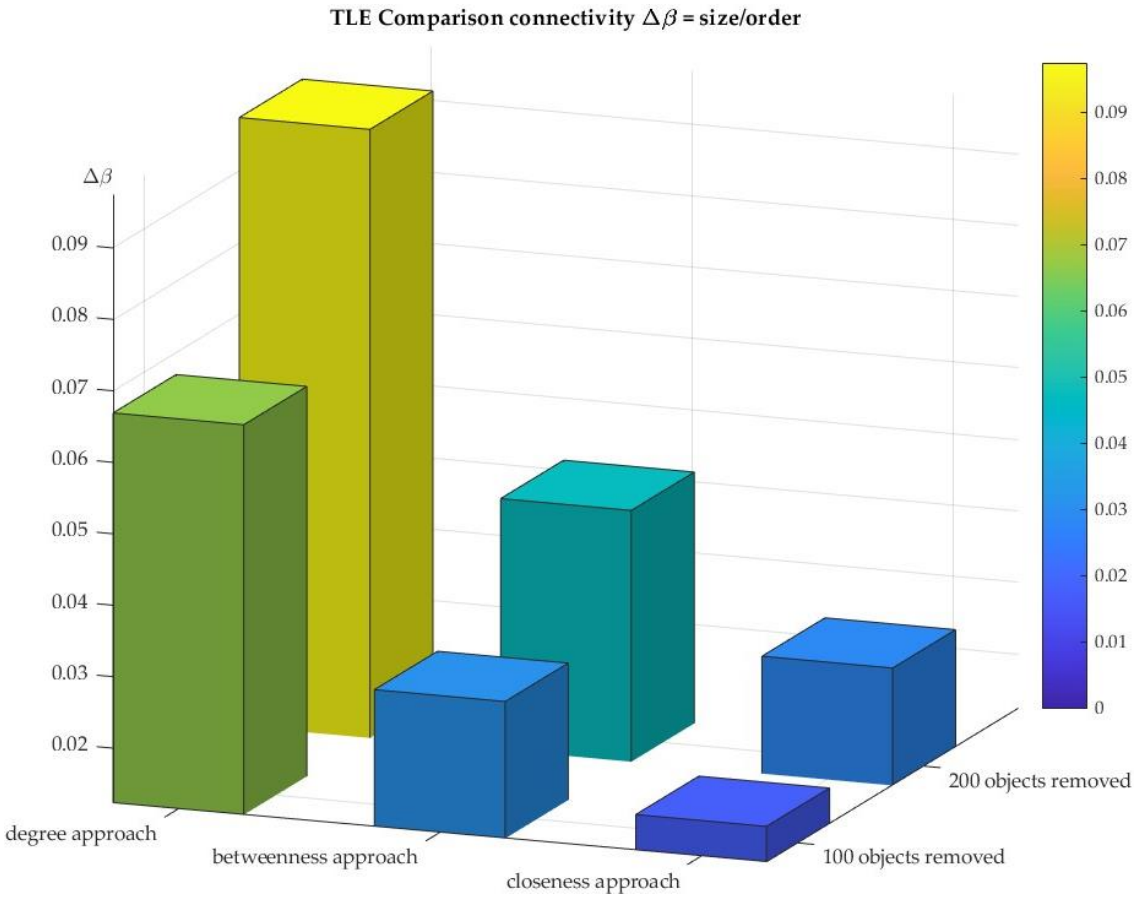

Figure 4.28: Change in connectivity after different strategies of removal (TLE).

The same conclusion of the case of CDM RSONet applies. Finally, to conclude that vulnerability and N are directly proportional, and conclusions of the work apply despite the selection of N, a wide set of N, is defined: 200, 100, 50, 20, 10, 5 and 1 object with the highest degree are removed from the RSONet and the robustness is assessed. The Figure 4.29 resumes $\Delta\beta$ computations, for each case.

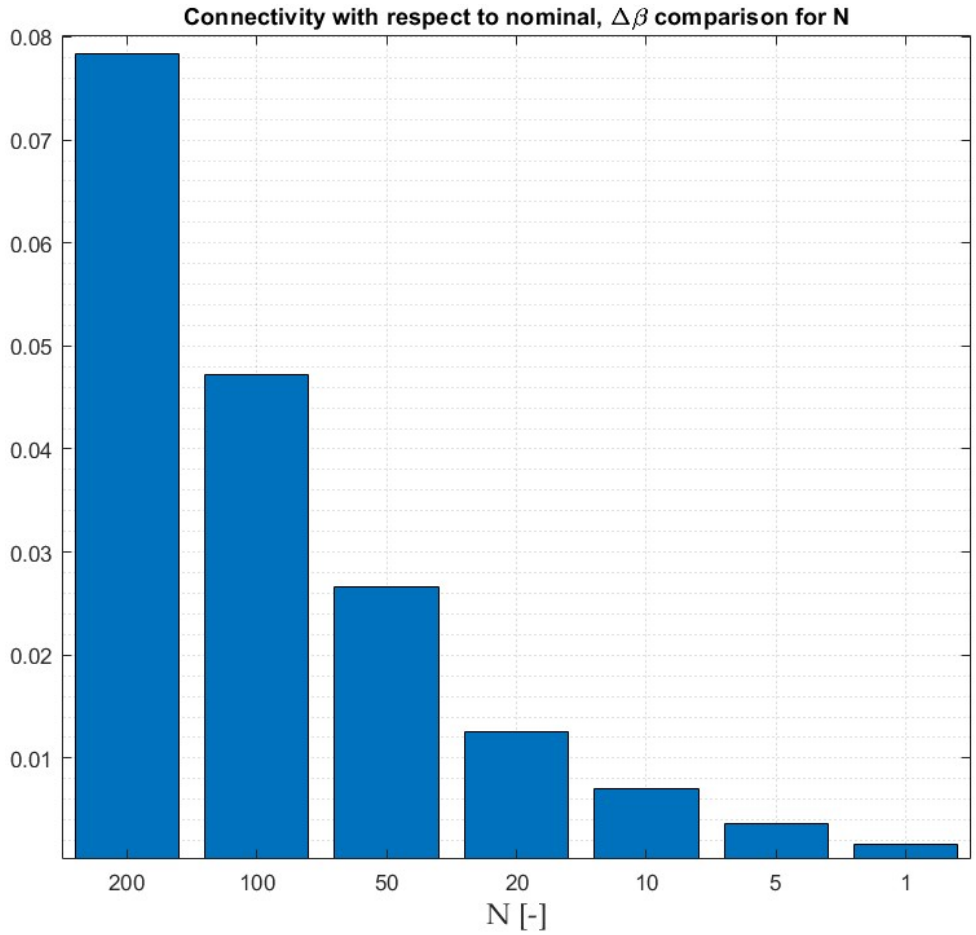

Figure 4.29: Δβ removing different N with highest degree.

The graph clearly shows the direct proportionality of N and connectivity. Similar findings were identified for the alternative strategies outlined throughout the thesis.

4.3.5. Comparison

The selection of the best strategy in terms of network robustness and danger score, among the previous case studies is hereby presented. Besides the mitigated populations previously identified, a strategy based on random removals is developed: the same N are removed randomly from the RSONet, utilising a simple built-in *MATLAB* function that casually selects numbers from given bounds.

In Figure 4.31, the connectivity β of each CDM-based case is depicted: the first bin corresponds to the initial CDM RSO population. The bin associated to the random removal strategy highlights the worst approach among them all, because the change in network connectivity is the smallest. The same conclusions can be done analysing the Figure 4.31, in which the $\Delta\beta$ is showed.

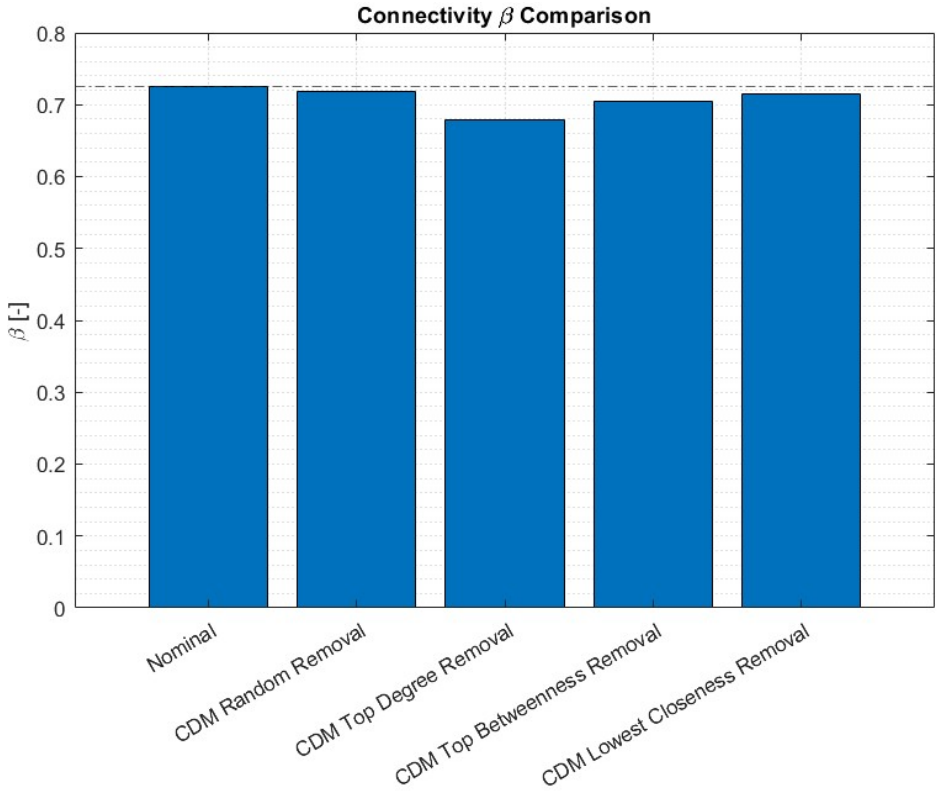

Figure 4.30: connectivity of CDM removal strategies.

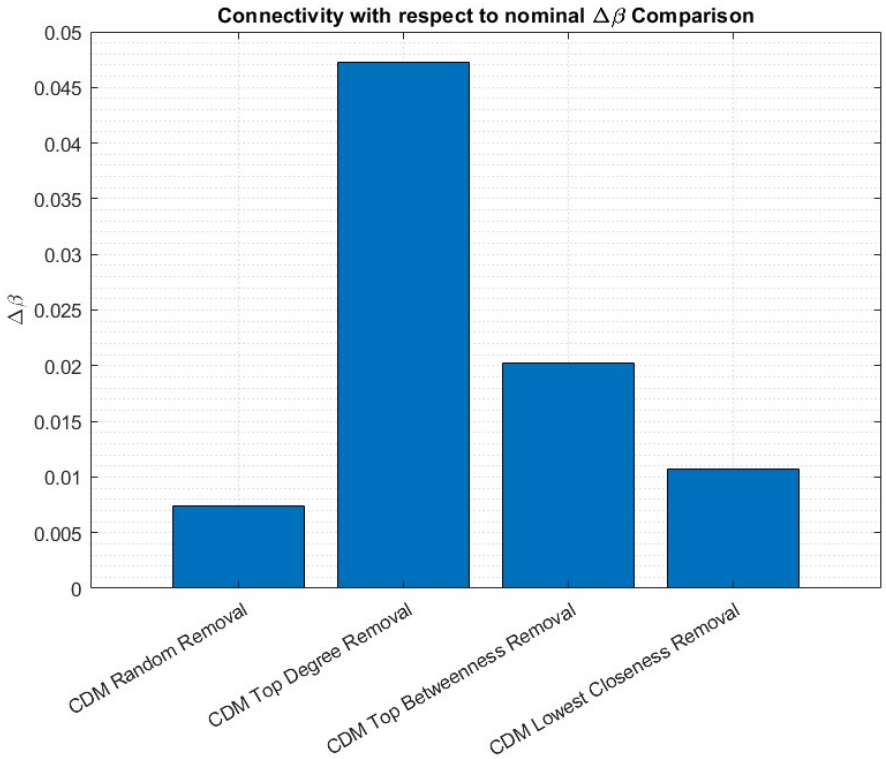

Figure 4.31: Δβ of CDM removal strategies.

Same exact conclusion for what regards average degree and betweenness, as showed in Figure 4.32 and Figure 4.33.

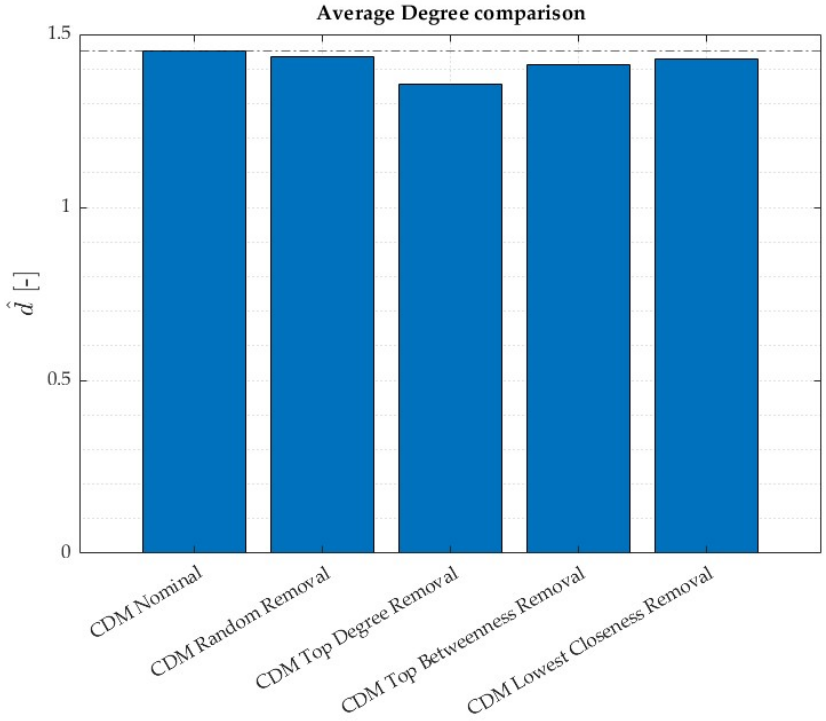

Figure 4.32: Average degree for each case.

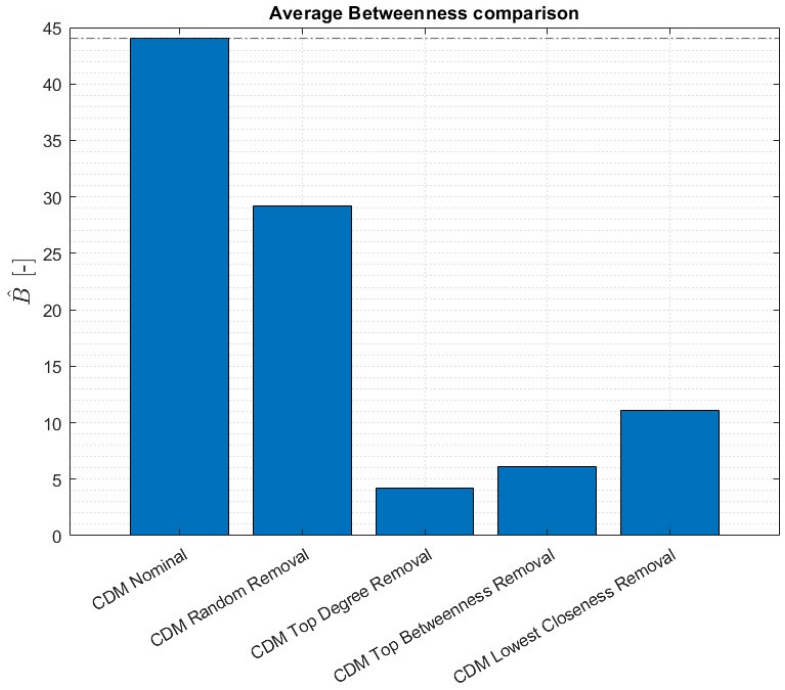

Figure 4.33: Average betweenness for each case.

Lastly, the average danger score is compared in Figure 4.34.

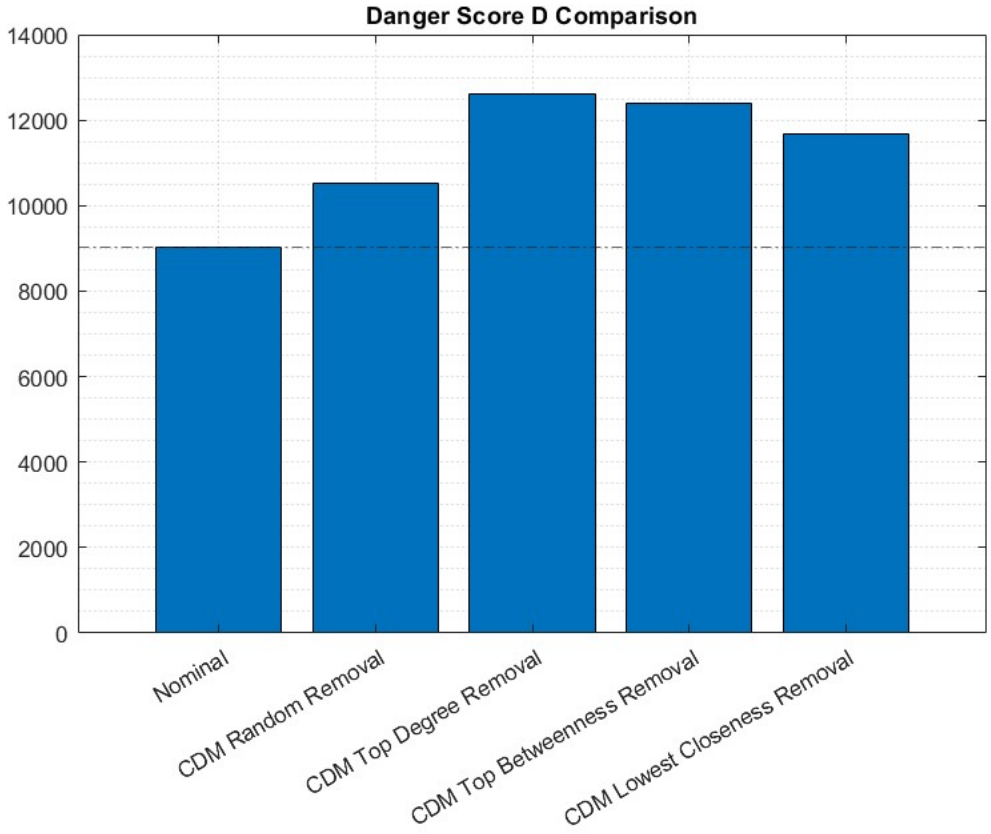

Figure 4.34: Average danger score for each case.

The best strategy in terms of robustness appears to be the less efficient in terms of danger score. As previously explained, this was expected: the danger score is depending on other parameters which are not related to network domain whereas the centrality measures do. Moreover, in CDM case, since the removal strategies almost completely focus on eliminating mostly only debris (i.e., objects with low mass) because of the way CDMs are defined (with 86% presence of debris), the average danger score increases with respect the nominal condition.

4.4. Network weighted measures approaches

In this section, removal strategies are based on weighted measures: 100 objects with highest strength, highest RSONet scores, highest danger score, and highest probability of collision are removed from the RSONet.

4.4.1. Probability of Collision

The removal from the RSONet of 100 objects belonging to the 100 pairs with highest collisional probability is performed, obtaining the mitigated network in Figure 4.35. The selection of the node to be removed from each pair is random. For visual clarity,

the Figure 4.36 depicts the biggest components of the RSONet before and after the strategical removal.

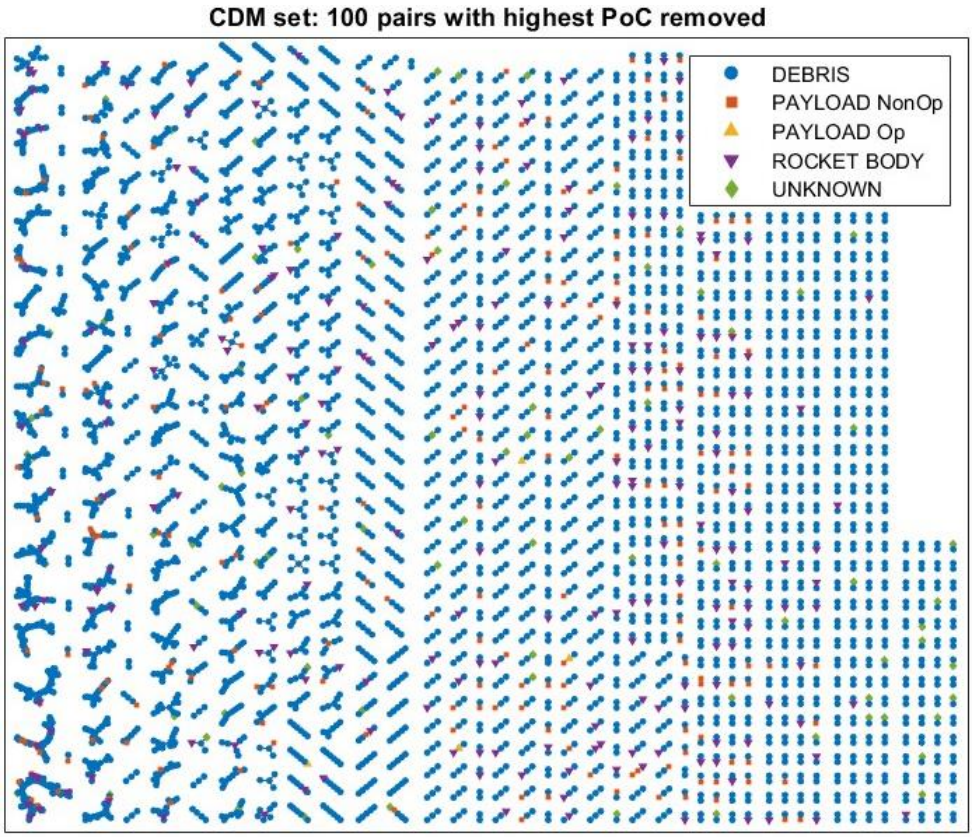

Figure 4.35: CDM dataset, RSONet representation after the removal.

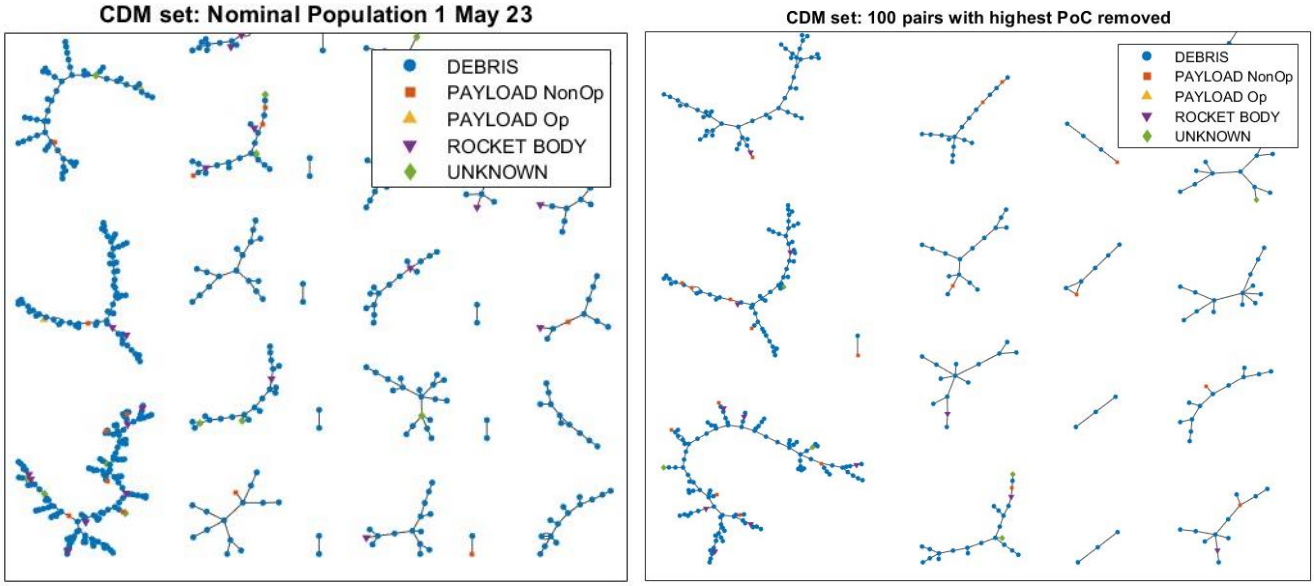

Figure 4.36: CDM dataset, RSONet before and after removals.

The highest probability of collision before the application of the strategy is associated to the conjunction between two debris: COSMOS-2251 DEB and FengYun-1C DEB,

with a $PoC = 0.147$. The two objects with highest PoC are not in any of the biggest components, while they are found in one of the smallest components instead.

After the removals, the highest PoC is between with a FengYun-1C DEB and a COSMOS-1867 COOLANT, with a $PoC = 0.003$.

The average value of collisional probability is decreased, from 6.24e-4 to 4.07e-4, as it is illustrated in Table 4.11.

Table 4.11: network measures for nominal and mitigated populations.

	n	m	β	$\hat{d}$	$\hat{B}$	PoC	S	R	D
Nominal CDM	4694	3406	0.73	1.45	4.41e1	6.25e-4	4.41e5	2.36	9019
PoC Approach	4506	3241	0.72	1.44	2.96e1	4.07e-4	2.96e5	1.45	6708

In total 188 are removed of which 88 were left with no conjunctions. The connectivity slightly decreased, together with the average degree and betweenness, similarly to the random removal strategy. The average danger score is decreased, thus, removed objects had higher danger score with respect to the average. This is primarily due to the considerable influence of the PoC on the refined score, which, along with mass, is a key determinant of the danger score: indeed, also the average refined score is decreased.

The Figure 4.37 shows how the RSONet refined score, clear indicator of the danger score, is changed after the removal.

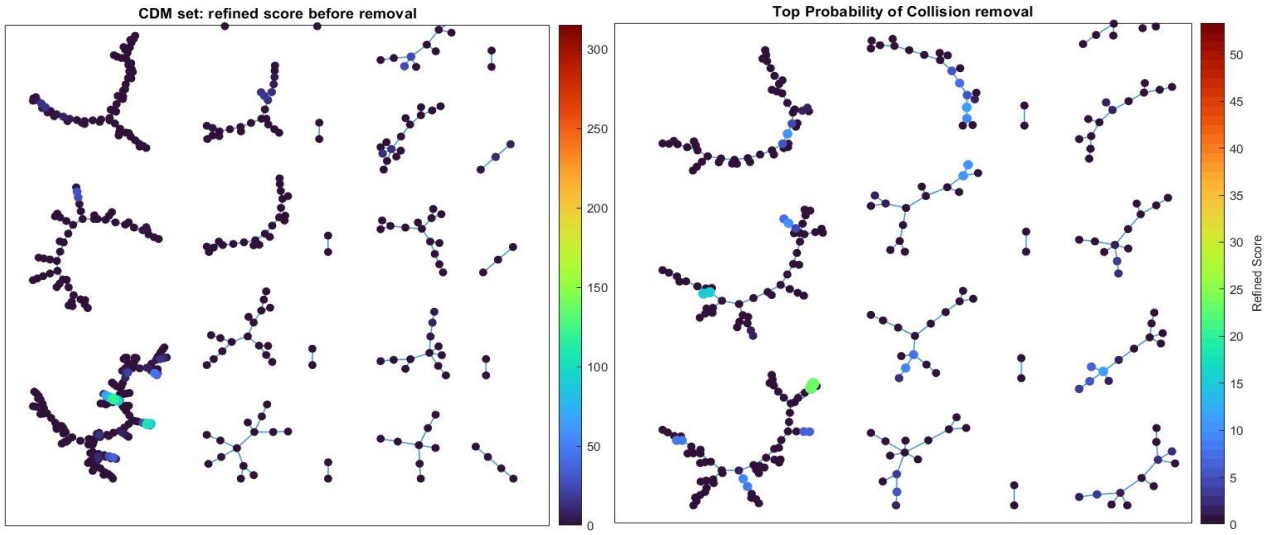

a) Biggest components nominal (b) Biggest components mitigated

Figure 4.37: RSONet refined score for the biggest components, before and after the removals.

4.4.2. Strength

The removal from the RSONet of 100 objects with highest strength is performed, obtaining the mitigated network in Figure 4.38. For visual clarity, the Figure 4.39 depicts the biggest components of the RSONet before and after the strategical removal.

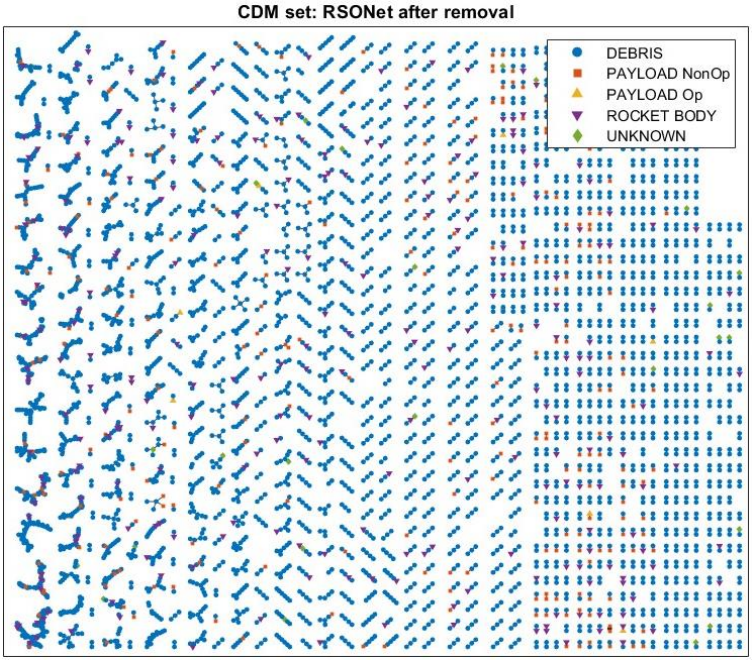

Figure 4.38: CDM dataset, RSONet representation after the removal.

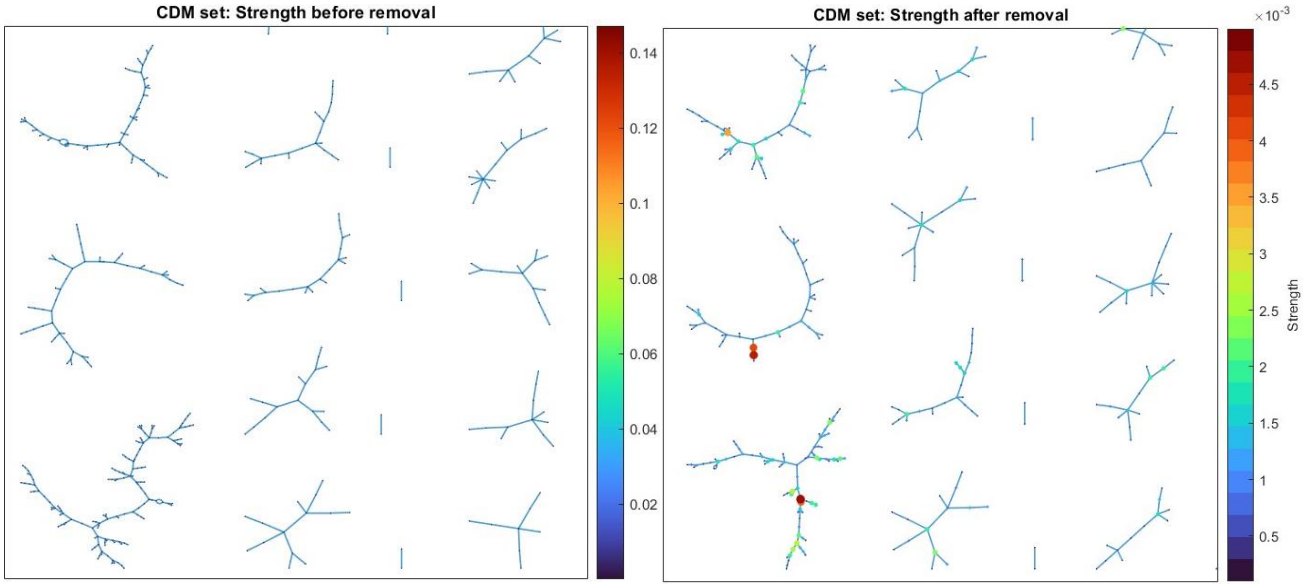

Figure 4.39: Biggest components before and after the removal.

A list of the 5 objects with the highest strength is reported in Table 4.12.

Table 4.12: Top 5 objects per strength.

	Strength	NORAD ID	Object Name
CDM	4.990963e-03	5731	METEOR 1-10
	4.904103e-03	43331	SCOUT G-1 DEB
	4.877587e-03	4973	THORAD AGENA D DEB
	4.858835e-03	41076	NOAA 16 DEB
	4.846475e-03	31088	FENGYUN 1C DEB

The ranking of the objects with highest strength differs from the one based on the degree (Table 4.5), because strength is a property which incorporates the probability of collision for each link, thus weighting the degree accordingly.

In Table 4.13 , network measures are reported.

Table 4.13: Network measures for nominal and mitigated populations.

	n	m	β	$\hat{d}$	$\hat{B}$	PoC	S	R	D
Nominal CDM	4694	3406	0.73	1.45	4.41e1	6.25e-4	4.41e5	2.36	9019
Strength Approach	4555	3272	0.72	1.44	1.89e1	4.45e-4	1.89e5	1.74	8539

In total 139 are removed of which 39 were left with no conjunctions. The connectivity slightly decreased, together with the average degree and betweenness, similarly to the random removal strategy. The approach is less effective in terms of robustness with respect the standard strategy based only on degree. On the contrary, the average danger score is decreased, meaning that removed objects had higher danger score with respect the average one. The reason is because the strength, is highly affecting the refined score, which is the main actor together with mass of the danger score: indeed, also the average refined score is decreased.

4.4.3. RSONet Refined Score

The removal from the RSONet of 100 objects with highest RSONet refined score is performed. In Figure 4.40, the obtained mitigated RSONet is depicted. The Figure 4.41 and Figure 4.42 illustrate the refined score per each node, before the removal and after the removal.

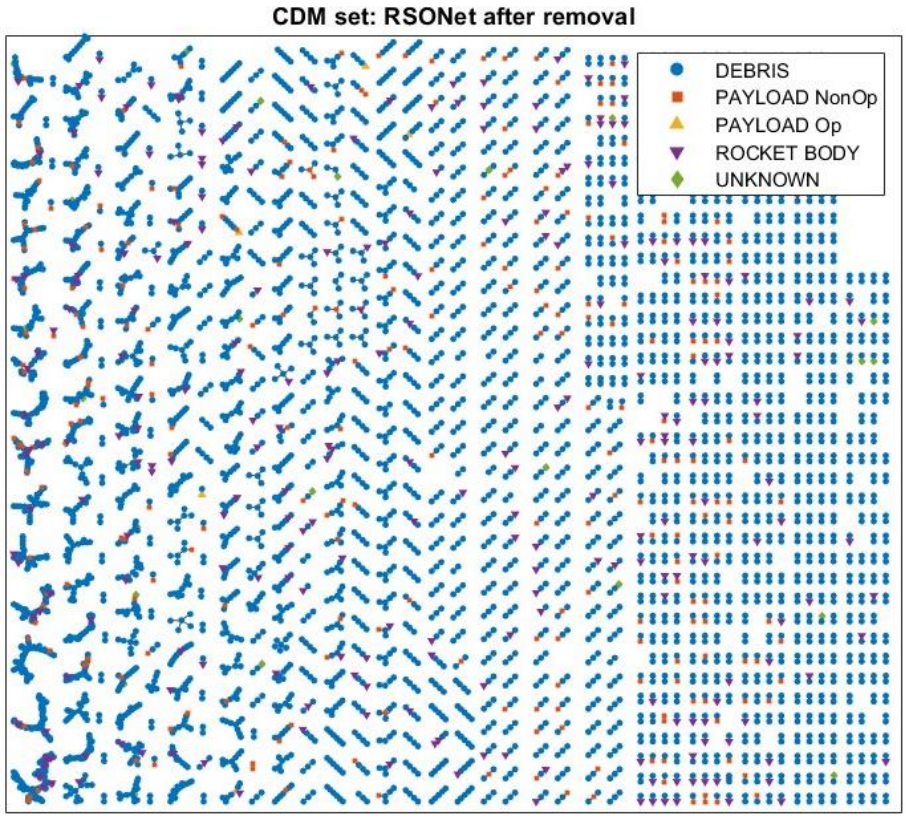

Figure 4.40: CDM dataset, RSONet representation after removal.

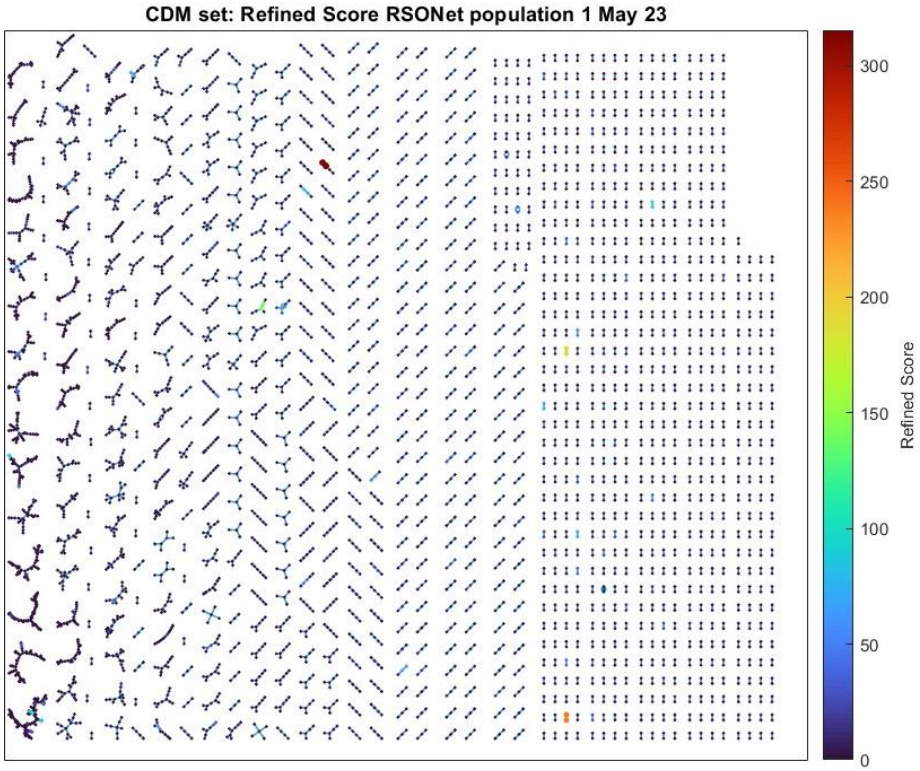

Figure 4.41: CDM dataset, refined score before the removal.

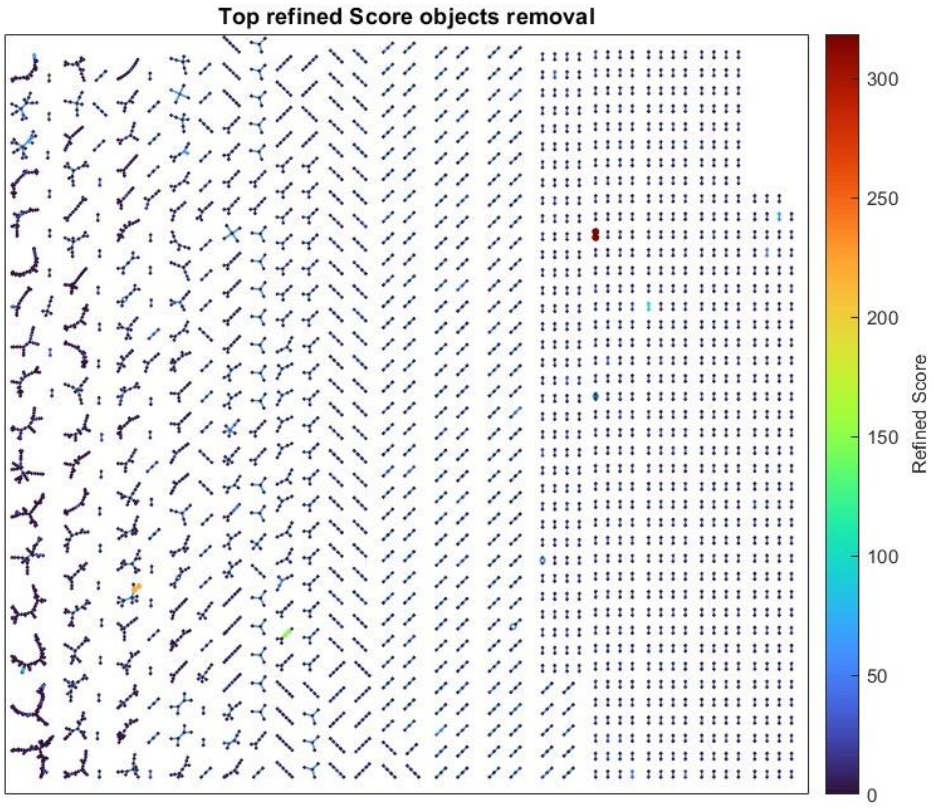

Figure 4.42: CDM dataset, refined score after the removal.

The objects with highest refined score are not in the biggest components, thus, the connectivity will be less affected by the removals, resulting in a network still highly connected.

A list of the 5 objects with the highest refined score is reported in Table 4.14.

Table 4.14: Top 5 objects per refined score.

	Refined score	NORAD ID	Object Name
CDM	3.153744e+02	6677	COSMOS 566
	3.131983e+02	14999	COSMOS 1560
	2.394487e+02	4821	THORAD AGENA D DEB
	2.394487e+02	4992	THORAD AGENA D DEB
	1.869292e+02	10288	COSMOS 942

The two objects with highest refined score, are two non-operative Russian satellites. As illustrated in the Figure 4.43, they represent one of the smallest components instead.

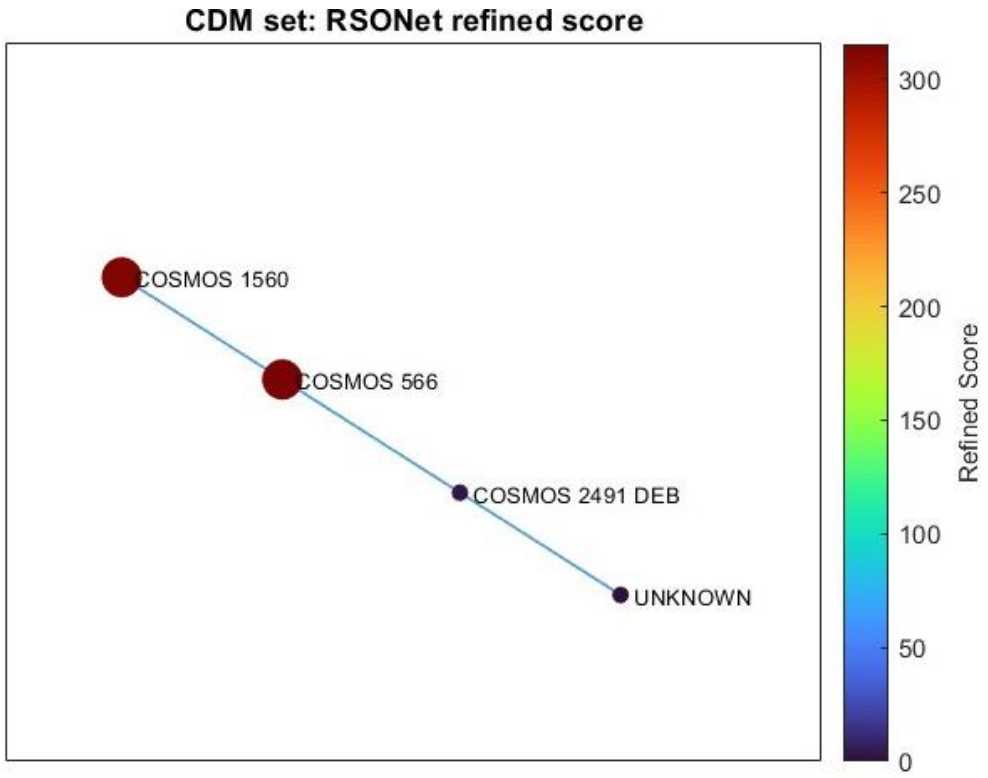

Figure 4.43: Component with the objects with highest refined score.

Besides the network visualizations, the evaluation of the adopted removal strategy, based on the refined score, is focused on the analysis of the measures, reported in Table 4.15.

Table 4.15: Network measures for nominal and mitigated populations.

	n	m	β	$\hat{d}$	$\hat{B}$	PoC	S	R	D
Nominal CDM	4694	3406	0.73	1.45	4.41e1	6.25e-4	4.41e5	2.36	9019
Refined score Approach	4561	3270	0.72	1.43	1.19e1	5.62e-4	1.93e5	1.90	6370

In total 133 are removed of which 33 were left with no conjunctions. The connectivity slightly decreased, together with the average degree and betweenness, less with respect to first strategy proposed in this chapter. On the contrary, the average danger score is decreased, thus, removed objects had lower danger score with respect the average one.

4.4.4. RSONet Simplified Score

In Figure 4.44, the obtained mitigated RSONet is presented, after the removals of 100 objects with highest RSONet simplified score. The Figure 4.45 and Figure 4.46 depict the simplified score per each node, before and after the removal strategy execution.

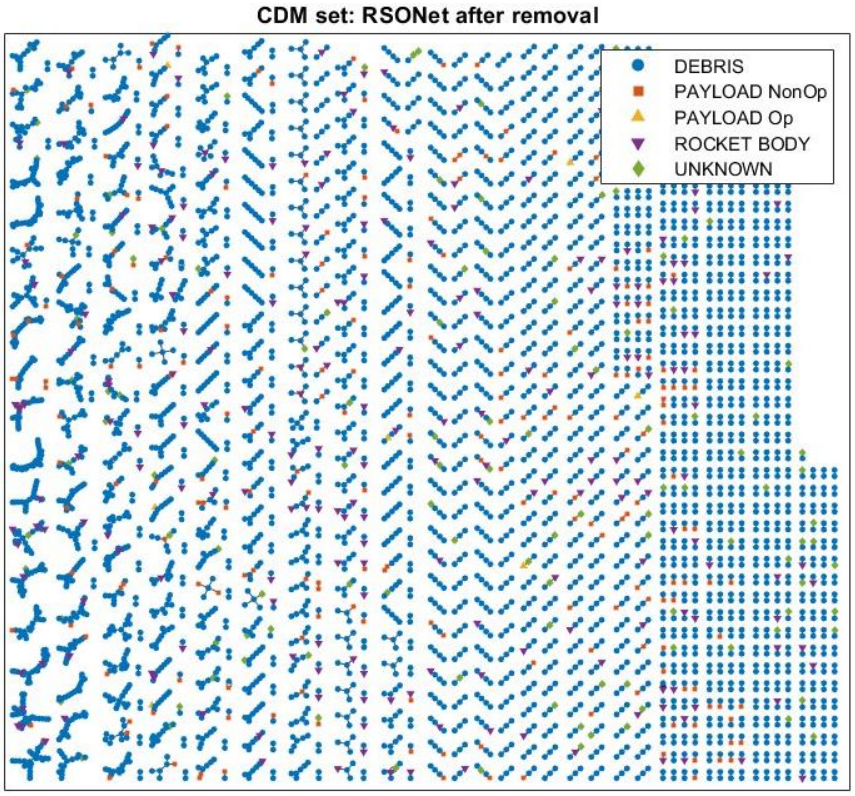

Figure 4.44: CDM dataset, RSONet representation after removal.

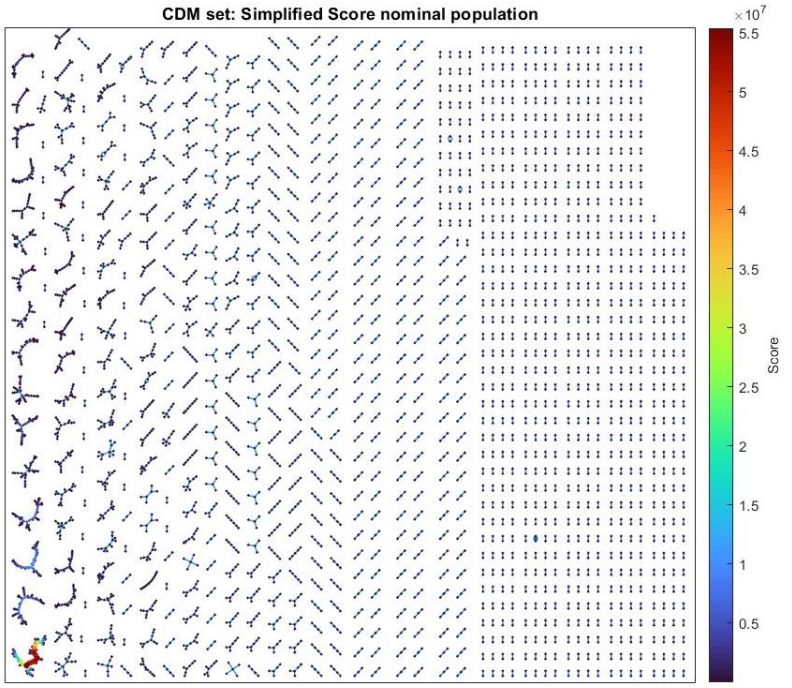

Figure 4.45: CDM dataset, simplified score before the removal.

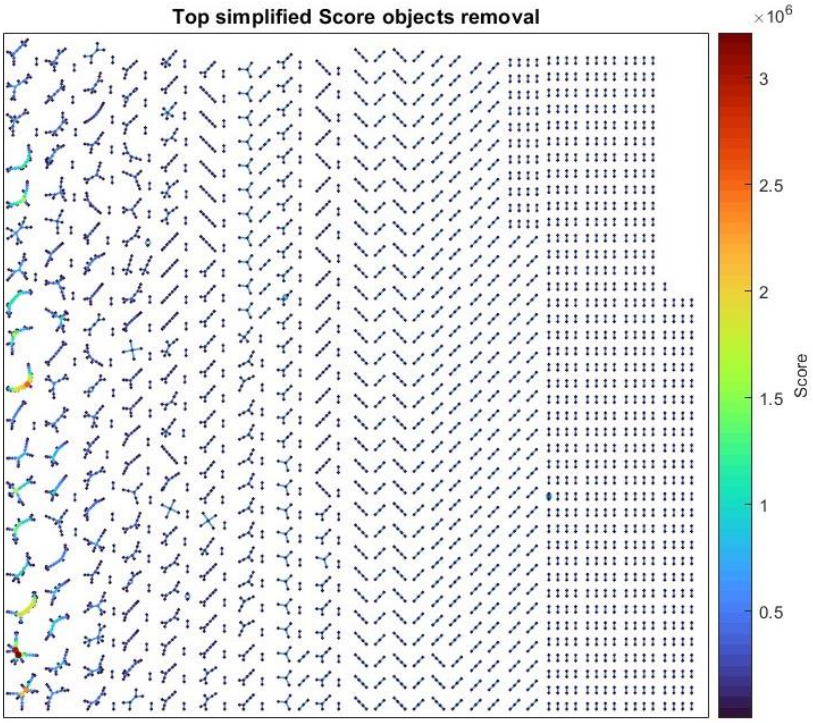

Figure 4.46: CDM dataset, simplified score after the removal.

The objects with highest simplified score are in the biggest components, thus, the connectivity will be way more affected by the removals, with respect the three previous strategies, resulting in a network less connected, as it is illustrated in Figure 4.47.

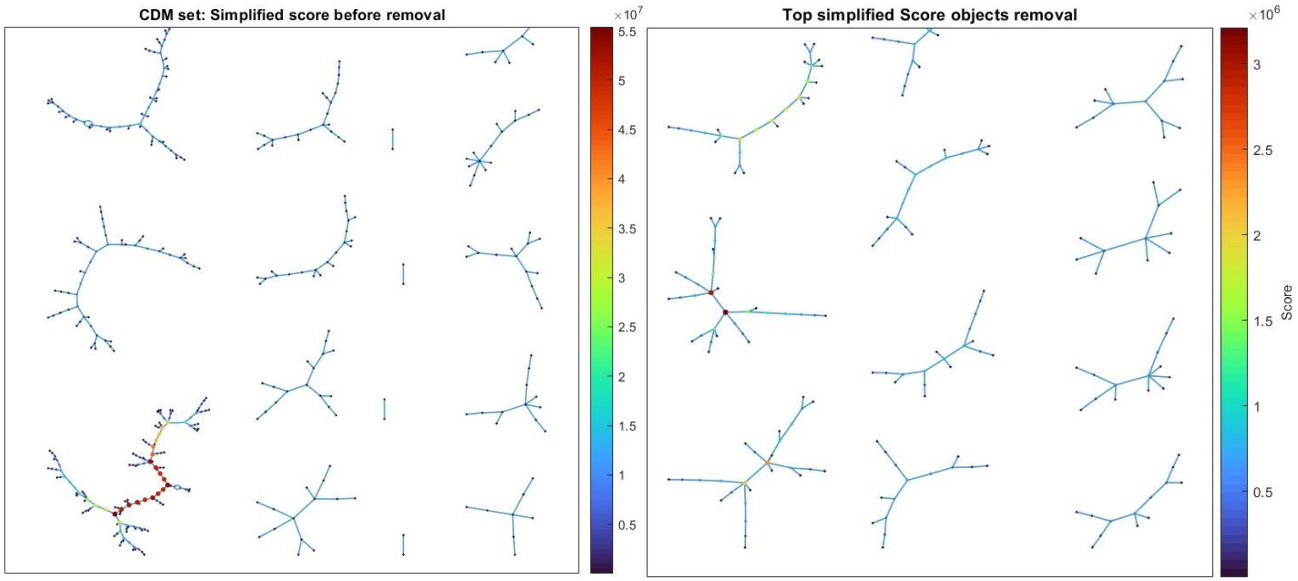

Figure 4.47: Biggest components before and after the removal.

A list of the 5 objects with the highest refined score is reported in Table 4.16.

Table 4.16: Top 5 objects per simplified score.

	Simplified score	NORAD ID	Object Name
CDM	5.538970e+07	50793	COSMOS 1818 COOLANT
	5.408970e+07	13719	SL-3 R/B
	5.303972e+07	38532	METEOR 2-1 DEB
	5.244970e+07	30092	FENGYUN 1C DEB
	5.174971e+07	36699	FENGYUN 1C DEB

Besides the network visualizations, the evaluation of the adopted removal strategy, based on the simplified score, is focused on the analysis of the measures, reported in Table 4.17.

Table 4.17: Network measures for nominal and mitigated populations.

	n	m	β	$\hat{d}$	$\hat{B}$	PoC	S	R	D
Nominal CDM	4694	3406	0.73	1.45	4.41e1	6.25e-4	4.41e5	2.36	9019
Simplified score Approach	4542	3204	0.70	1.41	6.11	6.35e-4	6.11e4	2.60	9877

In total 152 are removed of which 52 were left with no conjunctions. The connectivity is decreased, together with the average degree and betweenness, more with respect to previous three strategies proposed in this chapter, meaning that this removal strategy

is more effective in terms of network robustness: the network is more vulnerable to this elimination approach. On the contrary, the average danger score is increased, thus, removed objects had higher danger score with respect the average one. This behaviour was expected, because the simplified score is only depending on the centrality measures, by definition.

4.4.5. Danger Score

In Figure 4.48, the obtained mitigated RSONet is presented, after the removal of 100 objects with highest danger score. In Figure 4.49 and Figure 4.50 is illustrated the refined score for each node, before and after the application of the strategy.

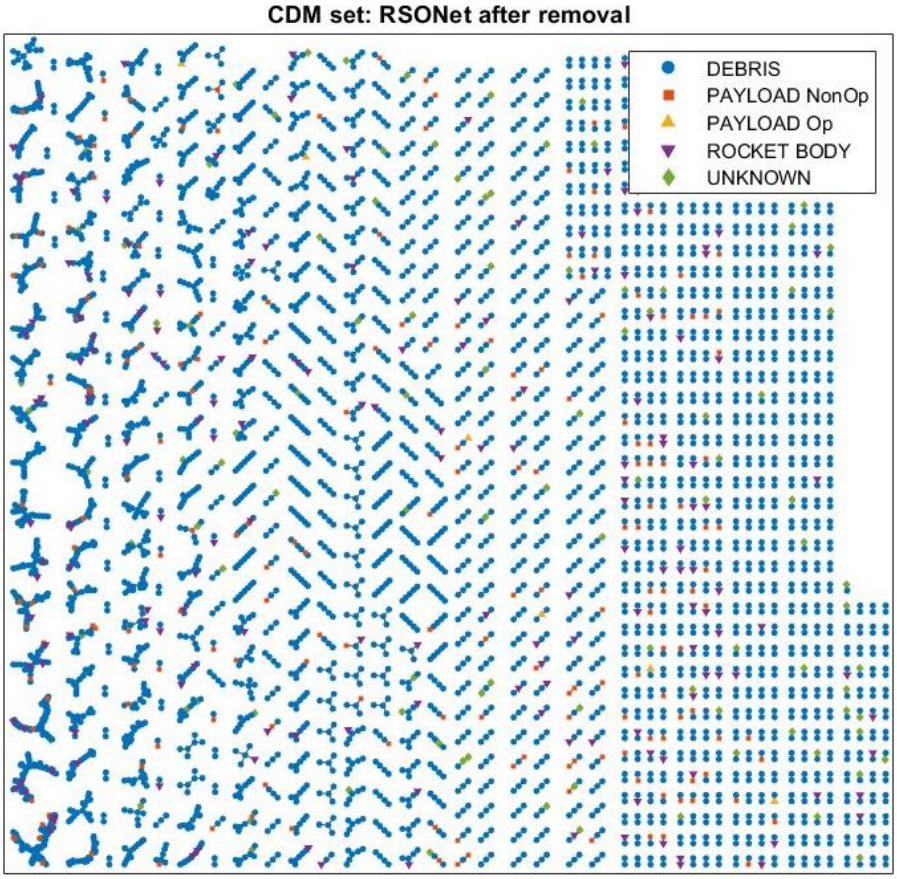

Figure 4.48: CDM dataset, RSONet representation after removal.

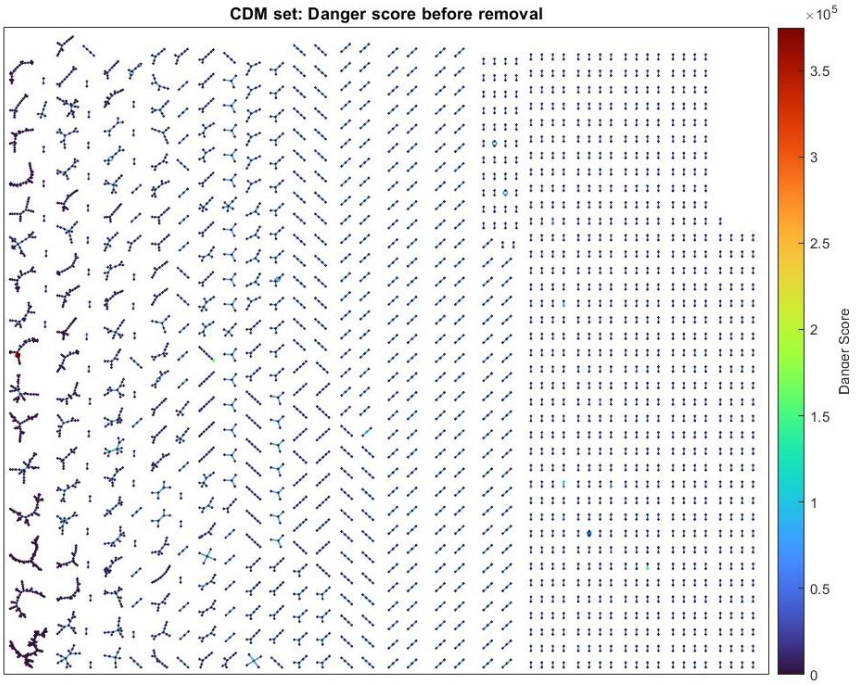

Figure 4.49: CDM dataset, danger score before the removal.

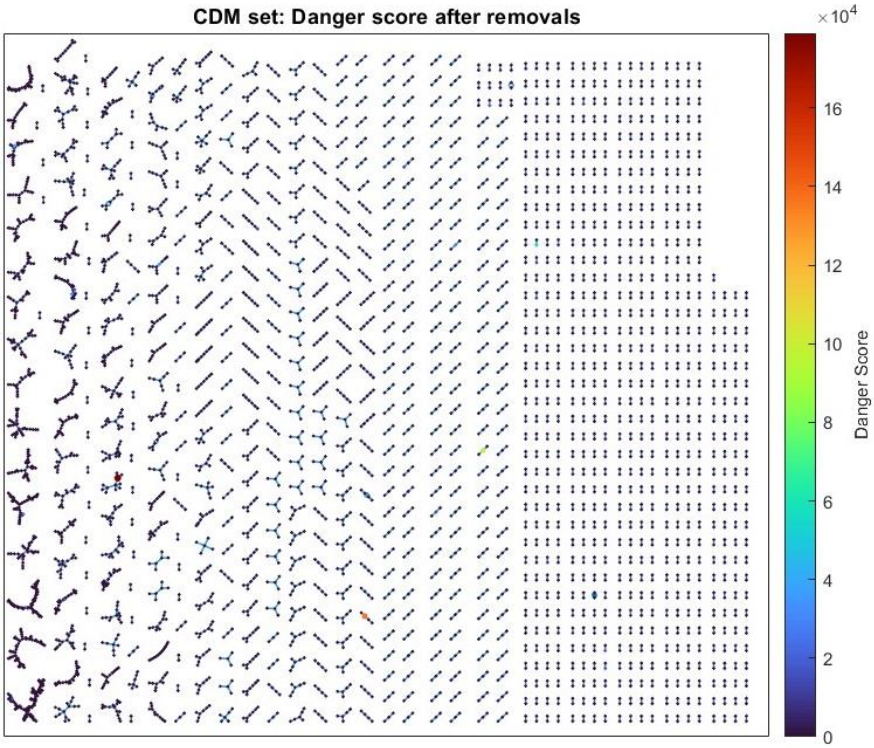

Figure 4.50: CDM dataset, danger score after the removal.

The objects with highest danger score are not in the biggest components, thus, the connectivity will be less affected by the removals, with respect the other strategies, resulting in a network still highly connected. The Figure 4.51 depicts the network largest components, before and after the execution of the strategy.

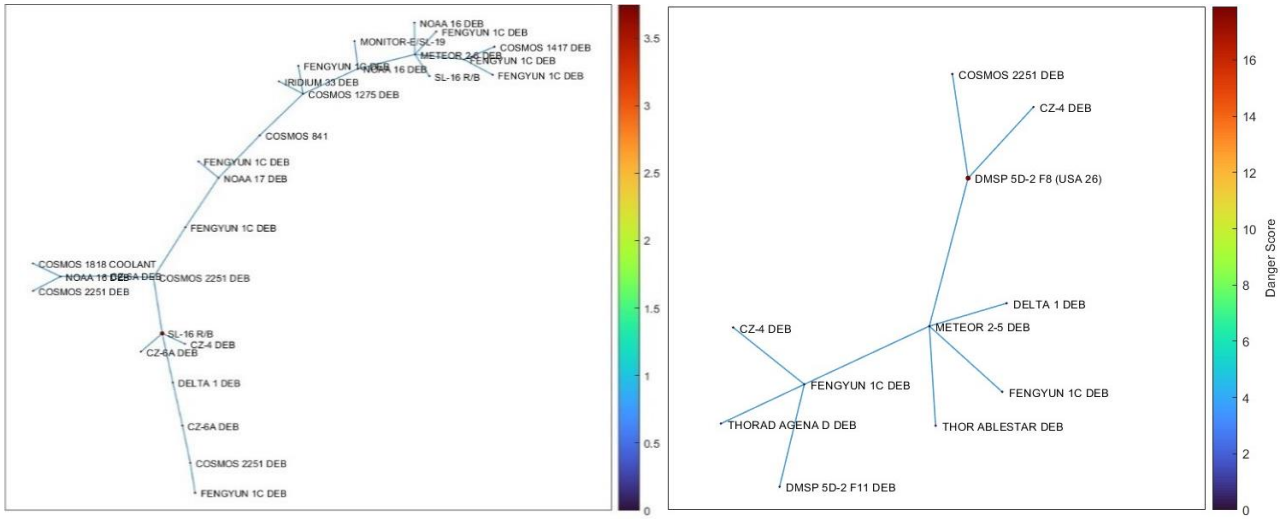

Figure 4.51: Biggest components before and after the removal.

A list of the 5 objects with the highest danger score is reported in Table 4.18.

Table 4.18: Top 5 objects per danger score.

	n	m	β	$\hat{d}$	$\hat{B}$	PoC	S	R	D
Nominal CDM	4694	3406	0.73	1.45	4.41e1	6.25e-4	4.41e5	2.36	9019
Danger score Approach	4531	3282	0.72	1.45	3.36e1	3.68e-4	3.36e4	1.67	5908

Besides the network visualizations, the evaluation of the adopted removal strategy, based on the danger score, is focused on the analysis of the measures, reported in Table 4.19.

Table 4.19: Network measures for nominal and mitigated populations.

	Danger score	NORAD ID	Object Name
CDM	3.747336e+05	25407	SL-16 R/B
	1.619594e+05	22219	COSMOS 2219
	1.575417e+05	25400	SL-16 R/B
	1.023590e+05	24306	SL-8 R/B
	7.278113e+04	10541	SL-14 R/B

In total 163 are removed of which 63 were left with no conjunctions. The connectivity is very slightly decreased, together with the average degree and betweenness, less with respect to all the previous strategies proposed in this chapter, meaning that this removal strategy is the least optimal in terms of connectivity.

4.4.6. Comparison

The selection of the best strategy in terms of network robustness and danger score, among the previous case studies is hereby presented and compared with random removal strategy.

In Figure 4.52, the connectivity β of each CDM case is depicted: the first bin corresponds to the initial RSO population. The bins associated to the random removal and the danger score strategies highlight the least optimal approaches among them all (in terms of connectivity), because the changes in the network connectivity are the smallest. The same conclusions can be done by analysing the Figure 4.53, in which the $\Delta\beta$ is showed.

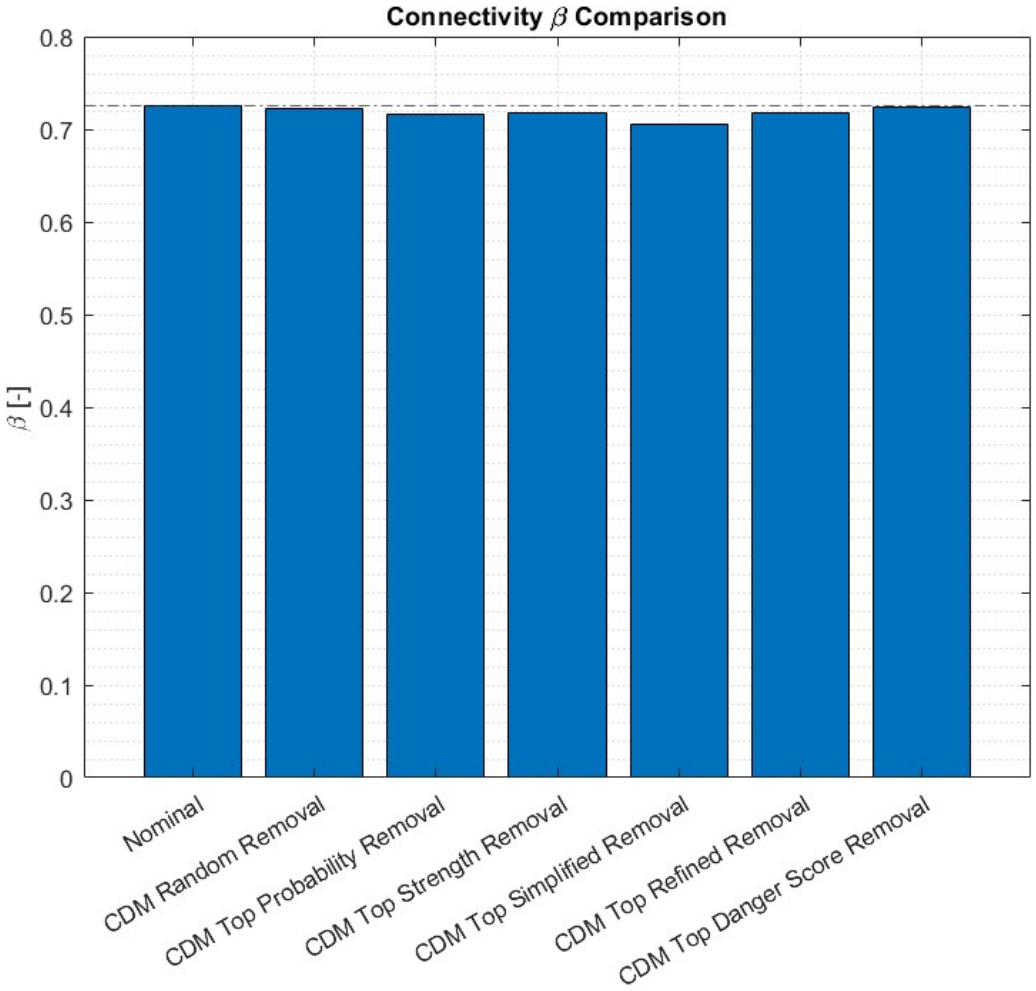

Figure 4.52: Connectivity of CDM removal strategies.

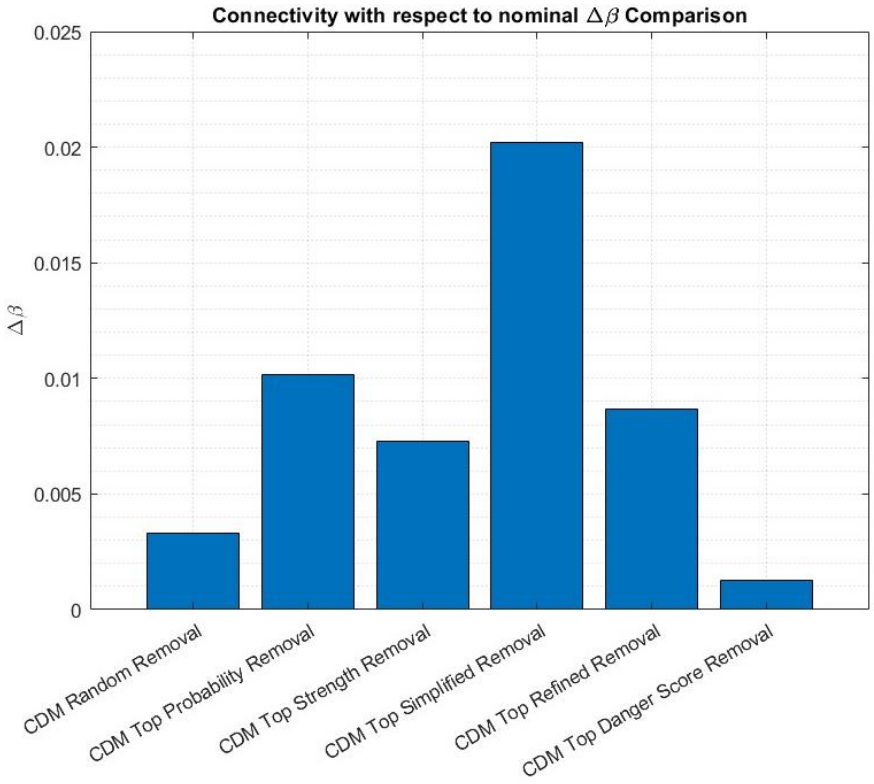

Figure 4.53: Δβ of CDM removal strategies.

Same exact conclusions apply regarding average degree and betweenness, as illustrated in Figure 4.54 and Figure 4.55.

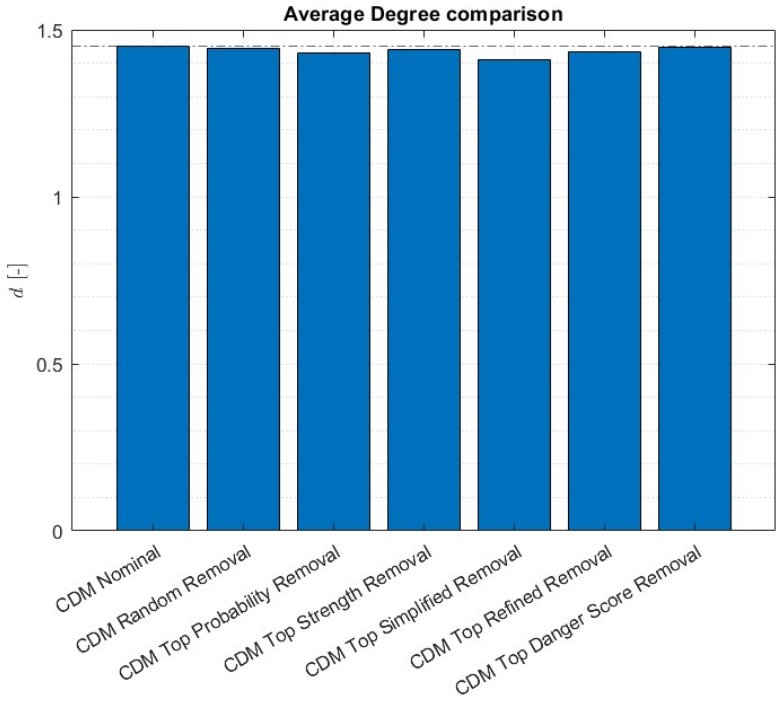

Figure 4.54: Average degree for each case.

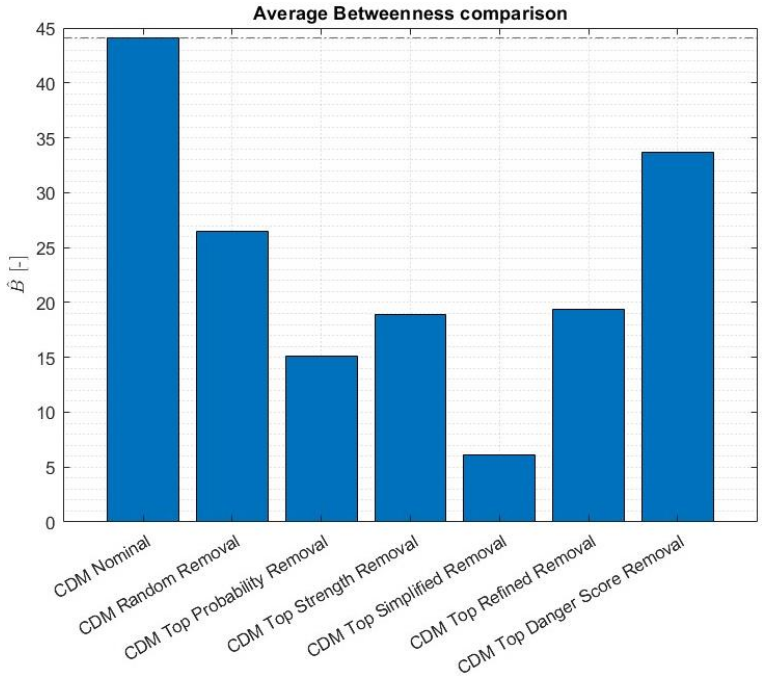

Figure 4.55: Average betweenness for each case.

The motivation behind the danger score is the least optimal in terms of connectivity is because it diverges conceptually from the network domain, even if it derives from that. The danger score is weighting also other parameters which do not depend on network. Lastly, the average danger score is compared. The Figure 4.56 depicts the cases.

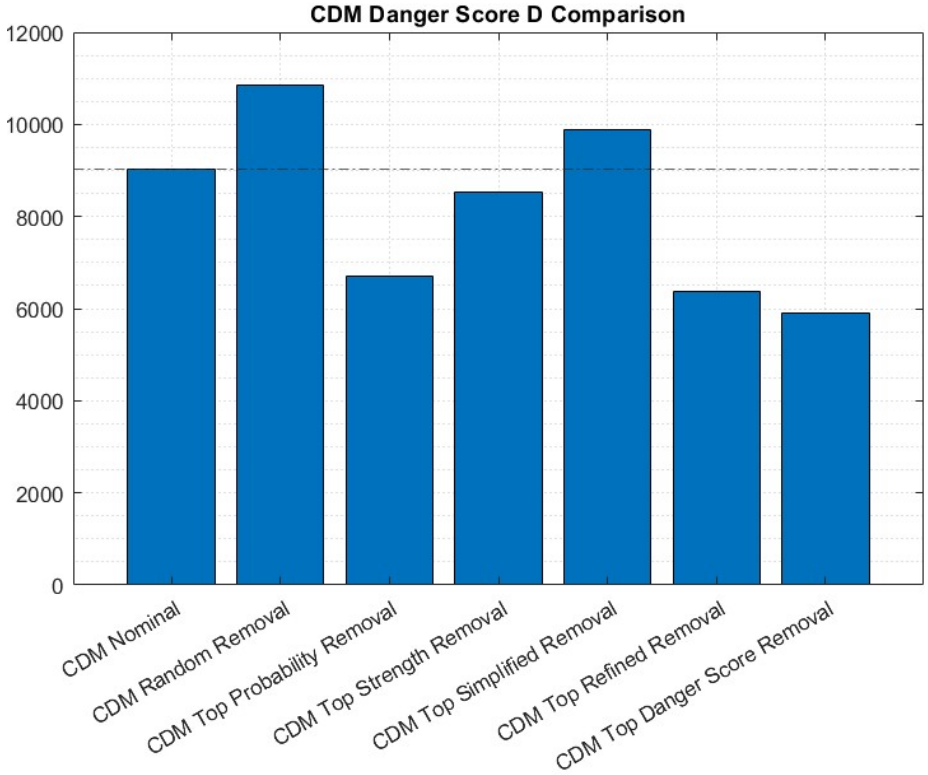

Figure 4.56: Average danger score for each case.

The best strategy in terms of robustness ends up being the least efficient in terms of danger score after the random removal case, which always represents the worst option. As previously explained, this was expected: the danger score is depending on other parameters which are not related to the network's structure as the centrality measures do. The best strategy here, besides removing objects with highest danger score, is the strategy based on the RSONet refined score.

4.5. Best strategy selection

Recent studies have shown that the selection for targets in debris removal missions, should be based on three principles:

- Mass of the object.
- Collisional probability.
- Altitude.

The higher these parameters are, the more suitable is the target [60]. The feasibility of the mission, connected to many other factors such as spin rate, size, etc., are beyond the scope of the thesis, as well as giving a definitive ranking list with best targets to be removed. This work is focused on the description of the proposed tool, as a new criterion for target selection, to highlight the impact of each removal on the rest of the space population by using network theory.

By comparing the tables listing objects with highest mass, with highest probability of collision, with highest danger score, it becomes apparent that they present different rankings.

In this work, the selection of the best strategy has been conducted, firstly by evaluating the network connectivity and robustness. The greater the decrease in connectivity following the application of a removal strategy, the less the network is robust to that kind of removal. Accordingly, the average degree and betweenness, indicate the same. Connecting to the real world, reduced connectivity implies less susceptibility to activate cascade collisions. Additionally, a decrease in the size of the network, is directly correlated to reduced effort required to manage the conjunction events of the entire space population.

The connection to the real world implies the importance of selecting removal strategies based on connectivity reduction. Nevertheless, other important parameters must be considered when removing objects: the mass, the probability of collision, the altitude, the size, the interactions with others, etc. Therefore, the developed strategies in the work are also compared based on the developed tool, which permits to take into account most of the mentioned factors.

In Table 4.20, the ranking based on the danger score is presented for the first 10 objects, belonging to the CDM RSONet population.

Table 4.20: 10 objects with highest danger score.

Danger score	Mass [kg]	NORAD ID	Object Name
3.747336e+05	8.225970e+03	25407	SL-16 R/B
1.619594e+05	3.221010e+03	22219	COSMOS 2219
1.575417e+05	8.225970e+03	25400	SL-16 R/B
1.023590e+05	1.421210e+03	24306	SL-8 R/B
7.278113e+04	1.387510e+03	10541	SL-14 R/B
6.388433e+04	1.280000e+03	5731	METEOR 1-10
5.813007e+04	1.434000e+03	3048	SL-8 R/B
5.343481e+04	1.427160e+03	7715	SL-3 R/B
4.996627e+04	6.937600e+02	7768	COSMOS 729
3.668693e+04	1.387510e+03	11672	SL-14 R/B

The object with the highest mass is at the 16th position, namely a SL-16 R/B of 9000kg.

On the one hand, the best strategy in terms of connectivity and the one that highlights the strongest vulnerability of the network, for both the TLE and CDM cases, is the strategy based on removing objects with the highest degree. The second place is occupied by two strategies: the one based on the betweenness, and the other one based on the simplified score. As expected, they both are related to network centrality, such as the connectivity. On the other hand, the best strategies in terms of danger score, for both the TLE and CDM cases, are the ones based on removing objects with highest danger score (trivially) and higher RSONet refined score.

Removing objects randomly proves to be always a poor strategy, both in terms of connectivity and danger score.

5 Conclusions and future developments

In this work, a newly developed tool, based on complex system and network theory, has been described to analyse space Earth orbiting object populations. Within this framework, the impacts of mega-constellations and space debris onto the rest of resident space objects have been individually assessed. Furthermore, several strategies to select targets for space object removal have been evaluated through the network theory and a novel developed danger score. Results clearly indicate that some strategies are better than others, in terms of network robustness and danger score. If the goal is to reduce the required effort for detection and monitoring of predicted conjunction events, the strategy based on removing objects with the highest network centrality degree is the most suitable. The net decrease of order, size, and connectivity, implies a reduction in the number of conjunctions within the selected period and beyond. Nevertheless, the concern about the space debris issue is not only a problem of numbers, but it also must take into account the severity of each potential collision. This issue brought the need of including unrelated network factors, which express the danger of likely collisions.

Without stepping away from the network domain, the thesis describes removal strategies based on general measures, which introduce collisional severity parameters such as the object mass, type, probability to collide with others, etc. Results highlight that the best removal strategy among them in terms of reduction of network connectivity is based on the RSONet simplified score, that, even if can be interpreted as a special case of the weighted refined score, is still not taking into account any collisional severity factors (it is related only to network centrality measures). Therefore, the second best option is held by two removal strategies: removal of objects with the highest probability of collision and with the highest RSONet refined score. By analysing the impact of these two strategies on the reduction of danger score, the one based on the RSONet refined score is better. Moreover, being related to centrality measures, this strategy causes greater reduction of average degree and betweenness with respect to one based only on collisional probability.

The strategy focused on eliminating objects with the highest danger score stands out as the most distant from the network domain compared to the other proposed approaches, because it introduces also the mass influence. This distinction is evident in the network connectivity, where this strategy has a minor impact compared to the others. However, it is essential to note that considering the mass in this context is of supreme significance: collisions between more massive objects would generate more threats to other space objects, leading faster to a space impracticability.

Given the instrument's relatively recent inception, there exists ample opportunities for numerous improvements. The main assumption to build the RSONet is considering all conjunctions to happen independently from time, leading to the computation of conservative probability scores (RSONet scores). The implementation of temporal networks would eliminate this assumption, increasing inevitably the complexity of the RSONet scores definitions.

Strategies based on adding satellites can be a turning point for mission design: through this framework, the analysis of new satellites to assess the influence of new satellites on the rest of population is possible by adding synthetic nodes in the network.

Furthermore, a more precise tool with respect to SGP4 orbital propagator would permit to have longer time windows and/or bigger populations to analyse.

The implementation of further parameters in the scores, such as the object altitude, its ability to perform collision avoidance manoeuvres, its size, etc., can refine the judgment of the strategies.

Moreover, new strategies can be assessed, based on either network characteristics or collisional parameters.

Bibliography

[1] IADC, "IADC Space Debris Mitigation Guidelines," IADC Steering Group and Working Group 4, October 2002, revised in June 2021.

[2] L. Hall, "The History of Space Debris," in *Space Traffic Management Conference*, Daytona Beach, November 2014.

[3] T. S. Kelso, "Satellite Times - Space Surveillance," September 1997. [Online]. Available: https://celestrak.org/columns/v04n01/. [Accessed January 2024].

[4] H. Klinkrad, "The Current Space Debris Environment and its Sources," *Space Debris: Models and Risk Analysis*, 1st ed., Springer Praxis Books, pp. 5-57, 2006.

[5] D. S. F. Portree and J. P. Loftus, "Orbital Debris: A Chronology," NASA, 1999.

[6] NASA, "Solar cycle sensitivity study of breakup events in LEO," *Orbital Debris Quarterly News,* vol. 19, no. 1, p. 6, January 2015.

[7] C. Pardini and L. Anselmo, "Environmental sustainability of large satellite constellations in low earth orbit," *Acta Astronautica,* vol. 170, pp. 27-36, 2020. https://doi.org/10.1016/j.actaastro.2020.01.016

[8] J. Zhang, Y. Cai, C. Xue, Z. Xue and H. Cai, "LEO mega constellations: Review of development, impact, surveillance, and governance," *Space: Science and Technology,* vol. 2022, no. 1, 2022.

https://doi.org/10.34133/2022/9865174

[9] A. Boley and B. Michael, "Anti-satellite weapon tests to disrupt large satellite constellations," *Nature Astronomy,* vol. 8, no. 1, pp. 10-12, 2024. http://doi.org/10.1038/s41550-023-02173-9

[10] ESA, "Space Debris by numbers," 2023. [Online]. Available: https://www.esa.int/Space_Safety/Space_Debris/Space_debris_by_the_numbers. [Accessed November 2023].

[11] ESA, "About Space Debris," 2023. [Online]. Available: https://www.esa.int/Space_Safety/Space_Debris/About_space_debris. [Accessed November 2023].

[12] ESA Space Debris Office, "ESA'S Annual Space Environment Report," ESA, 2023.

[13] N. L. Johnson, P. H. Krisko, J. C. Liou and P. D. Anz-Meador, "NASA's new breakup model of EVOLVE 4.0," *Advances in Space Research,* vol. 28, no. 9, pp. 1377-1384, 2001.

http://doi.org/10.1016/S0273-1177(01)00423-9

[14] N. a. S. Khlystov, "Space Industry Debris Mitigation Recommendations - World Economic Forum," *Future of Space Network - Sustainable Space Initiative, Centre for the Fourth Industrial Revolution,* June 2023.

[15] ESA Space Debris Mitigation WG, "ESA Space Debris Mitigation Requirements," ESA, 2023.

[16] ISO, "Space systems-Space debris mitigation requirementS," ISO, 2023.

[17] I. V. Usovik, "Review of perspective space debris mitigation solutions," *Journal of Space Safety Engineering,* vol. 10, no. 1, pp. 55-58, 2023. https://doi.org/10.1016/j.jsse.2022.12.001

[18] B. B. Virgili and H. Krag, "Active Debris Removal for LEO missions," in *6th European Conference on Space Debris'*, Darmstadt, Paper ESA SP-723, April 2013.

[19] M. Nitta, Y. Yoshimura and T. Hanada, "Space Debris Mitigation by Passive Debris Removal in Large Constellation," in *First International Orbital Debris Conference (IOC)*, Houston, December 2019.

[20] A. C. Long and D. A. Spencer, "Deployable drag device for launch vehicle upper stage de-orbit," in *65th International Astronautical Congress*, Toronto, January 2014.

[21] D. Romagnoli and S. Theil, "De-orbiting satellites in LEO using solar sails," *Journal of Aerospace Engineering Sciences and Applications,* vol. 4, no. 2, pp. 49-59, 2012.

http://doi.org/10.7446/jaesa.0402.05

[22] I. Gkolias, E. M. Alessi and C. Colombo, "Dynamical taxonomy of the coupled solar radiation pressure and oblateness problem and analytical deorbiting configurations," *Celestial Mechanics and Dynamical Astronomy,* vol. 132, no. 11-12, 2020.

https://doi.org/10.1007/s10569-020-09992-2

[23] J. C. Liou, "Collision activities in the future orbital debris environment," *Advances in Space Research,* vol. 38, no. 9, pp. 2102-2106, 2006.

[24] B. B. Virgili, "DELTA (DEBRIS ENVIRONMENT LONG-TERM ANALYSIS)," ESA/ESOC Space Debris Office, 2015.

https://doi.org/10.1016/j.asr.2005.06.021

[25] H. G. Lewis, G. G. Swinerd, N. Williams and G. Gittins, "DAMAGE: A dedicated GEO debris model framework," in *3rd European Conference on Space Debris, ESOC*, Darmstadt, Paper SP-473, March 2001.

[26] A. Rossi, L. Anselmo, C. Pardini, R. Jehn and V. G. B., "The new space debris mitigation (SDM 4.0) long term evolution code," in *5th European Conference on Space Debris*, Darmstadt, Paper SP-672, March-April 2009.

[27] T. Hanada, Y. Ariyoshi, K. Miyazaki, K. Maniwa, J. Murakami and S. Kawamoto, "Orbital Debris Modeling at Kyushu University," *The Journal of Space Technology and Science,* vol. 24, no. 2, pp. 23-35, 2009.

https://doi.org/10.11230/jsts.24.2_23

[28] J. Radtke, S. Mueller, V. Schaus and E. Stoll, "LUCA2 - An enhanced Long-term Utility for Collision Analysis," in *7th European Conference on Space Debris*, Darmstadt, April 2017.

[29] J. Dolado-Perez, R. Di Costanzo and B. Revelin, "Introducing MEDEE - A new orbital debris evolutionary model," in *6th European Conference on Space Debris*, Darmstadt, Paper SP-723, April 2013.

[30] V. Braun, A. Horstmann, S. Lemmens, C. Wiedemann and L. Böttcher, "Recent developments in space debris environment modelling, verification and validation with MASTER," in *8th European Conference on Space Debris*, Darmstadt, April 2021.

[31] NASA, "The New NASA Orbital Debris Engineering Model ORDEM2000," NASA, Houston, 2002.

[32] H. G. Lewis, R. J. Newland, G. G. Swinerd and A. Saunders, "A new analysis of debris mitigation and removal using networks," *Acta Astronautica,* vol. 66, no. 1-2, pp. 257-268, 1 2010.

https://doi.org/10.1016/j.actaastro.2009.05.010

[33] R. J. Newland, H. G. Lewis and G. G. Swinerd, "Supporting the development of active debris removal using weighted networks," in *5th European Conference on Space Debris'*, Darmstadt, Paper SP-672, March-April 2009.

[34] R. J. Newland, "Assessing the use of network theory as a method for developing a targeted approach to Active Debris Removal," University of Southampton, Faculty of Engineering and the environment Aeronautics & Astronautics, PhD Thesis, 2012.

[35] G. Acciarini and M. Vasile, "A multi-layer temporal network model of the space environment," in *71st International Astronautical Congress (IAC)*, online, October 2020.

[36] G. Acciarini and M. Vasile, "A network-based evolutionary model of the space environment," in *8th European Conference on Space Debris*, Darmstadt, April 2021.

[37] E. Stevenson, V. Rodriguez-Fernandez, H. Urrutxua, U. Rey and J. Carlos, "Towards graph-based machine learning for conjunction assessment," in *Advanced Maui Optical and Space Surveillance Technologies Conference (AMOS)*, Maui, September 2022.

[38] E. Stevenson, V. Rodriguez-Fernandez, H. Urrutxua and D. Camacho, "Benchmarking deep learning approaches for all-vs-all conjunction screening," *Advances in Space Research,* vol. 72, no. 7, pp. 2660-2675, 2023. https://doi.org/10.1016/j.asr.2023.01.036

[39] Y. Wang, C. Wilson and M. Vasile, "Multi-layer temporal network model of the space environment," in *AAS/AIAA Astrodynamics Specialist Conference*, Big Sky, August 2023.

[40] M. Romano, T. Carletti, A. Lemaitre and J. Daquin, "A network-based risk analysis for space traffic management," in *73rd International Astronautical Congress (IAC)*, Paris, September 2022.

[41] CCSDS, "Conjunction Data Message, Recommended Standard," CCSDS Secretariat, Washington, DC, 2013.

[42] Space Assigned Numbers Authority (SANA), "Object Types," May 2017. [Online]. Available: https://sanaregistry.org/r/object_types/. [Accessed February 2024].

[43] CelesTrack, "SATCAT Operational Status," [Online]. Available: https://celestrak.org/satcat/status.php. [Accessed November 2023].

[44] "Space-Track," [Online]. Available: https://www.space-track.org/. [Accessed September 2023].

[45] "CelesTrack," [Online]. Available: https://celestrak.org/. [Accessed September 2023].

[46] "DISCOSweb," ESA, [Online]. Available: https://discosweb.esoc.esa.int/. [Accessed September 2023].

[47] F. J. Krage, "NASA Spacecraft Conjunction Assessment and Collision Avoidance Best Practices Handbook," NASA, Office of the Chief Engineer, February 2023.

[48] F. R. Hoots and R. L. Roehrich, "SPACETRACK REPORT NO. 3 Models for Propagation of NORAD Element Sets," 1980.

[49] D. A. Vallado, P. Crawford, R. Hujsak and T. S. Kelso, "Revisiting Spacetrack Report #3," AIAA, 2006.

https://doi.org/10.2514/6.2006-6753

[50] S. Aida and M. Kirschner, "Accuracy assessment of SGP4 orbit information conversion into osculating elements," in *6th European Conference on Space Debris*, Darmstadt, April 2013.

[51] F. R. Hoots, L. L. Crawford and R. L. Roehrich, "An analytic method to determine future close approaches between satellites," *Celestial Mechanics,* vol. 33, no. 2, pp. 143-158, 1984.

https://doi.org/10.1007/BF01234152

[52] D. Casanova, C. Tardioli and A. Lemaître, "Space debris collision avoidance using a three-filter sequence," *Monthly Notices of the Royal Astronomical Society,* vol. 442, no. 4, pp. 3235-3242, 2014.

https://doi.org/10.1093/mnras/stu1065

[53] M. Romano, A. Muciaccia, M. Trisolini, P. Di Lizia, C. Colombo, A. Di Cecco and L. Salotti, "PUZZLE software for the characterisation of in-orbit fragmentations," in *8th European Conference on Space Debris*, Darmstadt, April 2021.

[54] G. F. Gronchi and G. Tommei, "On the uncertainty of the minimal distance between two confocal Keplerian orbits," *Discrete and Continuous Dynamical Systems,* vol. 7, no. 4, pp. 755-778, 6 2007.

https://doi.org/10.3934/dcdsb.2007.7.755

[55] 18th & 19th Space Defense Squadron, "Spaceflight Safety Handbook for Satellite Operators," Combined Force Space Component Command, Vandenberg Space Force Base, California, April 2023.

[56] M. Romano, T. Carletti and J. Daquin, *The Resident Space Objects Network: a complex system approach for shaping space sustainability,* arXiv preprint arXiv:2310.14795, 2023, submitted to *The Journal of the Astronautical Sciences*.

[57] NASA, "Proper implementation of the 1988 NASA Breakup Model," *Orbital Debris Quarterly News,* vol. 15, no. 4, pp. 4-5, October 2011.

[58] NASA, "Two More On-orbit Fragmentations in 2022," *The Orbital Debris Quarterly News,* vol. 27, no. 1, March 2023.

[59] P. Holme, B. J. Kim, C. N. Yoon and S. K. Han, "Attack vulnerability of complex networks," *The American Physical Society,* vol. 65, no. 5, pp. 14-28, 2002. https://doi.org/10.1103/PhysRevE.65.056109

[60] R. Le Letty, O. Dubois-Matra, K. Wormnes, R. Le Letty, L. Summerer, R. Schonenborg, O. Dubois-Matra, E. Luraschi, A. Cropp, H. Krag and J. Delaval, "ESA technologies for space debris remediation," in *6th European Conference on Space Debris*, Darmstadt, Paper SP-723, April 2013.

[61] M. E. J. Newman, "Mathematics of Networks," in *The New Palgrave Dictionary of Economics*, Palgrave Macmillan UK, 2008, pp. 1-8.

https://doi.org/10.1057/978-1-349-95121-5_2565-1

[62] M. E. J. Newman, "The Structure and Function of Complex Networks," *Society for Industrial and Applied Mathematics,* vol. 45, no. 2, pp. 167-256, 2003. https://doi.org/10.1137/S003614450342480

A Appendix A

A brief explanation of network theory and its key topics is provided to aid in understanding the thesis.

A.1. Network Theory

The network theory is employed for mathematical analysis of graphs, which are also referred to as networks in the literature. Networks serve as tool for investigating systems composed of multiple and connected members, whose collective behaviour cannot be predicted from behaviours of individual elements. Those systems are called complex systems and RSO population is an example.

Networks consist of nodes (also known as vertices) connected by links (also referred to as edges) based on their interactions. Nodes that are linked to one, are called neighbours of that node.

There are different types of networks, such as multi-edges, multi-relational, weighted, directed, and temporal networks, along with their respective counterparts. This thesis focuses on networks with specific properties. Firstly, it examines unweighted networks, where links among nodes are considered equal in importance. Additionally, it investigates weighted networks, where connections between nodes carry a numerical weight representing their induvial strength. In this context, the weight is represented by the probability of collision of each conjunction. Moreover, the analysis concentrates on uni-directional networks, where links do not have a specific direction. Furthermore, the thesis explores multi-edge networks, which permit to accommodate multiple connection between the same pair of nodes: in this instance, multiple conjunctions belonging to different close approaches, are possible. Lastly, networks are time-invariant, meaning that they do not incorporate changes over the selected period of propagation time. This last assumption contradicts reality, which instead involves conjunction event between space objects occurring at precise time instants. However, this framework allows to build mathematical instruments (RSONet scores) which appear to be conservative, because they consider conjunctions can interact and occur all independently from time.

Mathematically, to express the connections among nodes, it is exploited a matrix, known as adjacency matrix A of order nxn, where n is the number of nodes in the network.

$$A=\begin{bmatrix} 0 & \dots & A_{1,j} & \dots & A_{1,n} \\ \vdots & & & & \\ A_{i,1} & & \ddots & & \vdots \\ \vdots & & & & \\ A_{n,1} & & \dots & & 0 \end{bmatrix}$$

If there is a link between the node i and j, $A(i,j) > 0$. The exact value of $A(i,j)$ is 1 if the network is unweighted, otherwise equal to the probability of collision between the nodes i and j in case of weighted network. In this last instance, the matrix is called weighted adjacency matrix $\check{A}$. Since RSONets are undirected networks, A and $\check{A}$ are always symmetric.

Various measures exist to determine global statistics of a network. The most fundamental ones are the order n, the size m, and the connectivity β. The order is the number of nodes in the network, the size refers to the number of links among nodes, the connectivity represents the ratio of size to order.

Space networks describing conjunction events, usually comprise multiple components also known as subgraphs, some of which are bigger in order with respect to others. In RSONet the smallest component has at least 2 nodes, aligning with its aim to represent conjunctions among objects.

Additional valuable metrics include centrality measures such as degree, betweenness, closeness, and clustering. The measures are termed "centrality" because they expressed how much a node occupies central importance within the network. In this thesis, centrality measures have been computed using MATLAB built-in functions.

Hereafter, their theoretical definitions:

- The degree of a node *i* is the number of links connected to *i*, therefore the count of conjunctions performed by node *i* within the set propagation period.
- The betweenness of a node *i* quantifies the fraction of shortest path between nodes that pass through *i.* The shortest path, or geodesic path, denotes the minimal number of nodes traversed between two given nodes.
- The closeness of a node *i* denotes the reciprocal of the sum of the average shortest path distances from *i* to other reachable nodes.
- The clustering of a node *i* reflects its tendency to form connections within triangles with its neighbouring nodes [61].

The strength is a weighted measure, related to the degree of a node and the weight of its links. In RSONet, the strength quantifies the total weight of links of each node by summing the probability of collision of each conjunction that it is performing.

The robustness of the network refers to its ability to withstand disruptions caused by node removals. The network's response to node removals determines whether it is vulnerable or resilient (i.e., robust) [62]. The response is measured through the change in connectivity and the centrality measures, after the removal. When removals lead to

decreased network robustness, there is typically a decrease in connectivity and centrality measures such as average degree and betweenness.

In RSONet, high values of closeness are preferred, as they indicate greater stability against activation of cascade conjunction effects.

B Appendix B

Hereafter, the scheme of the MATLAB post-processing algorithm is presented.

B.1. Post-Processing Code

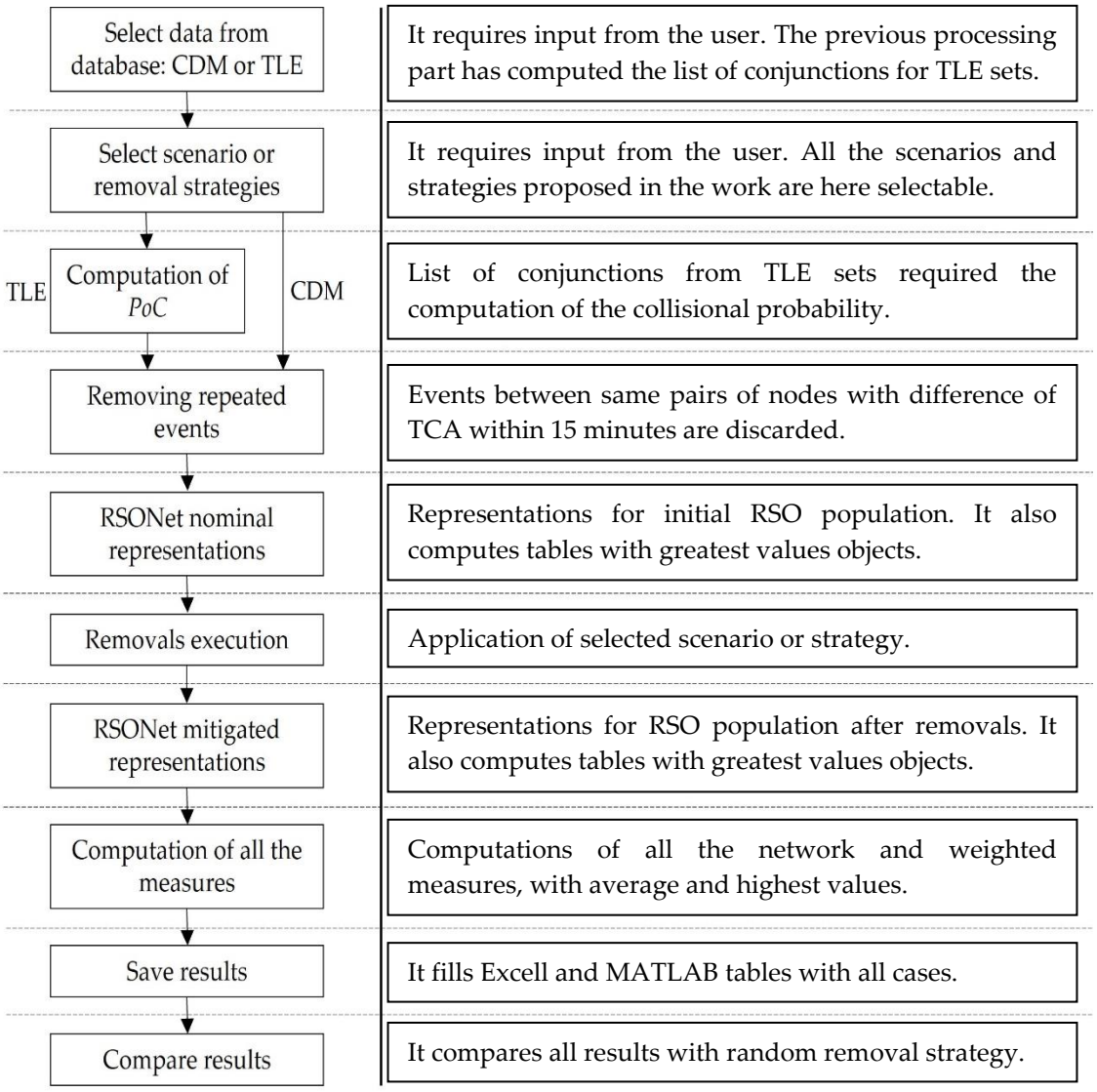

List of Figures

List of Tables

List of symbols

Variable	Description	SI unit
$\boldsymbol{\psi}$	Object Type Coefficient	[-]
$\boldsymbol{A}$	Adjacency Matrix	[-]
$\breve{\boldsymbol{A}}$	Weighted Adjacency Matrix	[-]
$\boldsymbol{\beta}$	Connectivity	[-]
$\Delta\boldsymbol{\beta}$	Connectivity with respect to nominal	[-]
$\boldsymbol{B_i}$	Betweenness for node	[-]
$\widehat{\boldsymbol{B}}$	Average Betweenness	[-]
$\boldsymbol{C_i}$	Clustering for node	[-]
$\widehat{\boldsymbol{C}}$	Average Clustering	[-]
$\boldsymbol{clos_i}$	Closeness for node	[-]
$\widehat{\boldsymbol{clos}}$	Average Closeness	[-]
d	Conjunction Distance Threshold	[km]
$\boldsymbol{d_i}$	Degree for node	[-]
$\boldsymbol{d_k}$	Keplerian distance function	[km]
$\widehat{\boldsymbol{d}}$	Average Degree	[-]
$\boldsymbol{D_i}$	Danger Score for node	[-]
D	Average Danger Score	[-]
e	Eccentricity	[-]
m	Network Size	[-]
MOID	Minimum Orbital Intersection Distance	[km]
n	Network Order	[-]
N	Number of objects removed	[-]
$\boldsymbol{N_f}$	Number of fragments	[-]
PoC	Probability of Collision	[-]
r	Geocentric Distance	[km]
R	Average RSONet Refined Score	[-]
$\boldsymbol{R_i}$	RSONet Refined Score for node	[-]
$\boldsymbol{s_i}$	Strength for node	[-]
$\boldsymbol{S_i}$	RSONet Simplified Score for node	[-]
S	Average RSONet Simplified Score	[-]
t	Time	[s]
$\boldsymbol{t_s}$	Time Step	[s]
T	Propagation Time	[s]
$\boldsymbol{T_0}$	Orbital Period	[min]

Acknowledgments

Vorrei ringraziare la Professoressa Colombo per avermi dato l'opportunità di poter svolgere questo lavoro in un contesto internazionale come quello belga, in cui ho avuto modo di accrescere le mie conoscenze accademiche e personali.

Un grazie particolare anche ai miei co-supervisori, Jérôme e Matteo, che hanno fatto sì che potessi trovarmi a mio agio in un ambiente nuovo come Namur, e che mi hanno aiutato in tutto e per tutto. Grazie di cuore.

Vorrei ringraziare anche il Professore Timoteo Carletti per il suo contributo e la sua grande disponibilità nell'aiutarmi.

Un grazie infinito alla mia Famiglia, che mi ha permesso di portare avanti gli studi e mi ha sempre sostenuto. Un "grazie" che non sarà mai abbastanza e che spero un giorno di ripagare con orgoglio e fierezza.

Infine, un grazie a tutti quelli che hanno fatto parte della mia vita durante questo percorso, a chi non c'è più, a chi mi ha aiutato, o semplicemente mi ha fatto compagnia.